

# Modern Statistical Models and Methods for Estimating Fatigue-Life and Fatigue-Strength Distributions from Experimental Data

William Q. Meeker\* Luis A. Escobar† Francis G. Pascual‡ Yili Hong§  
 Peng Liu ¶ Wayne M. Falk|| Balajee Ananthasayanam \*\*

16 November 2023

## Abstract

Engineers and scientists have been collecting and analyzing fatigue data since the 1800s to ensure the reliability of life-critical structures. Applications include (but are not limited to) bridges, building structures, aircraft and spacecraft components, ships, ground-based vehicles, and medical devices. Engineers need to estimate *S-N* relationships (Stress or Strain versus Number of cycles to failure), typically with a focus on estimating small quantiles of the *fatigue-life* distribution. Estimates from this kind of model are used as input to models (e.g., cumulative damage models) that predict failure-time distributions under varying stress patterns. Also, design engineers need to estimate lower-tail quantiles of the closely related *fatigue-strength* distribution. The history of applying incorrect statistical methods is nearly as long and such practices continue to the present. Examples include treating the applied stress (or strain) as the response and the number of cycles to failure as the explanatory variable in regression analyses (because of the need to estimate strength distributions) and ignoring or otherwise mishandling censored observations (known as runouts in the fatigue literature). The first part of the paper reviews the traditional modeling approach where a fatigue-life model is specified. We then show how this specification induces a corresponding fatigue-strength model. The second part of the paper presents a novel alternative modeling approach where a fatigue-strength model is specified and a corresponding fatigue-life model is induced. We explain and illustrate the important advantages of this new modeling approach.

*Keywords:* Bayesian inference, censored data, failure-time regression, fracture, maximum likelihood, nonlinear regression, reliability, *S-N* curves.

---

\*Department of Statistics, Iowa State University

†Department of Experimental Statistics, Louisiana State University

‡Department of Mathematics and Statistics, Washington State University

§Department of Statistics, Virginia Tech

¶JMP Statistical Discovery LLC

||U.S. Food and Drug Administration

\*\*Honda Aero

# 1 Introduction

## 1.1 Motivation

Engineers and scientists have been collecting and analyzing fatigue data since the 1800s to ensure the reliability of life-critical structures. Applications include (but are not limited to) bridges, building structures, aircraft and spacecraft components, ships, ground-based vehicles, and medical devices. Because of its importance, fatigue has been and continues to be the most widely studied failure mechanism. Many hundreds of technical papers describing fatigue data are published each year. Even today, many of these papers are not using appropriate statistical methods. *Current* standards and handbooks such as [ISO \(2012\)](#), [ASTM \(2015\)](#), and [MMPDS \(2021\)](#) describe and recommend *archaic statistical methods* developed from the late 1940s to the late 1960s. Modern statistical methods and the availability of computational power allow engineers to fit needed nonlinear regression models and properly handle runouts (right-censored observations). The modern statistical methods that provide improved statistical inference, however, are not presented in engineering standards. While this paper will not immediately remedy the omission of these topics, the information presented in this paper can guide inclusion in future revisions.

## 1.2 Laboratory Experiments to Obtain $S$ - $N$ Data

Under cyclic stress (ideally, a sine wave where “stress level” generally implies stress amplitude), test units accumulate damage—crack initiation and subsequent growth. The damage accumulation rate depends on levels of stress (or strain). A representative sample of specimens from some production process (e.g., selected from multiple heats or batches) will be tested. These should be randomly assigned to test conditions and order of testing. The number and location of stress levels, the number of test specimens, and the allocation of the test specimens needs to be specified in a purposeful way (described further in Section 6). Fatigue tests can be conducted to control displacement, stress amplitude, or strain amplitude. For consistency, we will generally use the word “stress” when writing generically. Some fatigue testing machines can test only one specimen at a time. Other machines are available to do stressing simultaneously on multiple specimens. Typically units are tested at a fixed stress amplitude until failure or a pre-specified censoring point, whichever comes first. Unfailed units are known as runouts or right-censored observations and are an important part of the data.

## 1.3 Motivating Examples

This section presents motivating examples based on fatigue tests with three different materials: a composite material and two metals with different characteristics. As will be shown in the following sections, the features of the different data sets will suggest regression models with different characteristics.

**Example 1.1 Fatigue-Life Data from a Test on a Laminate Panel.** Four-point out-of-plane bending tests were run on 25 specimens of carbon eight-harness satin/epoxy laminate panels at each

of five different stress levels. There were ten runouts at the two lowest stress levels. Fatigue life was considered to be the number of cycles until a specimen fractured. These data were previously analyzed (using different models) in [Shimokawa and Hamaguchi \(1987\)](#), [Pascual and Meeker \(1999\)](#), and [Meeker et al. \(2022, Chapter 17\)](#).

Figure 1(a) is a log-log scatterplot of the laminate panel *S-N* data with the response (thousands of cycles) on the vertical axis. Figure 1(b) plots the same data with the response on the horizontal axis. It is common practice to plot a regression response on the vertical axis. In the fatigue literature, however, the response is plotted on the horizontal axis and we will follow that convention here. Although it is partially obscured by the runouts, there is strong statistical evidence of curvature in the data on log-log scales. Such curvature is ubiquitous in *S-N* data, especially when there are tests at low stress levels resulting in long failure times (e.g., HCF or high-cycle fatigue).

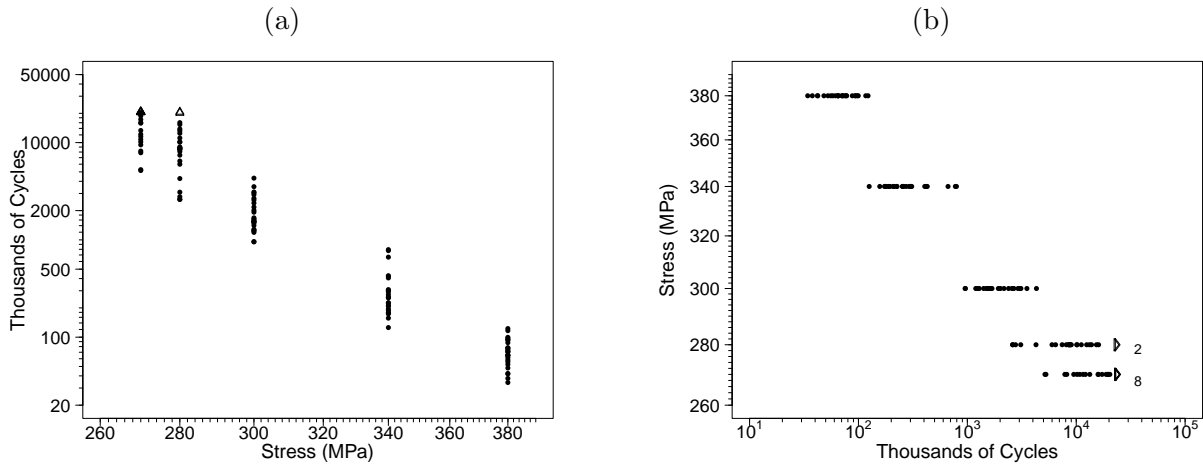


Figure 1: Laminate panel *S-N* data with number of cycles on the vertical axis (a) and the horizontal axis (b).

Figure 2 shows Weibull and lognormal probability plots for the laminate panel fatigue-life data with estimates of the cdfs (the lines going through the nonparametric estimate points) at each level of stress. These plots suggest that the lognormal distribution provides a better description of the data. The slopes of the cdf-estimate lines tend to decrease from left to right. This implies more spread in the data at lower stress levels, another common characteristic of *S-N* data. Section 2.6 will present an appropriate fatigue-life regression model to describe these data. ■

**Example 1.2 Fatigue-Life Data from a Test on Ti64 Specimens.** Ti-6Al-4V (Ti64) is an alloy of titanium, aluminum, and vanadium that has a high strength-to-weight ratio and corrosion resistance. Because of these properties, Ti64 is used widely in aerospace applications. Data from a fatigue test are shown in Figure 3(a). Units were subjected to cyclic loading at a temperature of 350°F with a stress ratio  $R = -1$  (fully reversed loading with a zero-mean stress) with stress amplitudes of 60 (37 specimens), 70 (12 specimens), 80 (11 specimens), and 90 (12 specimens) ksi (kilopound per square inch). More units were tested at 60 ksi because it was expected that a smaller proportion of tested

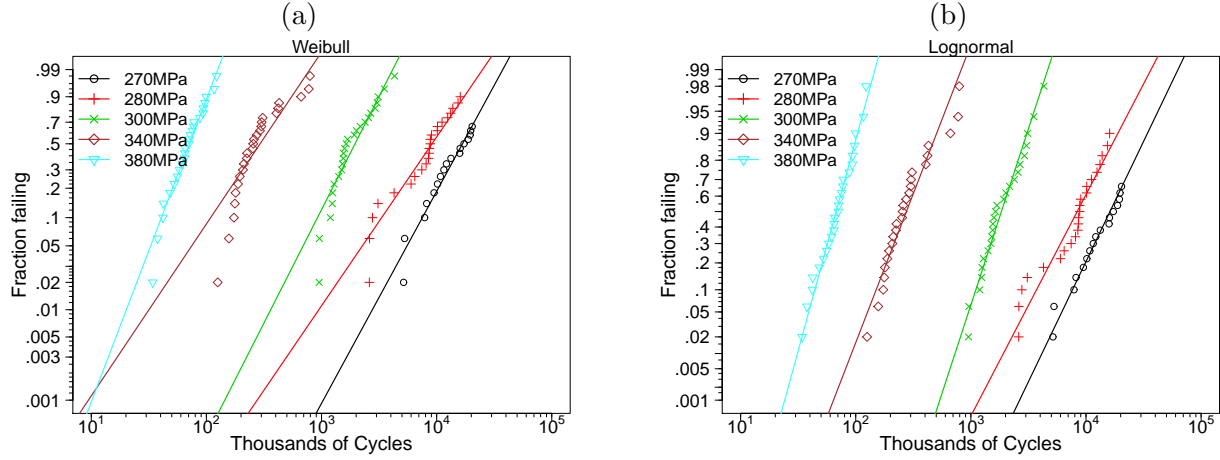


Figure 2: Laminate panel  $S$ - $N$  data Weibull (a) and lognormal (b) probability plots with separate distributions fit to each level of stress.

units would fail there. Of the 37 specimens tested at 60 ksi, 28 were runouts that survived between 30,000 and 46,505 thousand cycles (indicated by the triangles pointing to the right in the figure). The plot indicates strong curvature in the  $S$ - $N$  relationship and increasing spread at lower stress levels. Figure 3(b) is a lognormal probability plot for the Ti64 data. For these data, the lognormal

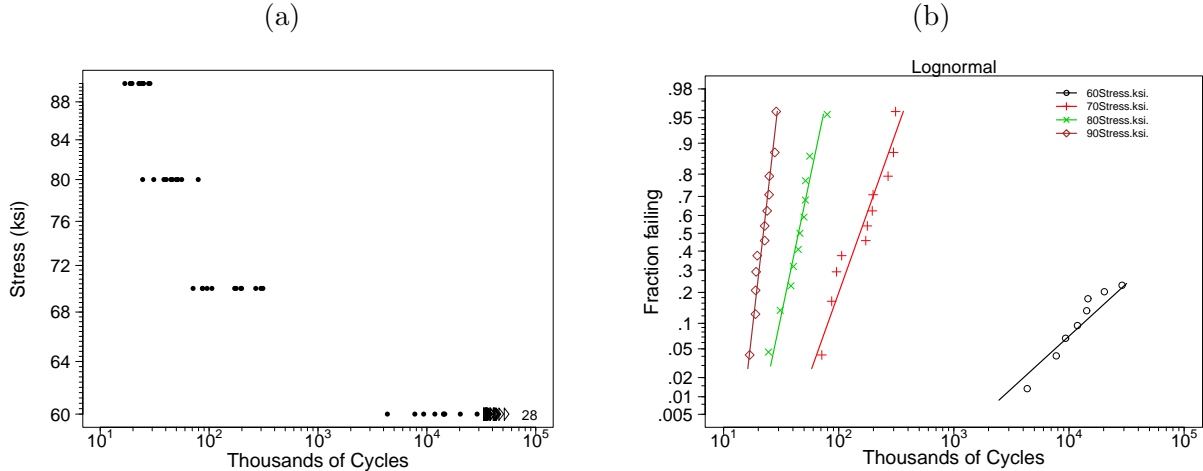


Figure 3: Ti64  $S$ - $N$  Data scatter plot (a) and lognormal probability plot (b) with separate lognormal distributions fit to each level of stress.

distribution provides a better fit than the Weibull distribution (see Figure 22 in the Supplement for a side-by-side comparison). The changes in slopes of the fitted lines (corresponding to estimates of the lognormal shape parameters) indicate the increase in spread at lower stress levels. ■

**Example 1.3 Fatigue-Life Data from a Test on Superelastic Nitinol Specimens.** Nitinol is an alloy of nickel and titanium able to accommodate large recoverable strains via martensitic phase transition, an effect sometimes referred to as super-elasticity. Nitinol has found numerous successful

applications in implantable medical devices which are designed to remain durable beyond 100 million cycles. Rotary bend fatigue tests with nitinol straight wire specimens were conducted with target alternating strain ranging from 0.28 to 2.66%. The material specification, sample preparation and test procedure, and interpretation of the results can be found in [Weaver et al. \(2022\)](#). Rotating bend produces inherently fully reversed loading with a zero-mean stress. All tests were conducted in phosphate buffered saline maintained at  $37 \pm 2^\circ\text{C}$  to approximate *in vivo* conditions. Tests were run until fracture or until completion of 1 billion cycles. Surviving units are runouts. The data from tests conducted at one of two laboratories is plotted in Figure 4(a), resulting in 46 fractures and 20 runouts. The nitinol data set also contains a variable “Exact Strain” that results after applying a correction to five nominal strain values. Because the size of the small correction varies from unit to unit, this results in a substantial increase in the number of strain levels making it impossible to use some of the diagnostics we want to illustrate.

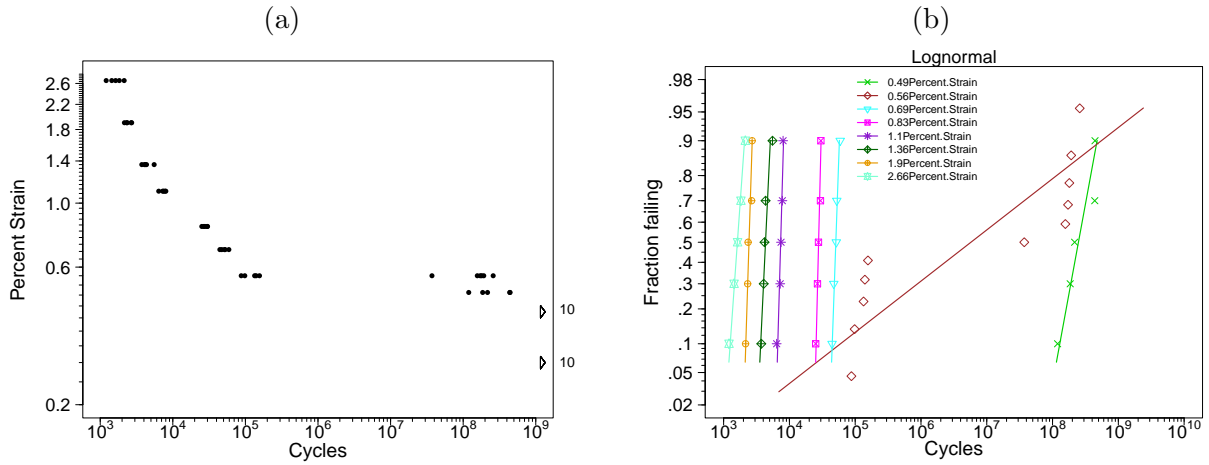


Figure 4: Nitinol *S-N* Data scatter plot (a) and lognormal probability plots (b) with separate distributions fit to each level of stress.

Similar to the Ti64 data in Example 1.2, the scatter plot in Figure 4(a) shows an *S-N* relationship with strong curvature and increased spread at low levels of strain. Figure 4(b) is a lognormal probability plot for the nitinol data. The most striking feature in the plot is at 0.56% strain where there were five early failures and, after a gap, five later failures. This kind of bimodal behavior is often seen in *S-N* data of standard metallic materials, especially at intermediate levels of stress or strain where cycling might be either elastic or plastic. In nitinol, however, fractures predominately initiate at small inclusions. The inclusions initiate propagation sooner under conditions of cyclic martensitic transformation than under conditions of purely elastic cycling. For the other levels of strain, either a lognormal or a Weibull distribution provides an excellent description of the data (see Figure 25 in the Supplement for a side-by-side comparison). ■

## 1.4 History and Literature Review

Scientific and engineering focus on understanding and managing fatigue as a failure mechanism accelerated in the 1950s after there were several fatigue-related failures in the rapidly growing area of aerospace applications. These and some other earlier fatigue-related reliability disasters are described in [Woo \(2020, Chapter 2\)](#). Engineers collecting fatigue data in the 1950s through the 1970s generally did not know how to properly handle censored data and other complications that arise in  $S$ - $N$  data. Stress was sometimes treated as the response variable (due to the desire to estimate strength distributions) and runouts were either ignored or treated as failures (practices that unfortunately still, in some places, continue today).

Examples of early development of statistical theory for the analysis of fatigue data include [Freudenthal and Gumbel \(1953, 1954, 1956\)](#). Wayne Nelson (while working at GE Corporate Research and Development) did pioneering work in developing appropriate statistical methods for modeling and making inferences from complicated *censored*  $S$ - $N$  data. [Nelson \(1984, 2004\)](#) illustrates these methods which include maximum likelihood estimation, model-checking diagnostics, and confidence intervals for fatigue-life distribution quantiles. He illustrated the methods on data from a strain-controlled experiment on a nickel-base super alloy used in high-temperature components of an aircraft engine. Log-life was modeled as a quadratic function of pseudo-stress (strain multiplied by Young's modulus, a covariate) to describe the characteristic curvature of most HCF  $S$ - $N$  data when plotted on log-log scales. He also employed a log-linear relationship for the lognormal shape parameter (also used in Section 2.3) to describe the often-seen increase in spread at lower stress levels.

As mentioned in Section 1.1, many thousands of papers have been published in the engineering literature describing methods for modeling fatigue data, often for specific applications. Dozens of models for fatigue data have been suggested in these papers. [Castillo and Fernández-Canteli \(2009\)](#) review and describe many of these models. We review several of the most commonly used  $S$ - $N$  models in Section 2. More complicated  $S$ - $N$  models are described and applied to the Ti64 and nitinol data in Section 5.

The publication of early papers using maximum likelihood methods, such as [Spindel and Haibach \(1979\)](#) and [Nelson \(1984\)](#), began a trend that continues today, of more analysts using appropriate methods for handling  $S$ - $N$  data with runouts. More recently, papers like [Babuška et al. \(2016\)](#) and [Castillo et al. \(2019\)](#) illustrate the use of Bayesian methods to fit and compare models fit to fatigue data. Bayesian methods can also properly handle runouts and correctly quantify statistical uncertainty.

## 1.5 Contributions

In addition to some review, this paper contains many new and important technical results.

1. A general, flexible, modular framework for statistical modeling  $S$ - $N$  data for which most of the models that have been used in the thousands of published papers in the engineering literature, can be viewed as special cases.

2. Engineers (and some statisticians) have, conceptually, known about the closely connected distributions of fatigue life and fatigue strength (e.g., [Freudenthal and Gumbel, 1956](#)). Because fatigue life is observable and fatigue strength is not, there has not been a unified and flexible estimation method for these distributions. For the first time, we present a unified flexible model that connects these two important distributions and allows for the efficient use of  $S$ - $N$  data to estimate both fatigue-life and fatigue-strength distributions. These connected distributions are at the heart of the framework in Contribution 1.
3. Perhaps most importantly, and building on Contribution 2, and a contribution by [Falk \(2019\)](#), we show how one can usefully specify a relatively simple fatigue-strength model that will then induce an appropriate fatigue-life model. We demonstrate and illustrate the important advantages of specifying the fatigue model for  $S$ - $N$  data in this manner.
4. We describe the physical explanation for the curvature in the  $S$ - $N$  relationship and show how this curvature induces fatigue-life distributions with an increased spread at lower levels of stress/strain.

## 1.6 Overview

The remainder of this paper is organized as follows. Section 2 outlines our general approach for modeling  $S$ - $N$  data and illustrates it on an example where a fatigue-life model is specified and the corresponding the fatigue-strength model is induced. Section 3 describes fatigue-strength models and shows how a specified fatigue-strength model induces a corresponding fatigue-life model. Section 4 briefly reviews likelihood and Bayesian methods for statistical inference, including residual analysis for censored data and general methods for estimating lower-tail quantiles of fatigue-life and fatigue-strength distributions that engineers need. Section 5 describes and compares additional widely-used models for  $S$ - $N$  data, describes the important advantages of specifying a fatigue-strength model that induces a fatigue-life model, and illustrates the approach with two additional HCF applications. Section 6 provides concluding remarks and outlines areas for future research. To save space and improve readability, proofs, various technical details, additional plots, and more detailed numerical results have been relegated to an online supplement (the Supplement).

## 2 Statistical Models for Fatigue $S$ - $N$ Data

As mentioned in Section 1.4, dozens of different statistical models have been suggested to describe  $S$ - $N$  data. This section introduces a modular framework that includes most of these models as special cases. For a given  $S$ - $N$  data set, appropriate model components are chosen to comprise a specific model or to describe the data. We encourage fitting and comparing alternative statistical models.

## 2.1 A Modular Framework for Modeling Fatigue $S$ - $N$ Data

A statistical model for fatigue  $S$ - $N$  experimental data has two closely related random variables. Fatigue life  $N$  is the number of cycles to failure (fracture) for a unit tested as a specified level of stress  $S_e$ . The fatigue-life model is an important input for some system-reliability models (e.g., Example 5.3 in [Meeker et al., 2022](#)).

Fatigue strength  $X$  is the lowest level of applied stress that would result in a failure at a specified number of cycles  $N_e$ . The fatigue-strength distribution (and especially small quantiles of the distribution) is important for engineering design and for assessing reliability with a stress-strength interference model (e.g., Section 23.2 in [Meeker et al., 2022](#)). There are some places in the fatigue literature where the distribution of  $X$  is called the “distribution of stress.” In fatigue experiments, stress (or strain) is a controlled experimental variable. For purposes of clarity and consistency with the vast majority of the fatigue literature, we will use *fatigue-strength distribution*. Fatigue resistance is another name for fatigue strength.

There are two different ways to specify a statistical model for  $S$ - $N$  data:

1. Specify a model  $F_N(t; S_e, \boldsymbol{\theta})$  for fatigue life  $N$  as a function of a specified stress amplitude  $S_e$  which will induce (imply) a corresponding fatigue-strength model (Section [2.4](#)).
2. Specify a model  $F_X(x; N_e, \boldsymbol{\theta})$  for fatigue strength  $X$  as a function of a given number of cycles  $N_e$ . This model will induce a corresponding fatigue-life model (Section [3.2](#)).

Here  $\boldsymbol{\theta}$  is a vector of unknown parameters (the nature of which depends on the particular model components) to be estimated from the  $S$ - $N$  data. To simplify notation, we will usually suppress the dependency of  $F_N(t; S_e)$ ,  $F_X(x; N_e)$ , or their corresponding density and quantile functions on  $\boldsymbol{\theta}$ .

Because  $N$  is *observable* (and  $X$  is not), the first approach for  $S$ - $N$  model specification has been used most commonly in practice and will be described and illustrated in the rest of this section. The second approach is new, has important advantages, and will be described in detail in Section [3.2](#) and illustrated in Examples [5.1](#) and [5.2](#). After deciding whether to specify the model for  $N$  or  $X$ , two model components need to be specified:

- A functional  $S$ - $N$  regression relationship (decreasing, usually nonlinear, continuous, and differentiable) describing how the observable  $N$  depends on the experimental factor stress amplitude  $S$ . Although it is possible to have other explanatory/experimental variables in a fatigue regression relationship, and such extensions are straightforward, we will focus on a model with just one experimental factor and describe the extensions in our concluding remarks.
- A probability model (e.g., a lognormal or Weibull distribution) to describe spread in the  $S$ - $N$  data.

In this paper we give examples of both types of components but the framework is flexible enough to accommodate other relationships and probability models not described explicitly in this paper.

## 2.2 Log-Location-Scale Probability Distributions

If  $Y$  has a location-scale distribution, then  $T = \exp(Y)$  has a log-location-scale distribution with cdf

$$F(t; \mu, \sigma) = \Phi\left[\frac{\log(t) - \mu}{\sigma}\right] = \Phi\left[\log\left(\left[\frac{t}{\exp(\mu)}\right]^{(1/\sigma)}\right)\right], \quad t > 0 \quad (1)$$

where  $\Phi(z)$  is the cdf for the particular standard location-scale distribution,  $\exp(\mu)$  is a scale parameter and  $\sigma$  is the shape parameter. The most well-known log-location-scale distributions are the lognormal ( $\Phi(z) = \Phi_{\text{norm}}(z)$  is the standard normal cdf), and Weibull ( $\Phi(z) = \Phi_{\text{sev}}(z) = 1 - \exp[-\exp(z)]$  is the standard smallest extreme value cdf) distributions. See Chapter 4 of [Meeker et al. \(2022\)](#) for more information about these and other log-location-scale distributions.

## 2.3 Some Simple $S$ - $N$ Relationships and Statistical Models for Fatigue Life

This section describes simple  $S$ - $N$  relationships that are useful for specifying a fatigue-life model for  $S$ - $N$  data. More complicated  $S$ - $N$  relationships that are better suited when a fatigue-strength model is specified are given in Section 5.

### 2.3.1 A statistical model for fatigue-life

Suppose that the logarithm of the fatigue-life random variable  $N$  at a *specified* stress level  $S_e$  is

$$\log(N) = \log[g(S_e; \boldsymbol{\beta})] + \sigma_N \epsilon, \quad (2)$$

where  $N = g(S; \boldsymbol{\beta})$  is a positive monotonically decreasing  $S$ - $N$  regression relationship of known form,  $\boldsymbol{\beta}$  is a vector of regression parameters, and  $\epsilon$  is a random error term from a location-scale distribution with  $\mu = 0$  and  $\sigma = 1$ . Then for any specified stress level  $S_e$ ,  $N$  has a log-location-scale distribution with cdf

$$F_N(t; S_e) = \Pr(N \leq t; S_e) = \Phi\left(\frac{\log(t) - \log[g(S_e; \boldsymbol{\beta})]}{\sigma_N}\right), \quad t > 0, \quad S_e > 0, \quad (3)$$

where  $g(S_e; \boldsymbol{\beta})$  is a scale parameter and  $\sigma_N$  is the shape parameter of the distribution of  $N$ . The fatigue-life  $p$  quantile is obtained by solving  $p = F_N(t_p(S_e); S_e)$  for  $t_p(S_e)$ , giving

$$t_p(S_e) = \exp(\log[g(S_e; \boldsymbol{\beta})] + \Phi^{-1}(p)\sigma_N), \quad 0 < p < 1, \quad S_e > 0. \quad (4)$$

### 2.3.2 The Basquin model

The [Basquin \(1910\)](#)  $S$ - $N$  relationship (sometimes referred to as the *inverse-power rule*) is

$$N = A \times S^{-B},$$

were  $A$  and  $B$  are parameters. As usually presented in the engineering literature, there is no random error term in the relationship, which is generally taken to represent the relationship between a particular failure-time distribution quantile (e.g., the median) and stress  $S$ . Taking logs, changing parameter names and a sign, and adding an error term gives the statistical model for fatigue life  $N$

$$\log(N) = \beta_0 + \beta_1 \log(S) + \sigma_N \epsilon. \quad (5)$$

For any specified level of stress  $S_e$ ,  $N$  has a log-location-scale distribution with constant  $\sigma_N$  with cdf and quantile functions given by (3) and (4), respectively, where  $\log[g(S_e; \beta)] = \beta_0 + \beta_1 \log(S_e)$ . Basquin is the simplest and most widely used model for fatigue life.

### 2.3.3 The Stromeier model

Stromeier (1914) introduced the *fatigue-limit*  $S$ - $N$  model

$$\log(N) = \beta_0 + \beta_1 \log(S - \gamma) + \sigma_N \epsilon, \quad (6)$$

which, as a generalization to the Basquin model in (5), describes the curvature commonly seen in  $S$ - $N$  data. For any specified level of stress  $S_e$ ,  $N$  has a log-location-scale distribution with cdf and quantile functions given by (3) and (4), respectively, where  $\log[g(S_e; \beta)] = \beta_0 + \beta_1 \log(S_e - \gamma)$ . In this model, if  $S_e$  is less than the fatigue-limit  $\gamma$  (also known as an endurance-limit), lifetime is infinite—stress is low enough that cycling does not cause permanent damage. Although there are dissenters, (e.g., Bathias, 1999), it is widely believed that fatigue-limits exist in hard metals like steel and some titanium alloys but not in soft metals like aluminum or copper. Even if fatigue-limits exist, it is unreasonable to assume that  $\gamma$  would be constant in a process/population because there are many additional sources of variability that would affect such fatigue-limits (e.g., surface finish, residual stresses, other manufacturing variabilities, and environmental variables). This motivates the random fatigue-limit (RFL) model described in Section 5.6.

The fatigue-limit  $\gamma$  in (6) is a horizontal asymptote for the  $S$ - $N$  relationship and therefore this model can usefully describe the kind of curvature seen in  $S$ - $N$  data from hard metals (e.g., the Ti64 data Example 1.2). The Stromeier model will not, however, describe any increase in spread often seen at low stress levels.

### 2.3.4 Box–Cox (power) transformation model

Nelson (2004, page 96) mentions the use of a power transformation of stress instead of a log transformation. Meeker et al. (2003) and Meeker et al. (2022, Section 18.5.5) use a Box–Cox transformation

*S-N* model

$$\log(N) = \beta_0 + \beta_1 \nu(S; \lambda) + \sigma_N \epsilon = \begin{cases} \beta_0 + \beta_1 \left( \frac{S^\lambda - 1}{\lambda} \right) + \sigma_N \epsilon & \text{if } \lambda \neq 0 \\ \beta_0 + \beta_1 \log(S) + \sigma_N \epsilon & \text{if } \lambda = 0 \end{cases} \quad (7)$$

instead. Here  $\nu(S_e, \lambda)$  is the Box–Cox power transformation of stress. This transformation is preferred because  $\nu(S_e, \lambda)$  is continuous in the power parameter  $\lambda$  and the special case  $\lambda = 0$  corresponds to the Basquin model. For any specified level of stress  $S_e$ ,  $N$  has a log-location-scale distribution with cdf and quantile functions given by (3) and (4), respectively, where  $\log[g(S_e; \beta)] = \beta_0 + \beta_1 \nu(S_e, \lambda)$ .

In contrast to the Stromeier model, there is no horizontal asymptote in this model but the model can usefully describe less extreme curvature that often arises in *S-N* data (e.g., the laminate panel data in Example 1.1). Like the Stromeier model, it will not describe any increase in spread at low stress levels.

As shown in Figure 5(a), for  $\lambda < 0$  and  $\beta_1 < 0$  (values expected in *S-N* applications) the Box–Cox relationship has a concave-up shape and a vertical asymptote at  $B = \beta_0 + \beta_1(-1/\lambda)$  as stress approaches infinity. As described in Sections 2.4.3 and 3.2.5, this asymptotic behavior can lead to physically unreasonable model features. When, however, the steep asymptotic behavior is outside the range where the model would be used (e.g., Example 2.2), there are no practical problems.

### 2.3.5 A model component to describe nonconstant $\sigma_N$

The models described earlier in this section do not account for nonconstant  $\sigma_N$  that is often seen in *S-N* data (e.g., the data introduced in Examples 1.2 and 1.3). Thus, for some data sets, it is necessary to add an additional model component such as

$$\sigma_N = \exp \left[ \beta_0^{[\sigma_N]} + \beta_1^{[\sigma_N]} \log(S_e) \right]. \quad (8)$$

Nelson (1984) used a quadratic *S-N* relationship and (8) to estimate *S-N* curves for a nickel-based superalloy. Pascual and Meeker (1997) used a Stromeier *S-N* relationship (Section 2.3.3) and (8) to describe the same data. In Section 2.6, our model for the laminate panel data will use (8) to describe the increase in spread at the lower stress levels seen in Figure 2.

When a model contains a special component to describe how  $\sigma_N$  depends on stress, it is no longer possible to find a closed-form expression for the fatigue-strength cdf like that in (10). It is still possible, however, to compute the cdf and quantiles of  $F_X(x; N_e)$  numerically by using the equivalence of fatigue-life and fatigue-strength quantile curves described in Section 2.4.4.

## 2.4 Linking Fatigue-Life and Fatigue-Strength Models

This section describes the relationship between a specified fatigue-life model and the corresponding induced fatigue-strength model.

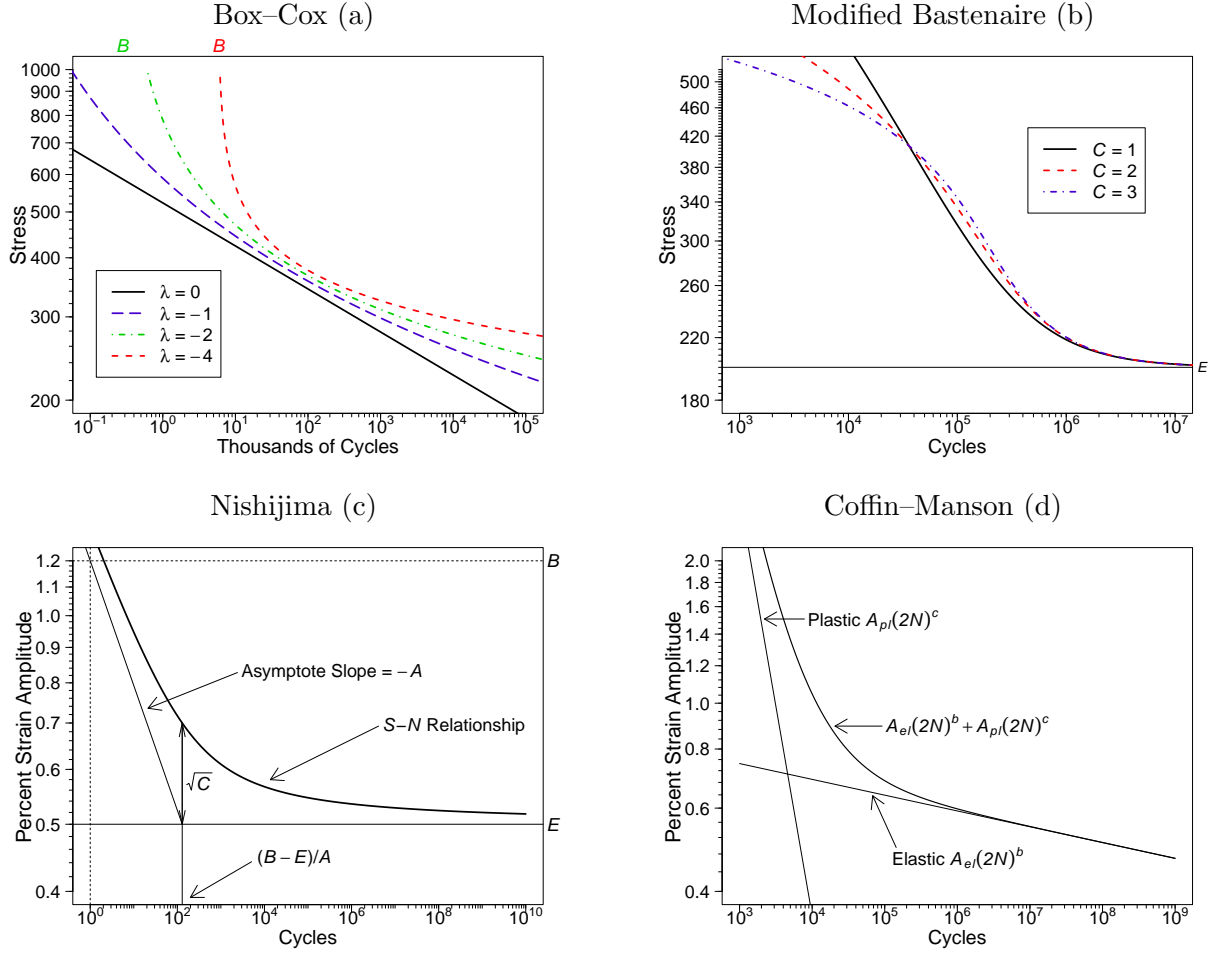


Figure 5:  $S$ - $N$  relationships: Box-Cox (7) (a), modified Bastenaire (5.2) (b), Nishijima (5.4) (c), and Coffin-Manson (5.5) (d).

#### 2.4.1 The induced fatigue-strength model when $\log[g(S; \beta)]$ has neither a vertical nor a horizontal asymptote

Section 2.1 defined the unobservable *fatigue-strength* random variable  $X$  as the lowest level of applied stress that would result in a failure at a specified number of cycles  $N_e$ . This definition describes the close relationship to the observable fatigue-life random variable  $N$ . In our model, based on this definition, the distributions of  $X$  and  $N$  share the same error term. For the moment, suppose that  $\log[g(S_e; \beta)]$  has neither a horizontal nor a vertical asymptote (e.g., the Basquin model). To derive the distribution of  $X$  from the distribution of  $N$  in (2), replace  $N$  with  $N_e$  and  $S_e$  with  $X$  giving

$$\log(N_e) = \log[g(X; \beta)] + \sigma_N \epsilon. \quad (9)$$

This shows that the common error term  $\sigma_N \epsilon$  drives the random variable  $X$  at fixed  $N_e$  as well as the random variable  $N$  at fixed  $S_e$ . Also, (9) implies that  $(\log(N_e) - \log[g(X; \beta)])/\sigma_N = \epsilon$  has a location-

scale distribution with  $\mu = 0$  and  $\sigma = 1$ . Then using (9) and the fact that  $g(S; \beta)$  is monotonically decreasing in  $S$ , the cdf of  $X$  is

$$\begin{aligned}
F_X(x; N_e) &= \Pr(X \leq x) = \Pr[g(X; \beta) > g(x; \beta)] \\
&= \Pr(\log[g(X; \beta)] > \log[g(x; \beta)]) = \Pr(-\log[g(X; \beta)] < -\log[g(x; \beta)]) \\
&= \Pr(\log(N_e) - \log[g(X; \beta)] < \log(N_e) - \log[g(x; \beta)]). \\
&= \Phi\left[\frac{\log(N_e) - \log[g(x; \beta)]}{\sigma_N}\right], \quad x > 0, \quad N_e > 0.
\end{aligned} \tag{10}$$

Note that (10) is a log-location-scale distribution if and only if the  $S$ - $N$  relationship  $\log[g(x; \beta)]$  is a linear function of  $\log(x)$  (i.e., the Basquin model in (5)). For nonlinear  $S$ - $N$  relationships, the induced distribution for  $X$  provides a theoretically justified method for making inferences about fatigue-strength distributions as a function of the fatigue-life model parameters  $(\beta, \sigma_N)$ .

Expressions for the corresponding pdf of  $X$  are given in Supplement Section B.4. The  $p$  quantile of the fatigue-strength distribution is obtained by solving  $F_X(x_p; N_e) = p$  in (10) for  $x_p$  giving

$$x_p(N_e) = g^{-1}(\exp[\log(N_e) - \Phi^{-1}(p)\sigma_N]; \beta), \quad 0 < p < 1, \quad N_e > 0. \tag{11}$$

**Example 2.1 The Induced Fatigue-Strength Model for the Basquin Relationship.** This example provides details for the special-case induced fatigue-strength model for the Basquin relationship, illustrated in Figure 6 for the lognormal and Weibull distributions. Substituting  $\log[g(x; \beta)] =$

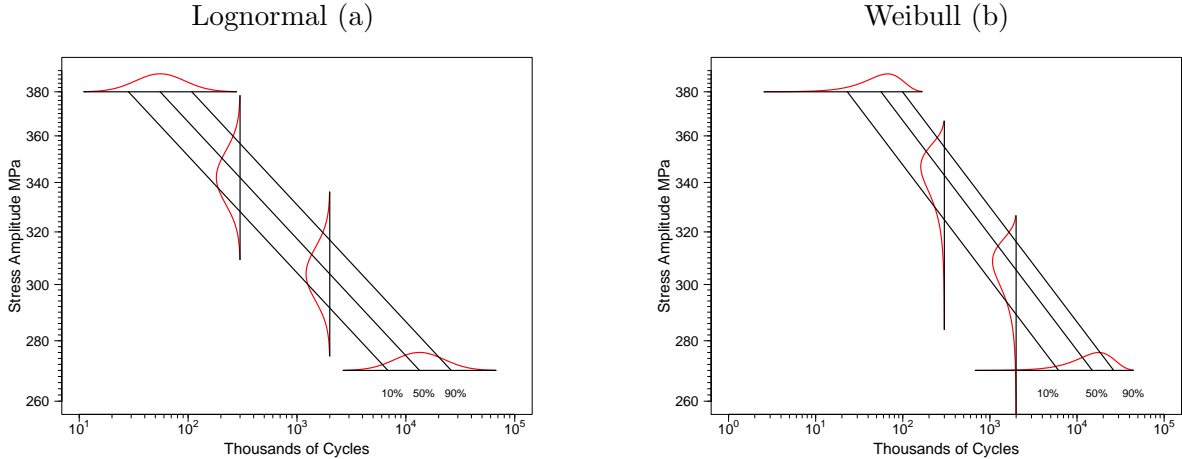


Figure 6: Lognormal (a) and Weibull (b) fatigue-life (horizontal) and fatigue-strength (vertical) distributions for the Basquin  $S$ - $N$  relationship.

$\beta_0 + \beta_1 \log(x)$  into (10), with  $\beta_1 < 0$  (because the  $S$ - $N$  relationship is strictly decreasing), gives

$$\begin{aligned} F_X(x; N_e) &= \Phi \left[ \frac{\log(N_e) - [\beta_0 + \beta_1 \log(x)]}{\sigma_N} \right], \quad x > 0, N_e > 0 \\ &= \Phi \left[ \frac{\log(x) - [\beta_0 - \log(N_e)]/|\beta_1|}{\sigma_N/|\beta_1|} \right] = \Phi \left[ \frac{\log(x) - [\beta_0^\dagger + \beta_1^\dagger \log(N_e)]}{\sigma_X} \right], \end{aligned}$$

where  $\beta_0^\dagger = -\beta_0/\beta_1$ ,  $\beta_1^\dagger = 1/\beta_1$ , and  $\sigma_X = \sigma_N/|\beta_1|$ , showing that, for the Basquin relationship, the induced fatigue-strength model has the same log-location-scale form with different parameters.  $\blacksquare$

#### 2.4.2 The induced fatigue-strength model when $\log[g(S; \beta)]$ has a horizontal asymptote

When  $\log[g(x; \beta)]$  has a horizontal asymptote at  $\log(S) = E$ ,  $\lim_{x \downarrow \exp(E)} \log[g(x; \beta)] = \infty$  as illustrated in Figure 5(b) and (c). Because  $(\log(N_e) - \log[g(x; \beta)])/\sigma_N$  is unbounded, the derivation of the cdf for  $X$  is the same as (10) but because of the asymptote, for given  $N_e$ ,

$$\lim_{x \downarrow \exp(E)} F_X(x; N_e) = \Phi \left( \frac{\log(N_e) - \infty}{\sigma_N} \right) = 0,$$

and thus

$$F_X(x; N_e) = \Phi \left( \frac{\log(N_e) - \log[g(x; \beta)]}{\sigma_N} \right), \quad x > \exp(E), N_e > 0.$$

The range of  $X$  depends on the unknown threshold parameter  $\exp(E)$ , so the model is not regular (e.g., Smith, 1985). The horizontal asymptote also implies that fatigue strength  $X$  will never be less than  $\exp(E)$ . The pdf of  $X$  is the same as (44) in Supplement Section B.4, except that it is positive only when  $x > \exp(E)$ . The quantiles of  $X$  are the same as (11) but as  $p \rightarrow 0$ ,  $x_p(N_e) \rightarrow \exp(E)$ . Section B.3.2 in the Supplement gives details for a particular example.

#### 2.4.3 The induced fatigue-strength model when $\log[g(S; \beta)]$ has a vertical asymptote

If  $\log[g(x; \beta)]$  has a vertical asymptote (e.g., the Box–Cox relationship in Section 2.3.4 and see Figure 5(a) with  $\lambda < 0$ ), then  $\lim_{x \rightarrow \infty} \log[g(x; \beta)] = B$  and thus  $B$  is a lower bound for  $\log[g(x; \beta)]$ . Consequently,  $[\log(N_e) - B]/\sigma_N$  is an upper bound for  $\epsilon$ , but the range of  $\epsilon$  is  $(-\infty, \infty)$ . To resolve this inconsistency, we modify (9) and use

$$\log(N_e) = \log[g(X; \beta)] + \sigma_N \epsilon I[-\infty < \epsilon < (\log(N_e) - B)/\sigma_N],$$

where  $I[\cdot]$  is the indicator function. The derivation of the cdf for  $X$  is the same as (10) but because of the asymptote, for given  $N_e$ ,

$$\lim_{x \rightarrow \infty} F_X(x; N_e) = \Phi \left( \frac{\log(N_e) - B}{\sigma_N} \right) < 1.$$

This implies that the distribution of  $X$  has a discrete atom of probability at  $\infty$ . The size of the discrete atom is

$$1 - \Phi\left(\frac{\log(N_e) - B}{\sigma_N}\right). \quad (12)$$

This discrete atom corresponds to the limiting proportion of units for which  $N > N_e$  as  $x \rightarrow \infty$ . This can be interpreted as the (physically questionable) proportion of units that would survive  $N_e$  cycles, even as stress approaches  $\infty$ . The pdf of  $X$  is the same as (44) in Supplement Section B.4 but it does not integrate to 1 because of the discrete atom of probability at  $\infty$ . The quantiles of  $X$  are the same as (11) but, because of the discrete atom at  $\infty$ ,  $x_p(N_e)$  are finite only for  $0 \leq p < \Phi[(\log(N_e) - B)/\sigma_N]$ . As an example, Section B.3.3 in the Supplement gives details for the Box–Cox *S-N* model.

#### 2.4.4 Equivalence of fatigue-life and fatigue-strength quantile curves

For *S-N* relationships that have neither a horizontal nor a vertical asymptote, the fatigue-life and fatigue-strength models have the same quantile curves and thus when estimating a fatigue-life model, one is simultaneously estimating the fatigue-strength model. For *S-N* relationships that have either a horizontal or a vertical asymptote the fatigue-life and fatigue-strength quantile curves are still equivalent except when there is a discrete atom of probability at  $\infty$ , as described in Sections 2.4.3 and Sections 3.2.4. Section F.1 provides a proof of the main result and more explanation about the exceptions.

### 2.5 Choosing a Fatigue-Life Probability Distribution

The lognormal and Weibull distributions are the most commonly used distributions in fatigue data analysis. This is because one or the other often fits well and because there is physical motivation for using them. Meeker et al. (2022, Section 4.6.2) give physics-of-failure arguments (based on cumulative damage mechanisms like fatigue) for using the lognormal distribution to describe time to fracture from fatigue in ductile materials like metals, when there is a single crack growing toward fracture. Mathematical justification for this physical/chemical motivation is given in Gnedenko et al. (1969, pages 36–37) and Mann et al. (1974, pages 133–134). Crowder et al. (Section 4.6 1994), Castillo and Fernández-Canteli (2009), and Meeker et al. (2022, Section 4.8.4) describe extreme-value-theory arguments for using the Weibull distribution to describe time to fracture from fatigue in brittle materials like ceramics or metals if there are potentially many cracks competing to be the first to cause fracture (e.g., in a wire, chain, gear, or bearing).

Although this kind of physical guidance is useful in deciding which distribution to use, it is important to use probability plots like those in Figures 2, 3(b), and 4(b) to help make a decision. It is also important to use sensitivity analysis to assess the effect of alternative choices in the distribution (especially when the data do not result in a definitive conclusion or when extrapolating into the lower tail of a fatigue-life or fatigue-strength distribution). For additional illustrations of this, Supplement

Section E provides a side-by-side comparison of lognormal and Weibull distributions fit to nine different  $S$ - $N$  data sets. For the four data sets where tests were on wire specimens, the Weibull distribution fits well (as predicted by extreme-value theory). For the others (e.g., notched or hour-glass shaped metal specimens), the data show that the lognormal distribution is a more appropriate distribution (as predicted by the cumulative damage theory).

## 2.6 An Example of Fitting a Simple Fatigue-Life Model

This section provides an example to illustrate the key ideas presented earlier in this section and to set the stage for the remainder of the paper.

**Example 2.2 Fitting the Box–Cox-Loglinear- $\sigma_N$   $S$ - $N$  Model to the Laminate Panel Data.** This example is a continuation of Example 1.1. A description of the noninformative/weakly informative prior distributions that were used and other details are in Supplement Section J.1. Figure 7(a) is a lognormal probability plot showing Bayesian cdf estimates. The estimates were computed by taking the median of the empirical distribution of the draws from the marginal posterior distributions of  $F_N(t; S_e)$  for a large number of values of  $t$  for each of the five levels of  $S_e$  used in the experiment. The Bayesian estimates agree well with the nonparametric estimates at all levels of  $S_e$ . For estimation at  $S_e = 270$  MPa, corresponding 95% credible intervals are also plotted. These were obtained from the 0.025 and 0.975 quantiles of the empirical distribution of the draws from the marginal posterior distribution  $F_N(t; 270)$  for the same values of  $t$  used to compute the cdf estimates. The credible intervals are narrow because of the large number of tested specimens with few runouts.

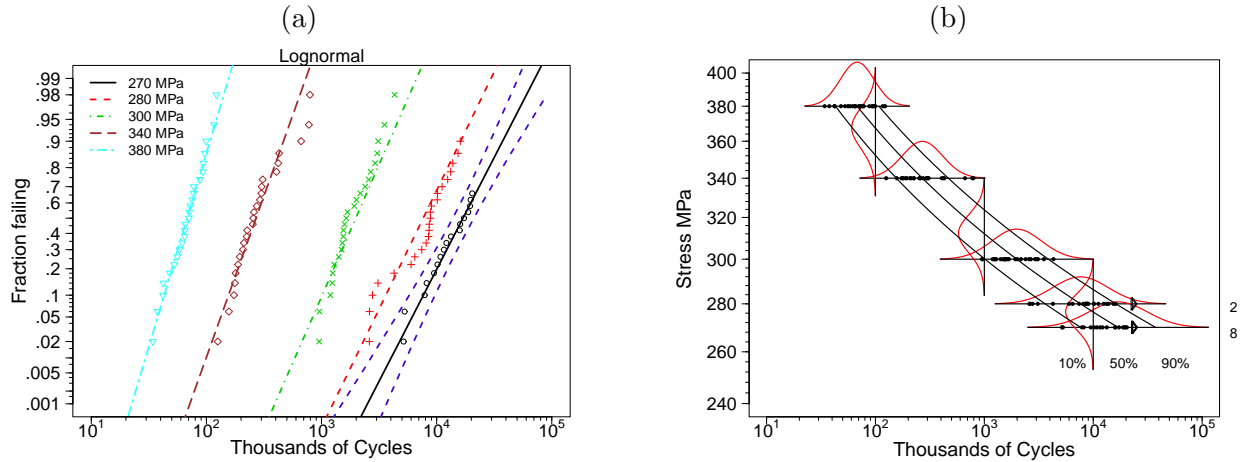


Figure 7: Lognormal probability plot showing the cdf estimates from the Box–Cox-loglinear- $\sigma_N$  model fit to the laminate panel  $S$ - $N$  Data (a) and the corresponding model plot showing the (shared) quantile curves and density estimates for fatigue life (horizontal) and fatigue strength (vertical) (b).

Figure 7(b) is a fitted *model plot* showing the estimates 0.10, 0.50, and 0.9 quantile curves, along with estimates of the fatigue-life and fatigue-strength densities superimposed on top of the  $S$ - $N$  data that we first saw in Figure 1(b). The increase in spread in the fatigue-life (horizontal) densities

(due to the loglinear- $\sigma_N$  component in the model) is evident. Interestingly, the spread in the *induced* fatigue strength (vertical) densities appears to be approximately constant. ■

## 2.7 Characteristics of *S-N* Models

[Bastenaire \(1972\)](#) and [Castillo and Fernández-Canteli \(2009, Chapter 2\)](#) describe various characteristics of *S-N* models that are required for the models to be sensible both physically and probabilistically. This section reviews some of these characteristics.

Perhaps the most important model characteristic is that the *S-N* relationship (e.g.,  $N = g(S)$ , corresponding to a particular quantile curve) be positive and monotonically decreasing—higher stress implies shorter life. Additionally, the fatigue-life model cdf  $F_N(t; S_e, \boldsymbol{\theta})$  should be

- Monotonically increasing in  $t$  for fixed  $S_e$  and
- Monotonically increasing in  $S_e$  for fixed  $t$ .

The first condition is generally met for any of the continuous cdfs typically used in fatigue-life models and used in this paper. Whether the second condition holds or not will depend on the nature of the regression model. Generally, the condition will hold if cdfs for different stress levels like those in Figure 7(a) do not cross. Equivalently, the condition will hold if quantile curves like those in Figure 7(b) do not cross. Although desirable, it is not essential that these not-cross conditions hold over the entire range of  $t$  and  $S_e$ . It is, however, essential that the conditions hold over the range of  $t$  and  $S_e$  where the model is used. [Bastenaire \(1972, page 10\)](#) makes a similar point.

For example, with the fitted quadratic model used in [Nelson \(1984\)](#) (mentioned in Section 1.4), the quantile curves are decreasing in pseudo-stress over the range of the data but begin to increase for larger values of the pseudo-stress used there—but this happens only outside of the range of pseudo-stress where the model would be used. The model used for the laminate panel data in Section 2.6 allows  $\sigma_N$  to be a loglinear function of stress. This causes the slopes of the estimates of the lognormal cdfs in a lognormal probability plot (see Figure 7(a)) to depend on stress, implying that the cdfs will cross. The crossing behavior, however, is far away from the region where the model would be used.

Similar conditions can be stated for the fatigue-strength model  $F_X(x; N_e)$ . Recognizing that the fatigue-life and fatigue-strength models have the same quantile curves (Section 2.4.4) shows that if the conditions hold for the fatigue-life model, they also hold for the fatigue-strength model and vice versa. This crossing behavior can be avoided by specifying a fatigue-strength model with constant  $\sigma_X$  which, if there is curvature in the *S-N* relationship, will result in a change in spread for the induced fatigue-life model for  $N$ . This illuminates an important advantage in specifying the *S-N* model in terms of the fatigue-strength distribution. This modeling approach is described in detail in Section 3.2.

### 3 Statistical Methods for Estimating Fatigue-Strength Distributions

#### 3.1 Estimating a Fatigue-Strength Distribution Using Binary Data

Because fatigue strength is not directly observable, the traditional way to estimate a fatigue-strength distribution at a specified level  $N_e$  (e.g., [Little and Jebe, 1975](#); [Nelson, 2004](#); [Awad et al., 2004](#); [Grove and Campean, 2008](#)) has been to

- Test a sample of  $n$  units at different fixed stress levels  $S_i$ ,  $i = 1, \dots, n$ . The units are tested until failure or the specified value of  $N_e$  cycles (whichever comes first).
- Dichotomize the data to consist of only the runouts (right-censored at  $S_i$  because  $X > S_i$ ) and failures (left-censored at  $S_i$  because  $X < S_i$ ). The actual failure times are ignored.
- Use binary regression methods (e.g., logit or probit regression, possibly on  $\log(S)$ ) to estimate the fatigue-strength distribution at  $N_e$  cycles.

Data from the well-known and commonly used staircase method (e.g., [Pollak et al., 2006](#); [Müller et al., 2017](#)) provide useful estimates of the *median* of the fatigue-strength distribution, but not small quantiles that are needed in high-reliability applications. This is because the method concentrates observations near the center of the fatigue-strength distribution. [Wu and Tian \(2014\)](#) review and suggest an alternative sequential method when the goal is to estimate a particular quantile of a distribution based on binary data. Section 3.2 shows how to estimate a fatigue-strength distribution more efficiently by using all of the available  $S$ - $N$  data (i.e., not ignoring the failure times). The methods build upon and extend the widely used methods for modeling  $S$ - $N$  data described in Section 2.

#### 3.2 Modeling $S$ - $N$ Data by Specifying a Fatigue-Strength Model

The relationship between  $F_N(t; S_e)$  and  $F_X(x; N_e)$  described in Section 2.4 suggests an alternative path for specifying a statistical model for  $S$ - $N$  data. Similar to [Falk \(2019\)](#), one can specify the form of the fatigue-strength distribution and use a specified  $S$ - $N$  relationship to *induce* a fatigue-life model that can be fit to the  $S$ - $N$  data using statistical methods (e.g., maximum likelihood or Bayesian estimation) that can accommodate censored data.

##### 3.2.1 The advantages of specifying the fatigue-strength model to describe $S$ - $N$ data

Specifying a fatigue-strength model and having it induce the corresponding fatigue-life model can have important advantages. For example, for many engineering materials, the variability in fatigue-strength distributions has been observed to be relatively constant across different values of  $N_e$  (e.g., [Hanaki et al., 2003, 2010](#)). Figure 13 in Supplement Section C provides six HCF examples where the vertical spread in the data is relatively constant. Thus a model component to describe increasing spread in fatigue life  $N$  will usually *not* be needed (further physical explanation is given in Section 5.1). As mentioned in Section 2.7, this implies that the quantile lines will not cross. More generally, especially

when there is a vertical or horizontal asymptote, the induced fatigue distributions (life or stress) have features that agree better with the actual physical nature of fatigue.

### 3.2.2 A statistical model for fatigue-strength

Suppose that the logarithm of the fatigue-strength random variable  $X$  at a *specified* number of cycles  $N_e$  is

$$\log(X) = \log[h(N_e; \boldsymbol{\beta})] + \sigma_X \epsilon, \quad (13)$$

where  $S = h(N; \boldsymbol{\beta})$  is a positive monotonically decreasing  $S$ - $N$  regression relationship of known form,  $\boldsymbol{\beta}$  is a vector of regression parameters, and  $\epsilon$  is a random error term from a location-scale distribution with  $\mu = 0$  and  $\sigma = 1$ . Then for any specified number of cycles  $N_e$ ,  $X$  has a log-location-scale distribution with cdf

$$F_X(x; N_e) = \Pr(X \leq x; N_e) = \Phi\left[\frac{\log(x) - \log[h(N_e; \boldsymbol{\beta})]}{\sigma_X}\right], \quad x > 0, \quad N_e > 0,$$

where  $h(N_e; \boldsymbol{\beta})$  is a scale parameter and  $\sigma_X$  is the shape parameter of the distribution of  $X$ . The fatigue-strength  $p$  quantile is obtained by solving  $p = F_X(x_p(N_e); N_e)$  for  $x_p(N_e)$ , giving

$$x_p(N_e) = \exp(\log[h(N_e; \boldsymbol{\beta})] + \Phi^{-1}(p)\sigma_X), \quad 0 < p < 1, \quad N_e > 0. \quad (14)$$

### 3.2.3 The induced fatigue-life model when $\log[h(N; \boldsymbol{\beta})]$ has neither a vertical nor a horizontal asymptote

For the moment, suppose that the positive monotonically decreasing  $S$ - $N$  relationship  $S = h(N; \boldsymbol{\beta})$  has neither a vertical nor a horizontal asymptote (e.g., the Basquin model). Replacing  $N_e$  with  $N$  and  $X$  with  $S_e$  in (13) gives

$$\log(S_e) - \log[h(N; \boldsymbol{\beta})] = \sigma_X \epsilon. \quad (15)$$

In this role switching,  $N$  at specified  $S_e$  replaces  $X$  at fixed  $N_e$ , but the random variables  $X$  and  $N$  have the same  $\sigma_X \epsilon$  error term. Equation (15) implies that  $(\log(S_e) - \log[h(N; \boldsymbol{\beta})])/\sigma_X = \epsilon$  has a location-scale distribution with  $\mu = 0$  and  $\sigma = 1$ . Thus the induced cdf of  $N$  is

$$\begin{aligned} F_N(t; S_e) &= \Pr(N \leq t) = \Pr[h(N; \boldsymbol{\beta}) > h(t; \boldsymbol{\beta})] \\ &= \Pr(\log[h(N; \boldsymbol{\beta})] > \log[h(t; \boldsymbol{\beta})]) = \Pr(-\log[h(N; \boldsymbol{\beta})] < -\log[h(t; \boldsymbol{\beta})]) \\ &= \Pr(\log(S_e) - \log[h(N; \boldsymbol{\beta})] < \log(S_e) - \log[h(t; \boldsymbol{\beta})]) \\ &= \Phi\left[\frac{\log(S_e) - \log[h(t; \boldsymbol{\beta})]}{\sigma_X}\right], \quad t > 0, \quad S_e > 0. \end{aligned} \quad (16)$$

Expressions for the corresponding pdf of  $N$  (needed to compute a likelihood function) is given in (44) in Supplement Section C.5. Note that (16) is a log-location-scale distribution if and only if  $\log[h(t; \beta)]$  is a linear function of  $\log(t)$  (i.e., the Basquin model in (5)). For nonlinear  $S$ - $N$  relationships, the induced distribution for  $N$  provides a theoretically justified method for making inferences about fatigue-life distributions as a function of the fatigue-strength model parameters  $(\beta, \sigma_X)$ . The  $p$  quantile of  $N$  is obtained by solving  $F_N(t_p; S_e) = p$  for  $t_p$  giving

$$t_p(S_e) = h^{-1}(\exp[\log(S_e) - \Phi^{-1}(p)\sigma_X]; \beta), \quad 0 < p < 1, \quad S_e > 0. \quad (17)$$

### 3.2.4 The induced fatigue-life model when $\log[h(N; \beta)]$ has a horizontal asymptote

When  $\lim_{t \rightarrow \infty} \log[h(t; \beta)] = E > -\infty$ ,  $\log[h(N; \beta)]$  has a horizontal asymptote, as illustrated in Figure 5(b) and (c). Note that both axes in these plots are logarithmic so  $E = \log(0.5)$  in Figure 5(c). Because  $E$  is a lower bound for  $\log[h(N; \beta)]$ ,  $[\log(S_e) - E]/\sigma_X$  is an upper bound for  $\epsilon$ , but the range of  $\epsilon$  in (15) is  $(-\infty, \infty)$ . To resolve this inconsistency, we modify (15) and use

$$\log(S_e) = \log[h(N; \beta)] + \sigma_X \epsilon I[-\infty < \epsilon < (\log(S_e) - E)/\sigma_X],$$

where  $I[\cdot]$  is the indicator function. The cdf for  $N$  is still (16) but because  $\lim_{t \rightarrow \infty} \log[h(t; \beta)] = E$ ,

$$\lim_{t \rightarrow \infty} F_N(t; S_e) = \Phi\left(\frac{\log(S_e) - E}{\sigma_X}\right) < 1, \quad (18)$$

which implies that the cdf  $F_N(t; S_e)$  has a discrete atom of probability at  $\infty$ . The size of the discrete atom is

$$1 - \Phi\left(\frac{\log(S_e) - E}{\sigma_X}\right). \quad (19)$$

This discrete atom corresponds to the limiting proportion of units for which fatigue strength  $X > S_e$ , as  $t \rightarrow \infty$ . This can be interpreted as the proportion of units that, if tested at stress  $S_e$ , would not fail because of the fatigue limit. The quantiles  $t_p(S_e)$  are the same as in (17), but because of the discrete atom of probability at  $\infty$ ,  $t_p(S_e)$  is only finite for  $0 < p < \Phi[(\log(S_e) - E)/\sigma_X]$ .

### 3.2.5 The induced fatigue-life model when $\log[h(N; \beta)]$ has a vertical asymptote

Consider, for example, the Box–Cox  $S$ - $N$  curves in Figure 5(a) which, for  $\lambda < 0$ , have vertical asymptotes at  $B = \log(N)$ . When  $t$  decreases to  $\exp(B)$ ,  $\log[h(t; \beta)]$  is unbounded. That is,  $\lim_{t \downarrow \exp(B)} \log[h(t; \beta)] = \infty$ . The cdf is obtained as in (16) except that  $\exp(B)$  is a threshold parameter (i.e.,  $\Pr[N \leq \exp(B)] = 0$ ) and thus

$$F_N(t; S_e) = \Phi\left(\frac{\log(S_e) - \log[h(t; \beta)]}{\sigma_X}\right), \quad t > \exp(B), \quad S_e > 0. \quad (20)$$

The quantiles  $t_p(S_e)$  of  $F_N(t; S_e)$  are the same as (17) but as  $p \rightarrow 0$ ,  $t_p(S_e) \rightarrow \exp(B)$ .

The interpretation of this threshold parameter is similar to that described in Section 2.3.4. For models with a vertical asymptote, even as stress increases to high levels, there is a positive value of  $N$  that a unit could survive. Of course that positive value could be a small fraction of a cycle. Even so, it could be argued that  $S$ - $N$  relationships with a vertical asymptote are inconsistent with what happens physically. As mentioned in Section 2.3.4, however, when the asymptotic behavior occurs far outside the range where the model would be used, any inconsistency is not of practical concern.

## 4 Estimating $S$ - $N$ Model Parameters, Model-Fitting Diagnostics, and Making Inferences about Fatigue Distributions

This section briefly describes maximum likelihood and Bayesian methods for fitting  $S$ - $N$  models, estimating tail probabilities and quantiles, and computing confidence or credible intervals for quantifying statistical uncertainty (i.e., uncertainty due to limited data). Both methods are well suited to handle runouts that appear in many fatigue tests. Ordinary least squares should not be used for estimation when there are runouts.

### 4.1 Likelihood-Based Methods

Likelihood is the primary tool for making non-Bayesian inferences when using advanced statistical methods and models. The method is general, versatile, and has been widely implemented in readily available software for many different kinds of statistical models. Under mild conditions (met in the applications in this paper), likelihood methods have desirable statistical properties in large samples and are generally difficult or impossible to beat even with small samples. For example, [Severini \(2000\)](#) and [Pawitan \(2013\)](#) provide detailed descriptions of likelihood theory and methods.

#### 4.1.1 Log-likelihood for an $S$ - $N$ regression model with runouts

Typical  $S$ - $N$  data are  $(S_i, N_i, \delta_i), i = 1, \dots, n$  giving stress level  $S_i$ , number of cycles  $N_i$ , and a censoring indicator  $\delta_i$  for each of  $n$  observations. The log-likelihood for these data is

$$\mathcal{L}(\boldsymbol{\theta}) = \sum_{i=1}^n \{\delta_i \log[f_N(N_i; S_i, \boldsymbol{\theta})] + (1 - \delta_i) \log[1 - F_N(N_i; S_i, \boldsymbol{\theta})]\}, \quad (21)$$

where

$$\delta_i = \begin{cases} 1 & \text{if } N_i \text{ is a failure time} \\ 0 & \text{if } N_i \text{ is a runout time.} \end{cases}$$

Here,  $F_N(N_i; S_i, \boldsymbol{\theta})$  is the fatigue-life cdf in (3) when the fatigue-life model is specified and (16) when the fatigue-strength model is specified (and the fatigue-life model is induced). Then  $f_N(t; S_i, \boldsymbol{\theta}) =$

$dF_N(N_i; S_i, \boldsymbol{\theta})/dt$  is the corresponding pdf. Supplement Sections B.2 and C.5 give expressions for the pdfs. Standard optimization algorithms can be used to maximize  $\mathcal{L}(\boldsymbol{\theta})$ . Implementation suggestions for the nonlinear models in this paper are given in Supplement Section I.

#### 4.1.2 Methods for computing confidence intervals when using likelihood-based inference

In engineering applications, inferences are generally needed for distribution tail probabilities and distribution quantiles. For non-Bayesian inference, basing confidence intervals for these quantities on the distribution of likelihood-ratio methods is perhaps the most natural method to use. Coverage probabilities tend to be close to the specified nominal confidence level. The method is computationally complicated but not hard to implement with modern computing capabilities. Supplement Section F.3.2 outlines methods for computing likelihood-based confidence intervals for cdf and quantiles of a specified fatigue-life model. Section F.3.3 does the same for an induced fatigue-strength model. Pascual and Meeker (1999) illustrate this approach for the RFL model, but the methods described there can be applied to any of the models suggested in this paper.

Wald confidence intervals are based on a quadratic approximation to the profile log-likelihood function (Meeker and Escobar, 1995) and are generally much easier to compute. Wald intervals, however, tend to have actual coverage probabilities that are smaller than the specified nominal confidence level. Bootstrap methods (e.g., Efron and Tibshirani, 1993) provide another method of potentially improving on the Wald approximation. There are, however, many ways to map bootstrap samples into confidence intervals (e.g., Chapters 13 and 14 in Meeker et al., 2017).

#### 4.1.3 Equivalence of likelihood pointwise confidence interval bands for cdfs and quantiles

Hong et al. (2008) showed that a band of pointwise confidence intervals for a cdf (e.g., the 270 MPa cdf estimate in Figure 7(a)) are exactly the same as the band of pointwise confidence intervals for quantiles if the confidence intervals are computed using the likelihood ratio method (and approximately the same for Wald intervals). There is a similar result relating bands of confidence intervals for cdfs and quantiles for both fatigue-life and fatigue-strength distributions for the models used in this paper. Technical details are given, respectively, in Supplement Sections F.3.4 and F.3.5.

Similarly, one can use confidence intervals for fatigue-life model quantiles to obtain confidence intervals for quantiles of the corresponding fatigue-strength model. For example, the value of stress  $S_e$  for which the likelihood-based lower confidence bound  $\underline{t}_p(S_e) = N_e$  is then equivalent to  $\underline{x}_p(N_e)$ , the likelihood-based lower confidence bound for the fatigue-strength distribution at  $N_e$ . Technical details are given in Supplement Section F.3.6. The importance of this result is that one can use existing software that computes confidence intervals for fatigue-life quantiles (or probabilities) to obtain confidence intervals for fatigue-strength quantiles (or probabilities).

## 4.2 Bayesian Inference Methods

Over the past thirty years, there has been an increasing trend in the proportion of applications where Bayesian methods are used. We use Bayesian inference methods for fitting  $S$ - $N$  regression models.

### 4.2.1 Motivation for using Bayesian methods

There are several reasons for using and recommending the use of Bayesian methods for  $S$ - $N$  modeling.

- Bayesian methods, with carefully chosen noninformative or weakly informative prior distributions, generally provide credible intervals with good coverage properties.
- Bayesian methods do not rely on large sample theory. Thus, even when there are few failures, credible intervals can be trusted (as long as a valid prior distribution has been specified).
- Putting aside highest posterior density intervals (that can have practically undesirable unequal coverage probabilities for the lower and upper endpoints), there is only one way to map posterior draws into Bayesian credible intervals. This is in contrast to non-Bayesian inference, where there are many methods (e.g., likelihood and numerous Wald, and bootstrap methods).
- Bayesian methods can handle, with relative ease and modeling flexibility, complicated data-model combinations for which no maximum likelihood software exists (e.g., combinations of nonlinear relationships, random parameters, and censored data).
- Bayesian methods allow an analyst to incorporate prior information into a data analysis/modeling problem to supplement limited data, often providing important improvements in precision.

### 4.2.2 Specifying the joint prior distribution

Bayesian inference requires the specification of a joint prior distribution for the model parameters. For most applications and certainly those considered here, there is usually a desire to use minimally informative priors. [Johnson et al. \(1999\)](#) describe how they developed a partially informative prior (while trying to be minimally informative) to fit the RFL model. [Gelman et al. \(2017\)](#) outline a general strategy for specifying weakly informative priors. In our examples, we tried to adhere to the principles in these references. Supplement Section [I.1.1](#) outlines our general strategy and Supplement Section [J](#) describes, for our examples, how we arrived at our minimally informative prior distributions.

### 4.2.3 Generating and using draws from the joint posterior distribution

For the examples in this paper (and the Supplement), we use Bayesian methods to fit the  $S$ - $N$  model and to compute credible intervals for quantities of interest like lower-tail quantiles of the fatigue-life and fatigue-strength distributions. For each of the  $S$ - $N$  models that we used, a Stan ([Stan Development Team, 2022b](#)) model was written and run using the RStan ([Stan Development Team, 2022a](#)) interface to R ([R Core Team, 2022](#)). For each model fit, 20,000 draws from the joint posterior distribution were

computed and saved. Then R functions were used to post-process these draws to compute estimates and credible intervals for quantities of interest (e.g., the results in Figure 7) and residuals used for diagnostic checking (e.g., the results in Figure 8).

#### 4.2.4 Numerical methods to obtain starting values and default joint prior distributions

Robust algorithms for estimating the parameters of nonlinear regression models (using either maximum likelihood or Bayesian estimation) require careful attention to parameterization and methods for finding starting values. “Ball park” starting values can often be obtained by using simple moment estimates (e.g., sample means, variances, and linear regression). Our approach is to define a parameterization where all parameters are unrestricted without any ordering relationships. Optimizers tend to perform best with such a parameterization and flat priors provide a natural default joint prior distribution. In some applications, it is necessary to replace the flat prior with an approximately flat normal (Gaussian) distribution with an extremely large standard deviation (e.g., 10 times the standard error obtained from maximum likelihood estimation). Exactly how these ideas are implemented depends on the particular model. Supplement Section I gives details for the models used in our examples.

### 4.3 Using Residuals as Model-Checking Diagnostics

Although probability plots like those in Figures 2, 3(b), 4(b), and especially 7(b) are useful for detecting departures from the assumed model, such plots are available only when experiments result in data with many observations at each of some number of stress levels. Frequently  $S$ - $N$  data have many stress levels with few repeats. In such cases, residuals can be computed and these can be displayed in various ways to see if they depart from what is expected under the assumed model.

Plotting residuals helps detect departures from model assumptions and should be part of any regression analysis. Most regression textbooks provide detailed guidance on how to do residual analysis, usually focused on graphical display of the residuals. [Nelson \(1973\)](#) describes regression analysis methods for censored data. The key idea is that the residual for a censored observation is correspondingly censored.

Here, residuals are defined as estimates of the  $\epsilon$  error variable in models such as (2) and (13). Such residuals are generally known as *standardized residuals* and should behave approximately like independent identically distributed observations with constant spread from the assumed distribution.

Scatter plots of the residuals versus other variables, such as the fitted values, stress, or other explanatory variables, and potential explanatory variables (e.g., test order and heat or batch) are useful. Systematic dependence of the residuals on any such variable or systematic change in spread versus such variables indicates a departure from the assumed model. Special symbols (e.g., an upward-pointing triangle) should be used to plot censored residuals. Heavy censoring can make residual scatter plots difficult to interpret ([Nelson, 1973](#)). For  $S$ - $N$  data, most censoring occurs at the lowest stress levels so scatter plots can detect model departures. Suppose no serious departures are detected in such scatter plots. In that case, probability plots of the residuals can be used to check the adequacy

of the assumed distribution of the  $\epsilon$  error variable. In addition to checking the model fit for individual fitted models, we have found that comparing residual plots for across different fitted models for the same data to be particularly useful. Supplement Section D gives a particular example.

Based on the *specified fatigue-life* regression model in (2), the standardized residuals (estimates of the  $\epsilon_i$  error for observation  $i$ ) are

$$\hat{\epsilon}_i = \frac{\log(N_i) - \log[g(S_i; \hat{\beta})]}{\hat{\sigma}_N}, \quad i = 1, \dots, n.$$

When there is a loglinear model for  $\sigma_N$ , as described in Section 2.3.5, the standardized residuals are

$$\hat{\epsilon}_i = \frac{\log(N_i) - \log[g(S_i; \hat{\beta})]}{\exp[\hat{\beta}_0^{[\sigma_N]} + \hat{\beta}_1^{[\sigma_N]} \log(S_i)]}, \quad i = 1, \dots, n. \quad (22)$$

Based on the *specified fatigue-strength* regression model in (13), the standardized residuals are computed from

$$\hat{\epsilon}_i = \frac{\log(S_i) - \log[h(N_i; \hat{\beta})]}{\hat{\sigma}_X}, \quad i = 1, \dots, n.$$

Then the  $\exp(\hat{\epsilon}_i)$  values should, if the assumed model is adequate, behave approximately like an independent, identically distributed (iid) sample from the assumed log-location-scale distribution.

Fatigue-life fitted values, a function of stress  $S$ , are defined as estimates of the median lifetime  $t_{0.50}(S)$ . Fatigue-strength fitted values, a function of the number of cycles  $N$ , are defined as estimates of the median strength  $x_{0.50}(N)$ . Because of the equivalence of fatigue-life and fatigue-strength quantile curves (as shown in Section F.1 in the Supplement), the functions  $t_{0.50}(S)$  and  $x_{0.50}(N)$  map out the same curve. For reasons described in Supplement Section J.2.4, it is better to plot residuals versus fatigue-life fitted values rather than fatigue-strength fitted values.

**Example 4.1 Residual Analysis for the Laminate Panel Box–Cox-Loglinear- $\sigma_N$  S-N Model.** This is a continuation of Example 2.2 where the Box–Cox-loglinear- $\sigma_N$  S-N model was fit to the laminate panel data. Figure 8(a) is a plot of the lifetime residuals versus stress, showing one column of residuals for each of the five stress levels. The residuals for stress levels between 280 and 380 have similar distributions, indicating that there is no evidence of model inadequacy. There were eight runouts at  $S = 270$  MPa and this is the reason that column is so short. ■

#### 4.4 Tolerance Bounds Versus Credible/Confidence Intervals for Quantiles

After an S-N model has been chosen and fit to the available data, the results are used by engineers in different ways. For many applications, estimates and confidence intervals for lower-tail quantiles of the fatigue-life distribution (at specified  $S_e$ ) and/or the fatigue-strength distribution (at specified  $N_e$ ) are of particular interest.

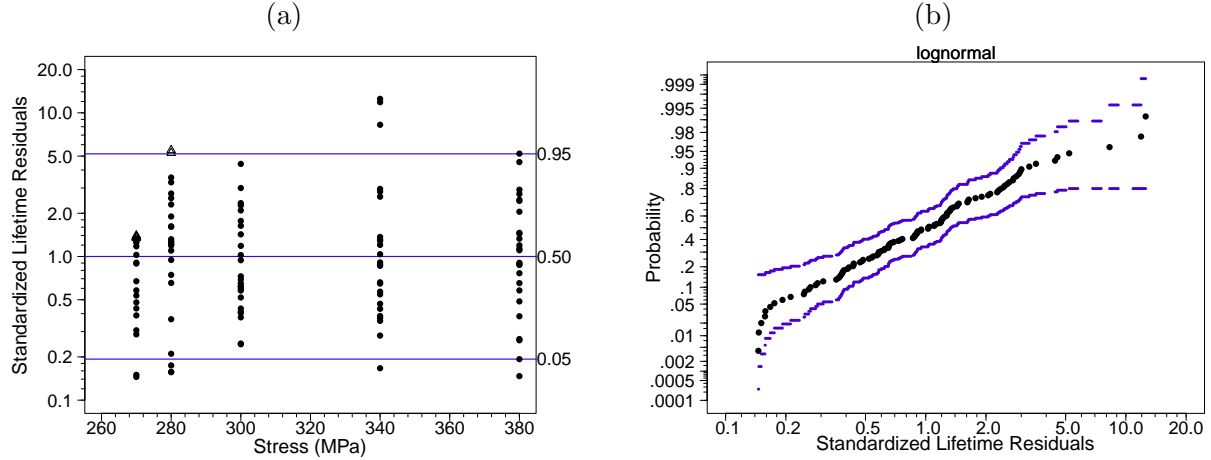


Figure 8: Fatigue-life residuals from the Box–Cox-Loglinear- $\sigma_N$   $S$ - $N$  model fit to the laminate panel data versus stress (a) and lognormal probability plot (b).

In some parts of the  $S$ - $N$  data modeling literature, there is discussion of lower one-sided tolerance bounds of the fatigue-life and/or the fatigue-strength distributions, which are sometimes called one-sided tolerance intervals (intervals, by definition, have two endpoints and having an infinite endpoint does not help explanation or understanding). As described in [Meeker et al. \(2017, Section 2.4.2\)](#), a one-sided lower  $100(1 - \alpha)\%$  confidence bound on the  $p$  quantile of a distribution is equivalent to a one-sided lower tolerance bound that one can claim, with  $100(1 - \alpha)\%$  confidence, is exceeded by at least a proportion  $1 - p$  of that distribution. In our pedagogical experience, engineers and other practitioners often confuse the  $100(1 - \alpha)\%$  confidence level with the  $1 - p$  exceedence probability of a tolerance bound but that the concept of a small- $p$  lower-tail quantile is easier to separate from the confidence level.

It is common to report (and most statistical software only provides) two-sided confidence intervals for specified quantiles. Note that the lower endpoint of a two-sided  $100(1 - \alpha)\%$  confidence interval can be interpreted as a one-sided lower  $100(1 - \alpha/2)\%$  confidence bound (e.g., the endpoints of a two-sided 90% confidence interval are one-sided 95% confidence bounds). A two-sided interval on a quantile, relative to a one-sided bound, provides more information. For a quantile in the lower tail of a fatigue-life or a fatigue-strength distribution, the lower bound tells how bad things might be; the upper bound tells *how good things might be*.

The relationship between one-sided confidence (credible) bounds and two-sided intervals presumes that the procedures provide, at least approximately, equal error probabilities for each tail and this is the reason that percentile credible intervals are recommended (as opposed to highest posterior density) and that simulation-based confidence intervals (e.g., Chapters 13 and 14 in [Meeker et al., 2017](#)) should calibrate each endpoint separately.

## 5 Other $S$ - $N$ Regression Relationships and Modeling Examples

Section 2 introduced three, relatively simple,  $S$ - $N$  regression relationships. Many other such relationships have been suggested. This section, while not exhaustive, describes several other  $S$ - $N$  relationships, illustrates how they fit within our modular framework, and illustrates the use of two of these relationships with the Ti64 and nitinol data that were introduced in Section 1.3.

### 5.1 Physical Explanation of the Curvature and Nonconstant Spread in $S$ - $N$ Data

Figures 3(a) and 4(a) are examples of  $S$ - $N$  data with strong curvature when plotted on log-log axes. Materials will exhibit this curvature differently depending on the damage accumulation mechanisms that are activated by cyclic loading. Curvature in the  $S$ - $N$  curve demonstrates that the rate of damage accumulated per cycle has a strong dependence on the magnitude of the load amplitude. Curvature will be greatest at load levels where the material transitions between micro-mechanical deformation regimes. A well documented example of this phenomena is the transition between elasto-plastic and purely elastic deformation in high-strength metallic materials. The  $S$ - $N$  relationship tends to be approximately linear (on log-log scales) when cycling is causing cyclic elasto-plastic deformation, but as one moves to lower stress/strain levels, the deformation becomes purely elastic leading to much longer life and this results in the concave-up curvature.

As noted in Section 3.2.3 (also see Example 2.1 and Figure 6) when the  $S$ - $N$  relationship is linear on log-log axes (i.e., the Basquin model) with  $\sigma_X$  not depending on  $N_e$ , the induced fatigue-life distribution will belong to the same family as the fatigue-strength distribution and will have constant spread. When, however, the  $S$ - $N$  relationship has the usual concave-up curvature described in the previous paragraph, the induced fatigue-life distribution will have increasing spread as stress/strain decreases. Technical details for this result are given in Supplement Section F.2. This behavior will be illustrated in Examples 5.1 and 5.2 (and corresponding Figures 9 and 11).

### 5.2 The Modified Bastenaire $S$ - $N$ Relationship

The original Bastenaire (1972) relationship is

$$N = g(S; \beta) = \frac{A \exp[-C(S - E)]}{S - E}.$$

As illustrated in Figure 5(b), this model has been modified (e.g., in ISO, 2012; Hauteville et al., 2022) to have more flexibility by adding a fourth parameter giving

$$N = g(S; \beta) = \frac{A \exp\left(-\left[\frac{S - E}{B}\right]^C\right)}{S - E}.$$

### 5.3 The Rectangular Hyperbolic $S$ - $N$ Relationship

The rectangular hyperbolic  $S$ - $N$  relationship can be written as

$$[\log(N) - B][\log(S) - E] = C,$$

where  $B$  is a vertical asymptote,  $E$  is a horizontal asymptote, and  $C$  controls how fast the  $S$ - $N$  curve approaches the respective asymptotes. All of these parameters are defined on the log-log scales that are used in this paper to display  $S$ - $N$  relationships. Supplement Figure 14(d) illustrates this relationship. For purposes of specifying a fatigue-strength model that can be used to induce a fatigue-life model and likelihood, the relationship can be expressed as

$$S = h(N; \boldsymbol{\beta}) = \exp \left[ \frac{C}{\log(N) - B} + E \right].$$

Model features that arise from the asymptotes depend on whether the fatigue-life model is specified (see Sections 2.4.2 and 2.4.3) or the fatigue-strength model is specified (see Sections 3.2.4 and 3.2.5).

### 5.4 The Nishijima $S$ - $N$ Hyperbolic Relationship

The Nishijima hyperbolic  $S$ - $N$  relationship (Nishijima, 1980, 1985), illustrated in Figure 5(c), is

$$[\log(S) - E][\log(S) + A \log(N) - B] = C.$$

where the regression parameters are  $\boldsymbol{\beta} = (A, B, C, E)$ . The parameters  $A$  and  $B$  are, respectively, the negative of the slope and the  $\log(N) = 0$  intercept of the large- $S$  asymptote;  $E$  is the horizontal asymptote;  $\sqrt{C}$  is the vertical distance between the  $S$ - $N$  curve and the point where the two asymptotes intersect (all on the log-log scales of the plot). For purposes of specifying a fatigue-strength model that can be used to induce a fatigue-life model, the relationship can be expressed as

$$S = h(N; \boldsymbol{\beta}) = \exp \left( \frac{-A \log(N) + B + E + \sqrt{[A \log(N) - (B - E)]^2 + 4C}}{2} \right). \quad (23)$$

**Example 5.1 Fitting the Nishijima/Lognormal Model to the Ti64  $S$ - $N$  Data.** This example is a continuation of Example 1.2. A description of the noninformative/weakly informative prior distributions that were used, additional residual plots, and other details are in Supplement Section J.2. The Nishijima hyperbolic regression model (23) was fit to the data under the assumption that fatigue strength has a lognormal distribution with a constant shape parameter  $\sigma_X$ . The induced fatigue-life model (Section 3.2.4) was used to define the log-likelihood in (21). Figure 9(a) is a lognormal probability plot showing, as symbols, the nonparametric estimate of fraction failing as a function of cycles and the corresponding regression-model estimates. The agreement is good. The early failures at 60 ksi deviate from the regression-model estimate but given the large amount of variability

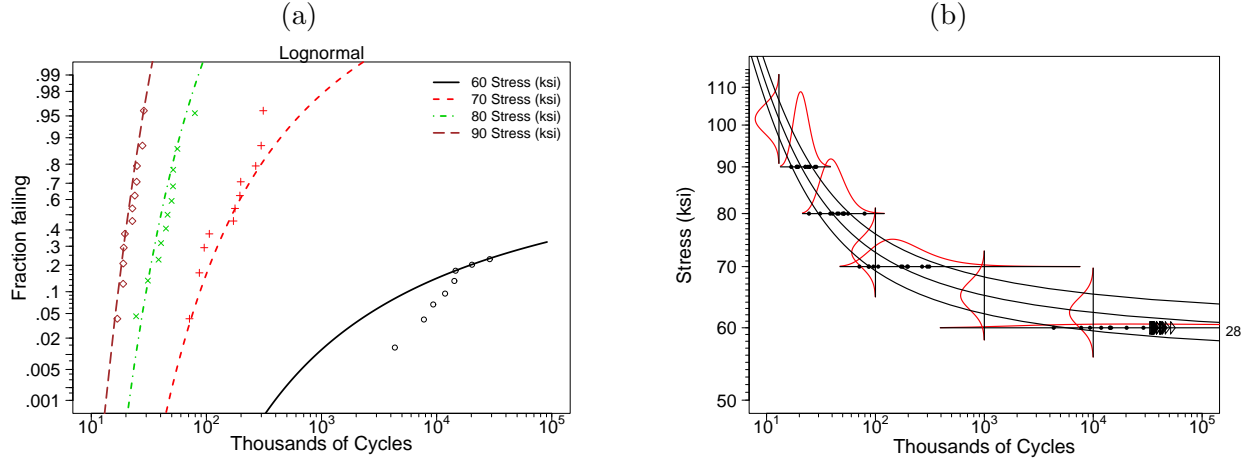


Figure 9: Lognormal probability plot showing the fatigue-life cdf estimates from the Nishijima model fit to the Ti64  $S$ - $N$  Data (a) and the corresponding model plot showing 0.10, 0.50, and 0.90 quantile curves and densities for fatigue strength (vertical) and fatigue life (horizontal) (b).

in small order statistics, this kind of deviation is consistent with the fitted model. As described in Section 3.2.4, the induced fatigue-life cdf (17) will level off to  $\Phi_{\text{norm}}([\log(S_e) - \bar{E}]/\hat{\sigma}_X)$  for large values of  $t$ . At 60 ksi, this limiting failure probability is (using point estimates from Supplement Section J.2)  $\Phi_{\text{norm}}([\log(60) - 4.039]/0.036) = 0.938$ . Figure 9(b) shows the fitted model superimposed on the same data in Figure 3(a). Note the vertical fatigue-strength densities with constant  $\hat{\sigma}_X = 0.036$  and the horizontal induced fatigue-life densities with increasing spread at lower stress levels. The residual plots

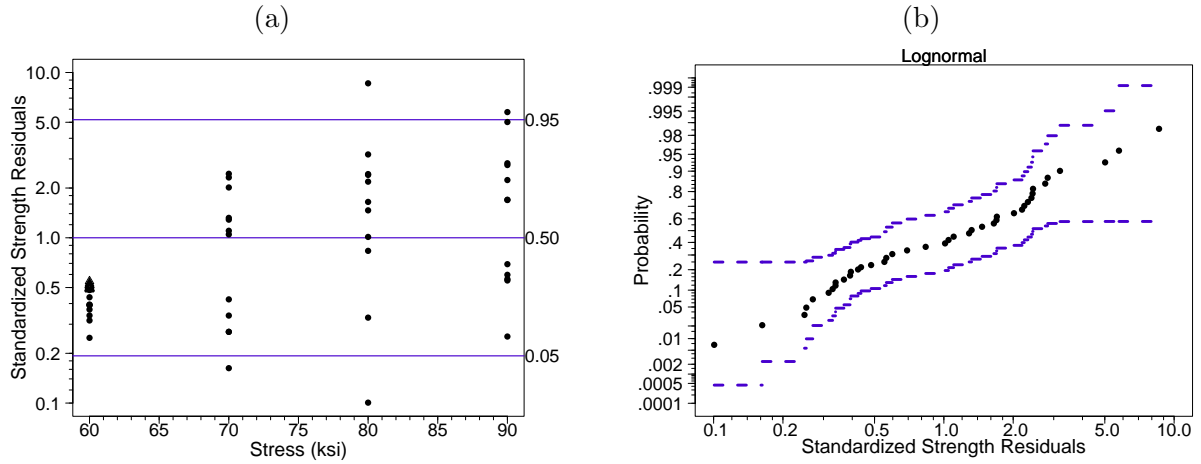


Figure 10: Fatigue-strength residuals from the Nishijima  $S$ - $N$  model fit to the Ti64 data versus stress (a) and lognormal probability plot (b).

in Figure 10 do not suggest departures from the assumed model. ■

## 5.5 The Coffin–Manson Relationship

The Coffin–Manson relationship (e.g., pages 748–754 in [Dowling, 2013](#)) is widely used to model fatigue-life data in strain-controlled experiments (but can also be used to describe  $S$ - $N$  data from stress-controlled experiments). For this model, fatigue life  $N$  and applied stress (or strain)  $S$  are related through the relationship

$$S = h(N; \boldsymbol{\beta}) = A_{el}(2N)^b + A_{pl}(2N)^c. \quad (24)$$

This relationship is illustrated in Figure 5(d). The terms  $A_{el}(2N)^b$  and  $A_{pl}(2N)^c$  represent separate Basquin relationships for the elastic and the plastic strain regimes. Here  $A_{el}$ ,  $A_{pl}$ ,  $b$ , and  $c$  are material-property parameters to be estimated from  $S$ - $N$  data. In particular,  $A_{el}$  and  $A_{pl}$  are the intercepts of the lines  $A_{el}(2N)^b$  and  $A_{pl}(2N)^c$ , respectively, when they are plotted on log-log axes;  $b$  and  $c$  are the corresponding slopes (note that the intercepts are defined as the value of strain at one half of a cycle when the response is in units of cycles). The sum of these lines provides a relationship with concave-up curvature commonly seen in  $S$ - $N$  data plotted on log-log scales.

**Example 5.2 Fitting the Coffin–Manson/Lognormal Model to the Superelastic Nitinol  $S$ - $N$  Data.** This example is a continuation of Example 1.3. A description of the noninformative/weakly informative prior distributions that were used, additional residual plots and other details are in the Supplement Section [J.3](#). The model fitting and likelihood construction and resulting plots are similar

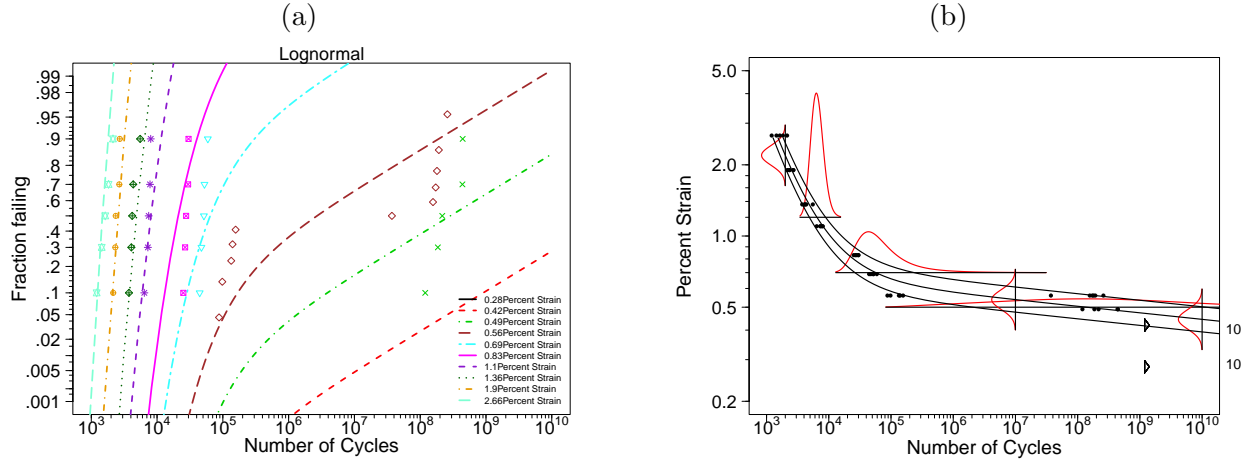


Figure 11: Lognormal probability plot showing the cdf estimates from the Coffin–Manson model fit to the nitinol  $S$ - $N$  Data (a) and the corresponding model plot showing 0.10, 0.50, and 0.90 quantile curves and densities for fatigue life (horizontal) and fatigue strength (vertical) (b).

to those described in Example 5.1, except that the Coffin–Manson  $S$ - $N$  relationship  $S = h(N; \boldsymbol{\beta})$  is defined by (24) and, because there is neither a horizontal nor a vertical asymptote, the induced fatigue-life model is given by (16) in Section 3.2.3. Figure 11(a) is a lognormal probability plot similar to Figure 4(b) but with the Coffin–Manson/lognormal regression model cdf estimates plotted for the eight

levels of strain. Interestingly, the upper tails of the plotted cdfs are linear, implying that the upper tail of the distributions behave like a lognormal distribution, in contrast to the horizontal asymptote in the Nishijima model illustrated in Figure 9(a).

The bimodality at 0.56% strain stands out again and is highly influential, inflating the estimate of spread in the induced fatigue-life distributions at the lower levels of strain and leading to lack of fit at the lower levels of strain (i.e., below 0.56% strain). [Weaver et al. \(2022\)](#) fit a mixture model to these nitinol data to accommodate the bimodality. Consideration of such a model is beyond the scope of this paper but is mentioned as an area for future research in Section 6.

Figure 11(b) shows the same data as Figure 4(a) but now has the 0.10, 0.50, and 0.90 quantile lines and estimated densities superimposed. Engineers demonstrating the reliability of an artificial heart valve would typically be interested in the 0.10 quantile of the fatigue-strength distribution at 600 million cycles (15 years). For the nitinol data, the marginal posterior draws of 0.10 quantile of the lognormal strength distribution at  $N_e = 600,000,000$  cycles is computed using (14) and these provide the point estimate 0.425 and a 95% credible interval [0.398, 0.449] in percent strain.

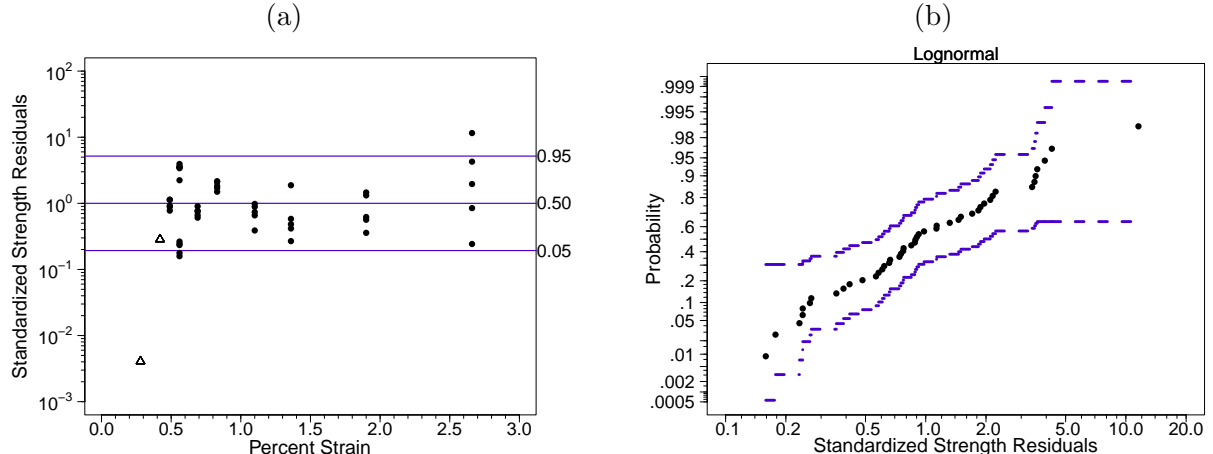


Figure 12: Fatigue-strength residuals from the Coffin–Manson  $S$ - $N$  model fit to the nitinol data versus strain (a) and lognormal probability plot (b).

Figure 12(a) plots the standardized residuals of the fatigue-strength distribution computed from (22) versus % strain. The bimodality can be seen in the two clusters of residuals at 0.56% strain. Other single clusters can be seen at 0.49, 0.69, and 0.83% strain. The small spread within these clusters suggests, in comparison with the overall spread in the residuals, that the residuals are not an iid sample. Such dependence could be due to lack of randomization with respect to factors like batch, test-machine effects, or the location of specimen wires cut from the spools. Figure 12(b) is a lognormal probability plot of the same residuals showing that the lognormal distribution fits well. ■

## 5.6 The Random Fatigue-Limit Model

Pascual and Meeker (1999) extended the Stromeier model (Section 2.3.3) by allowing the fatigue-limit  $\gamma$  to vary from unit to unit. The Random Fatigue-Limit (RFL) model describes both the curvature and the increased variability at lower stress levels when plotting  $S$ - $N$  data on log-log scales.

### 5.6.1 The RFL fatigue-life model

For stress  $S_e$  conditional on a fixed value of  $\gamma > 0$ ,

$$F_{N|\gamma}(t; S_e | \gamma) = \Pr(N \leq t; S_e | \gamma) = \Phi\left(\frac{\log(t) - \mu(S_e, \gamma)}{\sigma_\epsilon}\right), \quad t > 0, S_e > 0,$$

where  $\Phi$  is the standard location-scale distribution cdf corresponding to the conditional log-location-scale distribution for  $N$  (i.e.,  $N|\gamma$ ) and  $\mu(S_e, \gamma) = \beta_0 + \beta_1 \log(S_e - \gamma)$ . Then the unconditional distribution of  $N$  is obtained by averaging over the distribution of  $\log(\gamma)$

$$F_N(t; S_e) = \Pr(N \leq t; S_e) = \int_{-\infty}^{\log(S_e)} \frac{1}{\sigma_{\log(\gamma)}} \Phi\left(\frac{\log(t) - \mu(S_e, \nu)}{\sigma_\epsilon}\right) \phi_\gamma\left(\frac{\nu - \mu_{\log(\gamma)}}{\sigma_{\log(\gamma)}}\right) d\nu, \quad t > 0, S_e > 0, \quad (25)$$

where  $\phi_\gamma$  is the standard location-scale distribution pdf corresponding to the log-location-scale distribution of  $\gamma$ , and the parameters of the model are  $\boldsymbol{\theta} = (\beta_0, \beta_1, \sigma_\epsilon, \mu_{\log(\gamma)}, \sigma_{\log(\gamma)})$ . Pascual and Meeker (1999) illustrated all combinations Weibull and lognormal distributions for  $N|\gamma$  and  $\gamma$ .

### 5.6.2 The RFL fatigue-strength model

As with most other fatigue-life models for  $S$ - $N$  data, the RFL model can be used to define a distribution of fatigue strength  $X$  for a specified value of  $N_e$ . Similar to what was done in Sections 2.4 and 3.2, replacing  $t$  with  $N_e$  and  $S_e$  with  $x$  in the integral of (25) gives

$$F_X(x; N_e) = \Pr(X \leq x; N_e) = \int_{-\infty}^{\log(x)} \frac{1}{\sigma_{\log(\gamma)}} \Phi\left(\frac{\log(N_e) - \mu(x, \nu)}{\sigma_\epsilon}\right) \phi_\gamma\left(\frac{\nu - \mu_{\log(\gamma)}}{\sigma_{\log(\gamma)}}\right) d\nu. \quad (26)$$

Interestingly, as  $N_e \rightarrow \infty$  in (26), the cdf in the integrand approaches one and the cdf of fatigue strength  $X$  approaches the cdf of the random fatigue-limit  $\gamma$ . There are no closed-form expressions for the quantiles of the RFL model fatigue-life or fatigue-strength distributions but they can be readily computed by numerically inverting the cdfs.

## 5.7 The Castillo et al. $S$ - $N$ Model

Castillo et al. (e.g., in Castillo et al., 1985, Castillo and Galambos, 1987, Castillo et al., 2008, Castillo and Fernández-Canteli, 2009, and Equation (2) of Castillo et al., 2019) suggest an  $S$ - $N$  model based

on the rectangular hyperbolic  $S$ - $N$  relationship and a three-parameter Weibull distribution given by

$$F(t, x) = 1 - \exp \left\{ - \left[ \frac{[\log(t) - B][\log(x) - E] - \gamma}{\eta} \right]^\beta \right\} \quad (27)$$

with parameters  $\boldsymbol{\theta} = (B, E, \gamma, \eta, \beta)$  where  $B$  is a vertical asymptote for log fatigue life (i.e., minimum value for  $\log(N)$ ),  $E$  is a horizontal asymptote for log fatigue strength (i.e., a fatigue-limit and minimum value for  $\log(X)$ ), and  $\gamma$ ,  $\eta$ , and  $\beta$  are related to the Weibull distribution parameters. Their model derives from what they call a “compatibility condition,” which implies that the fatigue-life and the fatigue-strength quantile curves coincide, as described for our (different) models in Section 2.4.4.

Replacing  $x$  with  $S_e$ , (27) can be interpreted as the cdf for fatigue life  $N$  at a specified level of stress  $S_e$ . That is,

$$\begin{aligned} F_N(t; S_e) &= \Pr(N \leq t; S_e) = F(t, S_e) \\ &= 1 - \exp \left\{ - \left[ \frac{[\log(t) - B][\log(S_e) - E] - \gamma}{\eta} \right]^\beta \right\}, \end{aligned}$$

where  $t > \exp(B + \gamma/[\log(S_e) - E])$  and  $S_e > \exp(E)$ . Similarly, replacing  $t$  with  $N_e$ , (27) can be interpreted as the cdf for fatigue strength  $X$  at a specified number of cycles  $N_e$ . That is,

$$\begin{aligned} F_X(x; N_e) &= \Pr(X \leq x; N_e) = F(N_e, x) \\ &= 1 - \exp \left\{ - \left[ \frac{[\log(N_e) - B][\log(x) - E] - \gamma}{\eta} \right]^\beta \right\}, \end{aligned}$$

where  $x > \exp(E + \gamma/[\log(N_e) - B])$  and  $N_e > \exp(B)$ . Expressions for the Weibull parameters, quantile functions for  $N$  and  $X$ , and a plot of the quantile curves are given in Supplement Section H.

## 5.8 A Comparison and Operational Considerations for Choosing an $S$ - $N$ Model

Table 1 provides a summary of several  $S$ - $N$  models that fit within our modular framework and that we have either used in our examples or that are commonly used in the fatigue literature. The table is not meant to be an exhaustive list, but a sampling of the alternative models that are available. Broadly, there are two categories of models, depending on whether the fatigue-life or the fatigue-strength model is specified. Technically, any suitable  $S$ - $N$  relationship (such as those given in Sections 2.4, 2.3, and 5.2–5.5) could be used by specifying either the fatigue-life or the fatigue-strength model (and having the other be induced). The specification of Life or Strength given in the third column of Table 1 corresponds to the specification that we expect would be most useful given the properties of the resulting  $S$ - $N$  models and our experience with analyzing various  $S$ - $N$  data sets.

As part of our research, beyond the three examples presented in the paper, we fit the Basquin, Box–Cox-loglinear- $\sigma_N$ , Nishijima, Coffin–Manson, and RFL models to 18 different  $S$ - $N$  data sets (and other models to a smaller number of data sets) covering a wide range of materials, specimen types,

Table 1: Summary of Selected Models for  $S$ - $N$  Data

Model	# Param.	Model Specified for Fatigue	Vertical Asymptote for Large $S$	Horizontal Asymptote for Large $N$	Curvature and Nonconstant Spread
Basquin (inverse-power)	2+1=3	Life	No	No	No
Box–Cox-loglinear- $\sigma_N$	3+2=5	Life	Yes	No	Yes
Stromeyer-loglinear- $\sigma_N$	3+2=5	Life	No	Yes	Yes
Box–Cox	3+1=4	Strength	Yes	No	Yes
Stromeyer	3+1=4	Strength	No	Yes	Yes
Nishijima hyperbolic	4+1=5	Strength	No	Yes	Yes
Coffin–Manson	4+1=5	Strength	No	No	Yes
Bastenaire	3+1=4	Strength	No	Yes	Yes
Modified Bastenaire	4+1=5	Strength	No	Yes	Yes
Rectangular hyperbolic	3+1=4	Strength	Yes	Yes	Yes
Castillo et al.	3+2=5	Both	Yes	Yes	Yes
Random fatigue-limit	3+2=5	Life	No	Yes	Yes

The number of parameters in the # Param. column is the sum of the number of parameters in the  $S$ - $N$  relationship and those that describe variability in the statistical model.

and sample sizes. Based on those experiences and our knowledge of the nature of the different models, the remainder of this section provides recommendations on how to choose which model or models to use in a particular situation (as in most statistical modeling applications, it is generally important to fit and compare different models).

Key features of the various models are the existence (or not) of coordinate (i.e., vertical or horizontal) asymptotes in the  $S$ - $N$  relationship and the way that variability (including changes in variability as a function of stress) is described. Supplement Figure 14 illustrates the fitting of four  $S$ - $N$  models, with different combinations of the existence of asymptotes or not, to a version of the nitinol data. Figure 15 provides corresponding plots of the residuals versus strain. Plots like these helped inform the following discussion.

### 5.8.1 Models with no coordinate asymptotes

Because of its simplicity, the Basquin (inverse-power rule) statistical model (Section 2.3.2 and Figure 6) is the most common model fit to  $S$ - $N$  data and it is appropriate when testing is done at relatively high stress levels (plastic range) where the relationship between log-life and log-stress is approximately linear with constant spread. Such tests are frequently conducted to compare fatigue-life distributions for factors such as different treatments, test conditions like temperature or frequency, formulations of product materials, or different mechanical designs. When units are tested at high stress levels to estimate fatigue-life at lower stress levels (accelerated testing), the Basquin model will provide conservative estimates of low-stress fatigue-life quantiles, relative to models that describe the concave-up curvature typically seen at low stress levels (e.g., Examples 19.11–19.14 in [Meeker et al., 2022](#)).

The Coffin–Manson relationship (Section 5.5 and Figure 5(c)) is appropriate when there is curvature in the  $S$ - $N$  data plotted on log-log axes but no evidence for the existence of a fatigue limit. When used with a specified fatigue-strength distribution with constant  $\sigma_X$  (as suggested in Falk (2019) and as we recommend), the model describes the increase in spread at lower stress levels.

### 5.8.2 Models with a horizontal asymptote

The Stromeier (Section 2.3.3), Bastenaire (Section 5.2 and Figure 5(b)), Nishijima (Section 5.5 and Figure 5(d)), and the Random fatigue-limit (Section 5.6)  $S$ - $N$  models all have a horizontal asymptote that suggests the possible existence of a fatigue limit. A fatigue limit does not have to exist to use these models, as long as the model fits well and there is no extrapolation in stress. In such cases, the model provides valid inferences for lower-tail quantiles of the fatigue-life and fatigue-strength distributions. For  $S$ - $N$  data with the common concave-up shape when plotted on log-log axes, we found the properties of the induced fatigue-life model (for a specified fatigue-strength model with constant  $\sigma_X$ ) have better agreement with physical reality (also see Section 3.2.4) when compared to a specified fatigue-life model.

### 5.8.3 Models with a vertical asymptote

The Box–Cox model (Section 2.3.4 and Figure 5(a)) has a vertical asymptote. The rectangular hyperbolic model (Section 5.3 and Supplement Figure 14(d)) and the Castillo et al. model (Section 5.7 and Supplement Figure 19) have both vertical and horizontal asymptotes. The vertical asymptote is related to some interesting features of these models. First, the asymptote is related to the smallest number of cycles where a failure could occur, even as stress amplitude approaches infinity. Second (as noted, for example, in Section 4 of Toasa Caiza and Ummenhofer, 2018), the shape of the  $S$ - $N$  relationship does not agree with the most commonly seen behavior of  $S$ - $N$  data at higher stress levels. Finally, as shown in Supplement Figure 19, for small values of  $N_e$ , the spread in the induced distribution of fatigue strength  $X$  can increase dramatically. As described in Section 2.3.4, these issues are not of concern if this asymptotic behavior occurs outside the range where the model would be used (e.g., Figure 7(b)).

## 6 Concluding Remarks and Areas for Future Research

This paper outlines a modular framework for specifying, fitting, checking statistical models for  $S$ - $N$  fatigue data. The framework includes most of the  $S$ - $N$  relationships previously suggested in the fatigue literature. We illustrated the use of flexible Bayesian methods with noninformative or weakly informative prior distributions to estimate fatigue-life and fatigue-strength models. We illustrated the methods using  $S$ - $N$  /  $e$ - $N$  data from three different materials and specimen types and described our experiences with many other data sets and types of materials.

When modeling  $S$ - $N$  data, how should one choose whether to specify the fatigue-life model (resulting in an induced fatigue-strength model) or specify a fatigue-strength model (resulting in an induced fatigue-life model)? Given the manner in which it naturally describes increasing spread at lower stress levels (as explained in Section 5.1), especially in HCF applications, and other reasons given in Section 3.2.1, we strongly favor the approach that specifies the fatigue-strength model (Examples 5.1 and 5.2). What reasons are there to continue to use the approach that specifies the fatigue-life model (Example 2.2)? It is traditional, widely known, and software is readily available. We see no other advantages.

The following are areas where further research is needed.

- There is a need to develop practical methods for designing statistically efficient experiments to obtain  $S$ - $N$ / $e$ - $N$  data (how many and which levels of stress, number of specimens, and how to allocate them to stress levels). Although existing results for planning accelerated life tests (e.g., Chapter 6 in [Nelson, 2004](#)) may provide insight, there are important differences. Often there is no need to extrapolate in stress (although there may be extrapolation into the lower tails of both the fatigue-life and the fatigue-strength distributions). Depending on the application, inferences are generally needed for fatigue life over a range of stress values or fatigue-strength quantiles at particular points in time. Tools to quantify estimation precision for these quantities for proposed experimental designs are needed. [King et al. \(2016\)](#) describe such work for estimating fatigue-life distributions for a particular fatigue-life model. Their methods could be extended to focus on fatigue-strength distributions and other models.
- Our modeling has focused on experiments in which stress (or strain) *amplitude* is the experimental variable. Mean stress (or equivalently, the min/max stress ratio), temperature, cycling frequency, and surface condition/treatments are additional factors that are often studied in fatigue experiments. For example, [Pascual \(2003\)](#) and [King et al. \(2016\)](#) illustrate the use of such multiple explanatory variable fatigue modeling. The models and methods presented in this paper can be readily extended to allow for such additional explanatory variables.
- In experimental studies, it is important to understand and take account of important sources of variability. In fatigue testing, batch-to-batch (also called heat-to-heat or blend-to-blend) variability can be importantly large. Traditionally, careful experimenters would test the same number of specimens from each heat at each stress level. This equally represents the heats across the stress levels. [Nelson \(1984\)](#) provides an example and shows how to assess, graphically, whether there is heat-to-heat variability. A more quantitative approach would be needed to assess statistical significance of suspected batch-to-batch variability and assess whether efforts to reduce variability are successful. The methods presented in this paper could be readily extended to model batch-to-batch variability, in a manner similar to that used in [Meeker et al. \(2022, Section 23.4\)](#) to describe batch-to-batch variability in an accelerated life test.
- We have seen numerous examples of  $S$ - $N$ / $e$ - $N$  data where there is a bimodal distribution of

lifetimes (e.g., in the nitinol example presented here), usually at an intermediate level of stress (or strain). Various explanations have been suggested for this phenomenon. These include material defects (similar to multiple failure modes) and batch-to-batch variability. Appropriate models to describe such behavior need to be developed. [Weaver et al. \(2022\)](#) give an example of such a model.

- There is extensive existing knowledge of material properties. For example, [Dowling \(2013, page 751\)](#) provides a table containing nominal values for the parameters of the Coffin–Manson model for different materials. [MMPDS \(2021\)](#) contains a large amount of information about materials properties for different alloys that used in aerospace applications. This kind of information, combined with general engineering principles, could be used to help inform prior distributions for estimating the parameters of  $S$ - $N$  models.

## Acknowledgments

We would like to thank Charles Annis, Necip Doganaksoy, Woong Kim, Larry Leemis, Lu Lu, Wayne B. Nelson, and Peter Parker for providing helpful comments on a previous version of our paper. We would also like to thank Professors Enrique Castillo and Alfonso Fernández-Canteli for helping us to understand some aspects of their approach to modeling fatigue data.

## A Overview of the Supplementary Materials

The purpose of this supplement is provide additional technical details including derivations, additional examples, simulation results, and other technical details. Some of these details will be especially useful for those who want to write their own software to implement the methods described in the main paper.

This supplement is organized as follows. Section [B](#) provides additional technical details (beyond what is in the main paper) for  $S$ - $N$  regression models where the fatigue-life model is specified and the fatigue-strength model is induced. Section [C](#) provides additional technical details for  $S$ - $N$  regression models where the fatigue-strength model is specified and the fatigue-life model is induced. Section [D](#) compares the different basic  $S$ - $N$  model shapes and illustrates the importance of using residual analysis to help compare and choose such an  $S$ - $N$  relationship. Section [E](#) compares lognormal and Weibull probability plots for nine  $S$ - $N$  data sets based on fatigue tests for nine different materials and specimen types. Section [F](#) provides proofs of some of the technical results stated in the min paper. Section [G](#) describes an algorithm to compute the fatigue-strength distribution from the fatigue-life distribution when no closed-form expression is available. Section [H](#) provides, for the Castillo et al.  $S$ - $N$  model (described in Section [5.7](#)), additional technical details and characteristics. Section [I](#) describes numerical methods we developed for nonlinear regression models used in  $S$ - $N$  modeling. Section [J](#) gives the prior distributions, numerical results and other details from the three data analysis/modeling examples in the paper.

## B Technical Details for $S$ - $N$ Regression Models Where the Fatigue-Life Model is Specified and the Fatigue-Strength Model is Induced

This section outlines additional technical details of specifying a fatigue-life model and using it to induce a fatigue-strength model.

### B.1 Basic $S$ - $N$ Relationships for $N = g(S; \beta)$ and General Assumptions

Here we consider  $S$ - $N$  relationships of the type

$$N = g(S; \beta), \quad (28)$$

where  $\beta$  is a vector of regression model parameters and  $g(x; \beta)$  satisfies the following general conditions:

- $g(x; \beta)$  is positive; that is  $g(x; \beta) > 0$  for  $0 < x < \infty$ .
- $g(x; \beta)$  is strictly decreasing in  $x$ .
- $g(x; \beta)$  is differentiable for all  $x$ .

There are potentially two asymptotes for  $\log[g(S; \beta)]$ : A horizontal asymptote at  $E = \log(S)$  and a vertical asymptote at  $B = \log(N)$ , as illustrated in Figure 19.

### B.2 The Specified Fatigue-Life Model

The random variable  $N$  is the observed number of cycles for a unit at stress amplitude  $S_e$ . Based on the  $S$ - $N$  relationship (28), taking logs, replacing  $S$  with  $S_e$  and adding an error term  $\epsilon$  gives

$$\log(N) = \log[g(S_e; \beta)] + \sigma_N \epsilon, \quad (29)$$

where  $\epsilon$  has a location-scale distribution with  $\mu = 0$  and  $\sigma = 1$ , and  $\sigma_N$  is constant. Thus the log-location-scale cdf  $F_N(t; S_e)$  for fatigue life  $N$  is

$$\begin{aligned} F_N(t; S_e) &= \Pr(N \leq t) = \Pr[\log(N) \leq \log(t)] \\ &= \Phi\left[\frac{\log(t) - \log[g(S_e; \beta)]}{\sigma_N}\right], \quad t > 0, \quad S_e > 0. \end{aligned} \quad (30)$$

This cdf has the standard properties of a cdf for a positive random variable. In particular,  $\lim_{t \downarrow 0} F_N(t; S_e) = 0$  and  $\lim_{t \rightarrow \infty} F_N(t; S_e) = 1$ .

Then the pdf of  $N$  is

$$\begin{aligned} f_N(t; S_e) &= \frac{d}{dt} F_N(t; S_e) \\ &= \frac{1}{t\sigma_N} \phi \left[ \frac{\log(t) - \log[g(S_e; \beta)]}{\sigma_N} \right], \quad t > 0. \end{aligned} \quad (31)$$

The quantiles of  $F_N(t; S_e)$  are the solution to  $F_N(t_p) = p$ . Using (30),

$$t_p = \exp(\log[g(S_e; \beta)] + \sigma_N \Phi^{-1}(p)), \quad 0 < p < 1, \quad S_e > 0. \quad (32)$$

### B.3 Additional Results for Induced Fatigue-Strength Models

The induced fatigue-strength cdfs (and corresponding quantile functions) are described, in general terms, depending on whether the  $S$ - $N$  relationship has asymptotes or not, in Sections 2.4.1, 2.4.2, and 2.4.3 of the main paper. This section provides some additional, potentially useful, results not given there.

#### B.3.1 The induced fatigue-strength cdf for the Basquin model

Example 2.1 in Section 2.4.1 of the main paper provides details on the induced fatigue-strength cdf for the Basquin model.

#### B.3.2 The induced fatigue-strength cdf for the Stromeier model

For the Stromeier model (Section 2.3.3 of the main paper), the induced fatigue-strength cdf  $F_X(x; N_e)$  is obtained from (10) by using

$$\log[g(x; \beta)] = \beta_0 + \beta_1 \log(x - \gamma), \quad x > \gamma.$$

Note that (with  $\beta_1 < 0$ ) there is a horizontal asymptote at  $E = \log(\gamma)$  and thus  $\lim_{x \downarrow \gamma} \beta_0 + \beta_1 \log(x - \gamma) = \infty$ . This implies  $\lim_{x \downarrow \gamma} F_X(x; N_e) = 0$ , and thus  $\gamma$  is a threshold parameter for the fatigue-strength distribution, implying that fatigue strength  $X$  will never be less than  $\gamma$ .

To obtain the quantile function  $x_p(N_e)$  for  $N_e$ , use (11) in the main paper with

$$g^{-1}(w; \beta) = \gamma + \exp \left[ \frac{\log(w) - \beta_0}{\beta_1} \right]. \quad (33)$$

Because of the horizontal asymptote, as  $p \rightarrow 0$ ,  $x_p(N_e) \rightarrow \exp(E) = \gamma$  is a lower bound on the fatigue-life quantile.

### B.3.3 The induced fatigue-strength cdf for the Box–Cox model

For the Box–Cox model (Section 2.3.4), the induced fatigue-strength cdf  $F_X(x; N_e)$  is obtained from (10) by using

$$\log[g(x; \boldsymbol{\beta})] = \beta_0 + \beta_1 \nu(x; \lambda) = \begin{cases} \beta_0 + \beta_1 \left( \frac{x^\lambda - 1}{\lambda} \right) & \text{if } \lambda \neq 0 \\ \beta_0 + \beta_1 \log(x) & \text{if } \lambda = 0. \end{cases} \quad (34)$$

Because  $\lambda < 0$ ,  $-1/\lambda$  is an upper bound for  $\nu(X; \lambda)$  and thus

$$B = \lim_{x \rightarrow \infty} \log[g(x; \boldsymbol{\beta})] = \lim_{x \rightarrow \infty} \log[\beta_0 + \beta_1 \nu(x; \lambda)] = \beta_0 - \frac{\beta_1}{\lambda}$$

is a vertical asymptote. As described in Section 2.4.3, this vertical asymptote results in a discrete atom of probability of size

$$1 - \Phi\left(\frac{\log(N_e) - (\beta_0 - \beta_1/\lambda)}{\sigma_N}\right)$$

at  $\infty$ . This discrete atom corresponds to the limiting proportion of units for which  $N > N_e$  as  $x \rightarrow \infty$ . This can be interpreted as the (physically questionable) proportion of units that would survive  $N_e$  cycles, even as stress approaches  $\infty$ .

To obtain the quantile function  $x_p(N_e)$  at  $N_e$ , use (11) in the main paper with

$$g^{-1}(t; \boldsymbol{\beta}) = \left\{ 1 + \lambda \left[ \frac{\log(t) - \beta_0}{\beta_1} \right] \right\}^{1/\lambda}.$$

The quantiles are finite for  $0 < p < \Phi([\log(N_e) - (\beta_0 - \beta_1/\lambda)]/\sigma_N)$ .

## B.4 Expressions for the Induced Fatigue-Strength Model pdfs

The pdf corresponding to the fatigue-strength cdf (10) in the main paper for the random variable  $X$  (induced from a specified fatigue-life distribution in Section 2.4.1) is

$$f_X(x; N_e) = \frac{dF_X(x; N_e)}{dx} = \frac{1}{\sigma_N} \left| \frac{d}{dx} \log[g(x; \boldsymbol{\beta})] \right| \phi \left[ \frac{\log(N_e) - \log[g(x; \boldsymbol{\beta})]}{\sigma_N} \right]. \quad (35)$$

Expressions for  $d \log[g(x; \boldsymbol{\beta})]/dt$  depend on the particular  $g(x; \boldsymbol{\beta})$  relationship and are given for some models in the following subsections.

#### B.4.1 Expression for the induced fatigue-strength pdf for the Basquin model

For the Basquin model, the fatigue-strength pdf can be obtained by substituting

$$\frac{d}{dx} \log[g(x; \boldsymbol{\beta})] = \frac{\beta_1}{x}, \quad x > 0,$$

into (35).

#### B.4.2 Expression for the induced fatigue-strength pdf for the Stromeier model

For the Stromeier model (Section B.3.2), the fatigue-strength pdf can be obtained by substituting

$$\frac{d}{dx} \log[g(x; \boldsymbol{\beta})] = \frac{\beta_1}{x - \gamma}, \quad x > \gamma,$$

into (35). Because  $\gamma$  is a threshold parameter, the pdf is positive only when  $x > \gamma$ .

#### B.4.3 Expression for the induced fatigue-strength pdf for the Box–Cox model

For the Box–Cox model (Section B.3.3), the fatigue-strength pdf can be obtained by substituting

$$\frac{d}{dx} \log[g(x; \boldsymbol{\beta})] = \frac{g'(x; \boldsymbol{\beta})}{g(x; \boldsymbol{\beta})} = \beta_1 x^{\lambda-1}, \quad x > 0,$$

into (35). Because of the discrete atom of probability at  $\infty$  (see Section 2.3.4 in the main paper), (35) will, in this case, integrate to

$$\Phi\left(\frac{\log(N_e) - (\beta_0 - \beta_1/\lambda)}{\sigma_N}\right).$$

## C Technical Details for *S-N* Regression Models Where the Fatigue-Strength Model is Specified and the Fatigue-Life Model is Induced

This section outlines additional technical details of specifying the fatigue-strength model and using it to induce a fatigue-life model.

### C.1 Basic *S-N* Relationships for $S = h(N; \boldsymbol{\beta})$ and General Assumptions

Here we consider *S-N* relationships of the type

$$S = h(N; \boldsymbol{\beta}), \quad (36)$$

where  $\boldsymbol{\beta}$  is a vector of regression model parameters and  $h(t; \boldsymbol{\beta})$  satisfies the following general conditions:

- $h(t; \beta)$  is positive; that is  $h(t; \beta) > 0$  for  $0 < t < \infty$ .
- $h(t; \beta)$  is strictly decreasing in  $t$ .
- $h(t; \beta)$  is differentiable for all  $t$ .

There are potentially two asymptotes for  $\log[h(N; \beta)]$ : A horizontal asymptote at  $E = \log(S)$  and a vertical asymptote at  $B = \log(N)$ , as illustrated in Figure 19.

## C.2 Additional Motivation for Specifying the Fatigue-Strength Distribution

Section 3.2 of the main paper outlined the important advantages of specifying the fatigue-strength distribution in  $S$ - $N$  modeling. Because the variability in fatigue-strength  $X$  tends not to depend strongly on the number of cycles  $N_e$  one can, if there is curvature in the  $S$ - $N$  relationship, avoid having to include an additional model component to describe nonconstant  $\sigma_N$  as was done in Section 2.6 of the main paper. Figure 13 shows scatter plots for six high-cycle-fatigue (HCF) data sets. The data sets in Figure 13 were chosen because cycling was done at a large number of levels of stress/strain (in contrast to the three examples in the main paper). Having so many stress/strain levels allows us to see, empirically, the relatively constant variability in fatigue-strength as a function of cycles. This approximate constancy in the fatigue-strength distribution spread is in contrast to the often sizable increase in spread in fatigue-life distribution at lower stress/strain levels. Thus, model specification is simplified. Also, for the reasons given Section 5.1 of the main paper, we have observed, in many of the data sets that we have analyzed, that the induced fatigue-life model tends to nicely describe fatigue-life data.

## C.3 The Specified Fatigue-Strength Distribution

The fatigue-strength random variable  $X$  is the (unobservable) lowest level of applied stress that would result in a failure at a specified number of cycles  $N_e$  cycles. Based on the  $S$ - $N$  relationship (36), taking logs, replacing  $S$  with  $X$  and replacing  $N$  with  $N_e$ , and adding an error term  $\epsilon$  gives

$$\log(X) = \log[h(N_e; \beta)] + \sigma_X \epsilon, \quad (37)$$

where  $\epsilon$  has a location-scale distribution with  $\mu = 0$  and  $\sigma = 1$ , and  $\sigma_X$  is constant. Thus the log-location-scale cdf  $F_X(x; N_e)$  for strength  $X$  is

$$\begin{aligned} F_X(x; N_e) &= \Pr(X \leq x) = \Pr[\log(X) \leq \log(x)] \\ &= \Phi\left[\frac{\log(x) - \log[h(N_e; \beta)]}{\sigma_X}\right], \quad x > 0, \quad N_e > 0. \end{aligned} \quad (38)$$

This cdf has the standard properties of a cdf for a non-negative random variable. In particular,  $\lim_{x \downarrow 0} F_X(x; S_e) = 0$  and  $\lim_{x \rightarrow \infty} F_X(x; S_e) = 1$ .

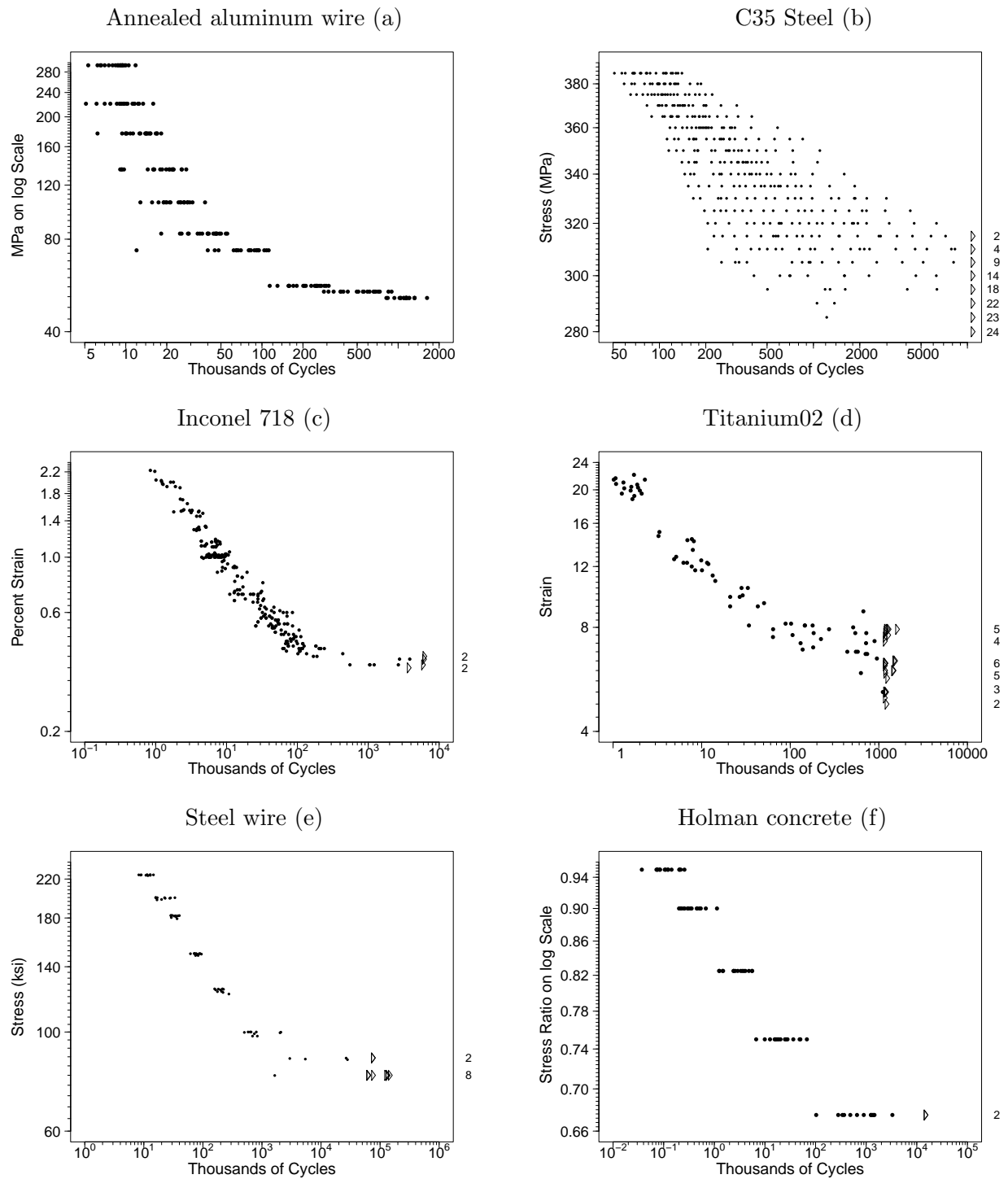


Figure 13: Scatterplots for the annealed aluminum wire (a), C35 steel (b), Inconel 718 (c), Titanium02 (d), steel wire (e), and Holman concrete (f)  $S$ - $N$  data.

## C.4 Additional Results for Induced Fatigue-Life Models

The induced fatigue-life cdfs (and corresponding quantile functions) are described, depending on whether the  $S$ - $N$  relationship has asymptotes or not, in Sections 3.2.3, 3.2.4, and 3.2.5 of the main paper. In this section we provide some additional results not given there.

### C.4.1 The induced fatigue-life distribution for the Stromeier model

The Stromeier (Section 2.3.3)  $S$ - $N$  relationship is

$$N = \exp[\beta_0 + \beta_1 \log(S - \exp(E))]. \quad (39)$$

Solving for  $S$  gives

$$S = h(N; \beta) = \exp(\gamma) + \exp\left(\frac{\log(N) - \beta_0}{\beta_1}\right), \quad (40)$$

where  $N > 0$  and  $\beta_1 < 0$ . Then the induced fatigue-life cdf  $F_N(t; S_e)$  is given by (16) in the main paper. The Stromeier model has a horizontal asymptote at  $E = \log(\gamma) = \log(S)$  because with  $\beta_1 < 0$ ,

$$\lim_{t \rightarrow \infty} \log[h(t; \beta)] = \log\left[\gamma + \exp\left(\frac{t - \beta_0}{\beta_1}\right)\right] = \log(\gamma).$$

Thus, as noted in Section 3.2.4 of the main paper,  $F_N(t; S_e)$  has a discrete atom of probability at  $\infty$  equal to the value in (19).

To obtain the quantile function  $t_p(S_e)$  for  $N$ , use

$$h^{-1}(S) = \exp[\beta_0 + \beta_1 \log(S - \gamma)] \quad (41)$$

in (17) of the main paper but, as noted in Section 3.2.4, because of the discrete atom of probability at  $\infty$ ,  $t_p(S_e)$  is only finite for  $0 \leq p < \Phi[(\log(S_e) - \log(\gamma))/\sigma_X]$  and thus there is a limit, depending on  $S_e$ , for the largest finite quantile.

### C.4.2 The induced fatigue-life cdf for the Box–Cox model

The Box–Cox  $S$ - $N$  relationship is  $N = \exp[\beta_0 + \beta_1 \nu(S; \lambda)]$ , where

$$\nu(S; \lambda) = \begin{cases} \frac{S^\lambda - 1}{\lambda} & \text{if } \lambda \neq 0 \\ \log(S) & \text{if } \lambda = 0. \end{cases} \quad (42)$$

In fatigue applications,  $\beta_1 < 0$  and  $\lambda \leq 0$ . For  $\lambda < 0$ , solving for  $S$  in (42),

$$S = h(N; \boldsymbol{\beta}) = \left[ 1 + \frac{\lambda}{\beta_1} [\log(N) - \beta_0] \right]^{1/\lambda}. \quad (43)$$

As described in Section 3.2.5 of the main paper, the induced fatigue-life cdf is given by (20). The Box–Cox model has a vertical asymptote at  $B = \beta_0 - \beta_1/\lambda$ , and this implies that  $N > \exp(\beta_0 - \beta_1/\lambda)$  and thus the cdf has a threshold parameter.

To obtain the quantile function  $t_p(S_e)$  for  $N$ , use

$$h^{-1}(S) = N = \exp[\beta_0 + \beta_1 \nu(S; \lambda)]$$

in (17) of the main paper. As noted in Section 3.2.5, because of the threshold parameter, the quantiles  $t_p(S_e)$  of  $F_N(t; S_e)$  are the same as (17) but as  $p \rightarrow 0$ ,  $t_p(S_e) \rightarrow \exp(\beta_0 - \beta_1/\lambda)$ . Thus the lower bound on the fatigue-life quantile is  $\exp(\beta_0 - \beta_1/\lambda)$ .

## C.5 Expressions for the induced Fatigue-Life Model pdfs

The pdf of an induced fatigue-life random variable  $N$  is

$$f_N(t; S_e) = \frac{dF_N(t; S_e)}{dt} = \frac{1}{\sigma_X} \left| \frac{d}{dt} \log[h(t; \boldsymbol{\beta})] \right| \phi \left[ \frac{\log(S_e) - \log[h(t; \boldsymbol{\beta})]}{\sigma_X} \right]. \quad (44)$$

Expressions for  $d \log[h(t; \boldsymbol{\beta})]/dt$  depend on the particular  $h(t; \boldsymbol{\beta})$  relationship and are given for some models in the following subsections.

### C.5.1 Expressions for the induced fatigue-life pdf for the Coffin–Manson model

For the Coffin–Manson model, following from (24) in the main paper and replacing  $N$  with  $t$  gives

$$S = h(t; \boldsymbol{\beta}) = A_{el}(2t)^b + A_{pl}(2t)^c$$

and thus

$$h'(t; \boldsymbol{\beta}) = d h(t; \boldsymbol{\beta})/dt = 2bA_{el}(2t)^{b-1} + 2cA_{pl}(2t)^{c-1}.$$

Then

$$\frac{d}{dt} \log[h(t; \boldsymbol{\beta})] = \frac{h'(t; \boldsymbol{\beta})}{h(t; \boldsymbol{\beta})} = \frac{2bA_{el}(2t)^{b-1} + 2cA_{pl}(2t)^{c-1}}{A_{el}(2t)^b + A_{pl}(2t)^c}.$$

This can be substituted into (44) to give the needed expression for the Coffin–Manson model pdf.

### C.5.2 Expressions for the induced fatigue-life pdf for the Nishijima hyperbolic model

For the Nishijima hyperbolic model, following from (23) replacing  $N$  with  $t$ , gives

$$S(t, \beta) = h(t, \beta) = \exp\left(\frac{-A \log(t) + B + E + \sqrt{[A \log(t) - (B - E)]^2 + 4C}}{2}\right).$$

and thus

$$\begin{aligned} \frac{d \log[h(t; \beta)]}{dt} &= \frac{1}{2} \frac{d}{dt} \left[ -A \log(t) + B + E + \sqrt{[A \log(t) - (B - E)]^2 + 4C} \right] \\ &= \frac{A}{2t} \left[ -1 + \frac{A \log(t) - (B - E)}{\sqrt{[A \log(t) - (B - E)]^2 + 4C}} \right]. \end{aligned}$$

This can be substituted into (44) to give the needed expression for the Nishijima hyperbolic model pdf. Note that this pdf does not integrate to 1 due to the discrete atom of probability at  $t = \infty$  (see Section 3.2.4) given in (19).

### C.5.3 Expression for the induced fatigue-life pdf for the Stromeier model

For the Stromeier model,

$$\frac{d \log[h(t; \beta)]}{dt} = \left( \frac{1}{t \beta_1} \right) \frac{\exp\left(\frac{\log(t) - \beta_0}{\beta_1}\right)}{\gamma + \exp\left(\frac{\log(t) - \beta_0}{\beta_1}\right)}.$$

This can be substituted into (44) to give the needed expression for the Stromeier fatigue-life pdf. Due to the discrete atom of probability at  $\infty$  (see Sections 3.2.4 and C.4.1), this pdf integrates to  $\Phi[(\log(S_e) - E)/\sigma_X] < 1$ .

### C.5.4 Expression for the induced fatigue-life pdf for the Box–Cox model

For the Box–Cox model,

$$\frac{d \log[h(t; \beta)]}{dt} = \left( \frac{1}{t \beta_1} \right) \frac{1}{1 + \frac{\lambda}{\beta_1}(\log(N) - \beta_0)}.$$

This can be substituted into (44) to give the needed expression for the pdf. Because of the threshold parameter, caused by the vertical asymptote in the  $S$ - $N$  relationship, noted in Sections 3.2.5 and B.3.3, this pdf is positive only when  $t > B = \exp(\beta_0 - \beta_1/\lambda)$ .

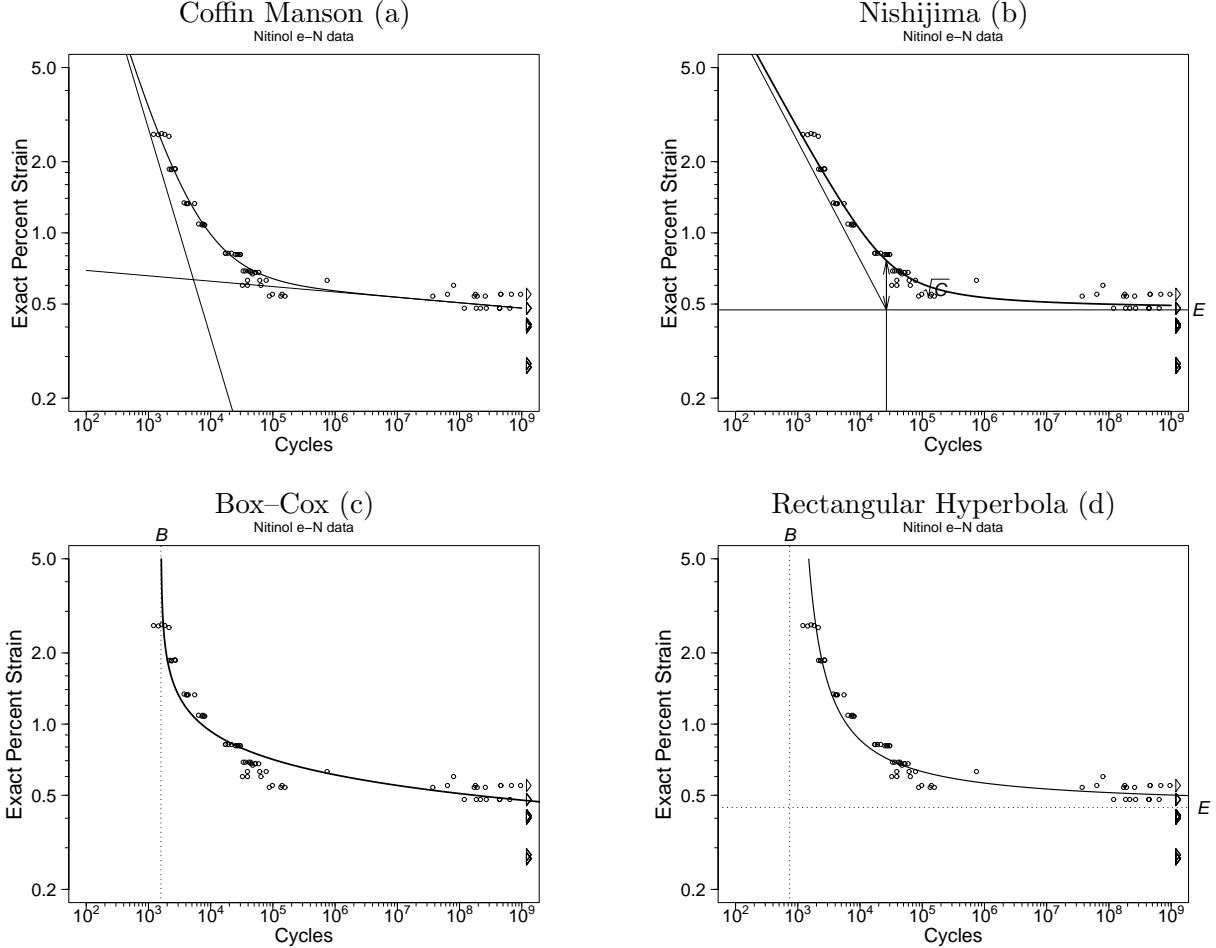


Figure 14: Median  $S$ - $N$  estimates for models fit to the complete nitinol data for the Coffin–Manson relationship with *no coordinate asymptotes* (a); Nishijima hyperbolic relationship with a *horizontal asymptote* (b); Box–Cox relationship with a *vertical asymptote* (c); and a rectangular hyperbola relationship with *both horizontal and vertical asymptotes* (d).

## D A Comparison of $S$ - $N$ Relationship Shapes and How to Choose the Right One

The existence of coordinate asymptotes is an important distinguishing characteristic of  $S$ - $N$  relationships. Figure 14 shows the  $S$ - $N$  relationships for four of the models considered in the main paper for all four combinations of the existence of coordinate asymptotes.

As described and illustrated in Section 4.3 and Examples 5.1 and 5.2 of the main paper, residual analysis is an important tool for statistical model building. Providing further compelling support for the use of residual analysis, Figure 14 shows the fitted median curve for four different  $S$ - $N$  models, fit to nitinol data used in Weaver et al. (2022) (including additional data taken at a different laboratory added). There is some evidence of lack of fit for the Box–Cox model and to a lesser degree for the rectangular hyperbola model. The residuals versus strain plots in Figure 15 provide more complete

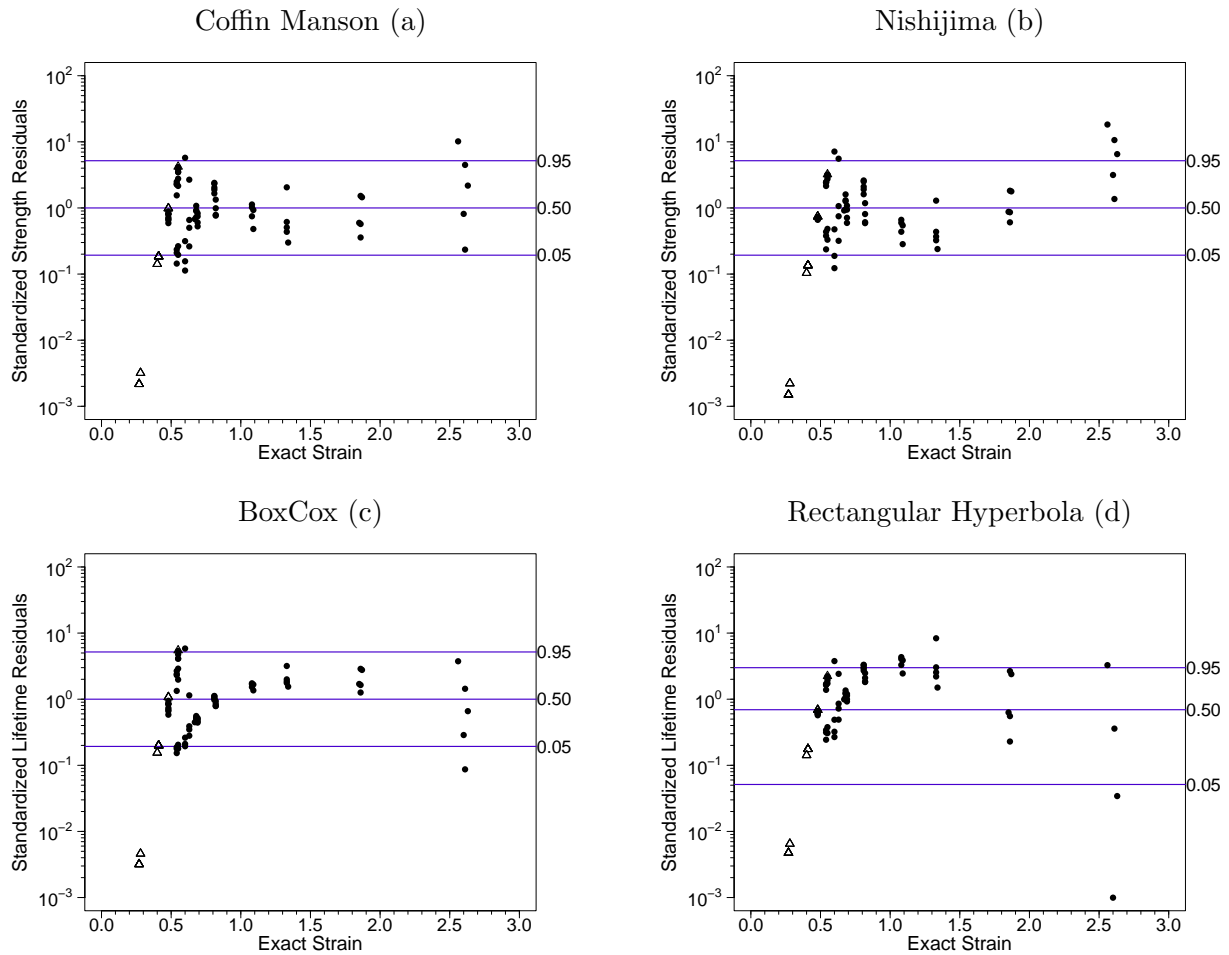


Figure 15: Residuals versus strain plots for models fit to the complete nitinol data: Coffin–Manson (a); Nishijima hyperbolic (b); Box–Cox (c); and rectangular hyperbola (d).

and accurate information about the adequacy of the different models. In particular, there appears to be an upside-down-U pattern for the Box–Cox and to a lesser degree for the rectangular hyperbola models, perhaps caused by the steeply increasing (due to the vertical asymptote)  $S$ - $N$  curve in the high-strain region. The residual plots highlight the more subtle differences between the Coffin–Manson and Nishijima hyperbolic models. Taking into account the runouts, across different values of stress/strain the distribution of the residuals for the Coffin–Manson have empirical distributions that are more constant than those for the Nishijima model.

## E Examples Comparing Lognormal and Weibull Distributions Fit to $S$ - $N$ Data from Different Materials and Specimen Types

Figure 2 in the main paper compared the lognormal and Weibull multiple probability plots for the laminate panel  $S$ - $N$  data, showing that the lognormal distribution fit much better, as would be suggested by the cumulative damage failure mechanism (Section 2.5). Figures 16, 17, and 18 provide side-by-side comparisons of lognormal and Weibull multiple probability plots for nine additional  $S$ - $N$  data sets of various different materials and specimen types.

The three wire data sets in Figure 16 came from [Freudenthal \(1952\)](#). In Figure 17, the aluminum 6061-T6 data were used in [Birnbaum and Saunders \(1969\)](#). For this data set, the failure times larger than 1800 thousand cycles were converted to right censored observations at that point because the fit in the upper tail was bad (interest is focused on the lower tail and those upper-tail observation could bias lower-tail estimates). The C35 steel data came from tests of slightly notched specimens and were given in [Maennig \(1968\)](#). These data were subsequently analyzed in [Castillo and Galambos \(1987\)](#) and [Castillo et al. \(2019\)](#). The concrete  $S$ - $N$  data came from [Holmen \(1979, 1982\)](#) and were subsequently analyzed in [Castillo and Hadi \(1995\)](#), the rejoinder of [Pascual and Meeker \(1999\)](#), and [Castillo et al. \(2007\)](#).

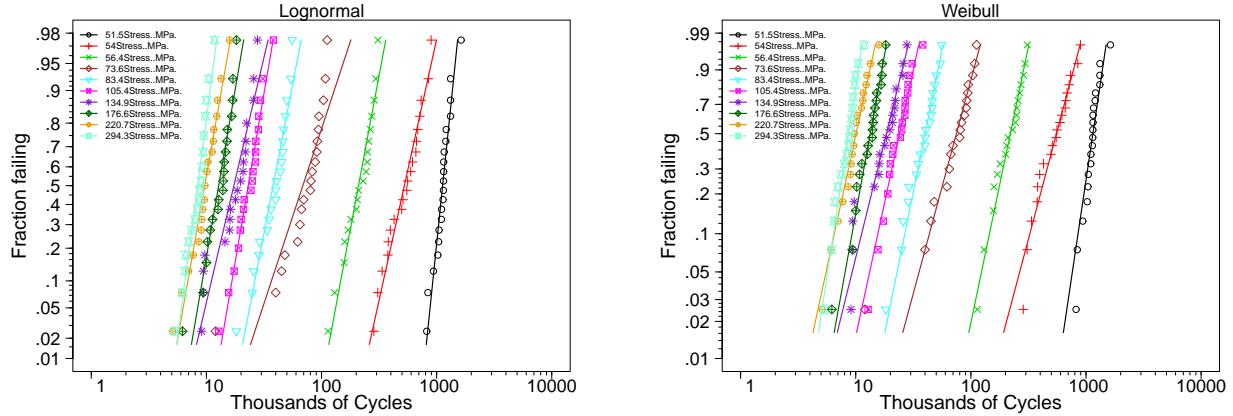
In Figure 18, the 0.02 inch diameter nitinol wire rotating bend  $S$ - $N$  data are a subset of the data presented in [Weaver et al. \(2022\)](#) that were generated in the FDA laboratories. The  $S$ - $N$  data based on sharply notched specimens of 2024-T4 aluminum alloy specimens were given in [Shimokawa and Hamaguchi \(1979\)](#) but also analyzed in [Shen \(1994\)](#). The Ti64 data (same as used in Examples 1.2 and 5.1) have not appeared in any previous publication.

## F Proofs of Technical Results Stated in the Main Paper

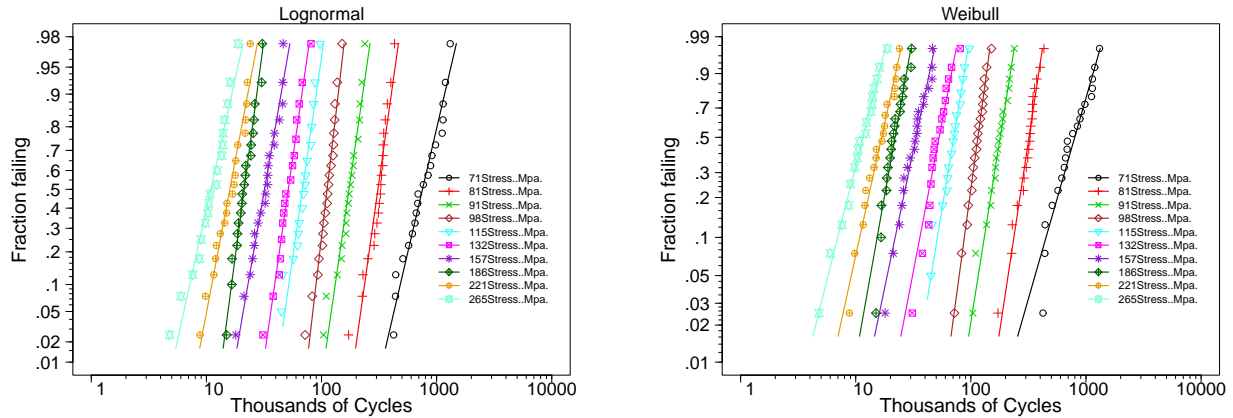
### F.1 Equivalence of Fatigue-Life and Fatigue-Strength Quantile Curves

Section 2.4.4 stated that, for  $S$ - $N$  relationships that have neither a horizontal nor a vertical asymptote, the fatigue-life and fatigue-strength models have the same quantile curves. Section F.1.1 proves that result and Section F.1.2 describes the behavior of the exceptional cases, for extreme values of  $p$ , when the  $S$ - $N$  relationship has one or two coordinate asymptotes.

Annealed Aluminum Wire *S-N* Data



Annealed Electrolytic Copper Wire *S-N* Data



Annealed ARMCO Iron Wire *S-N* Data

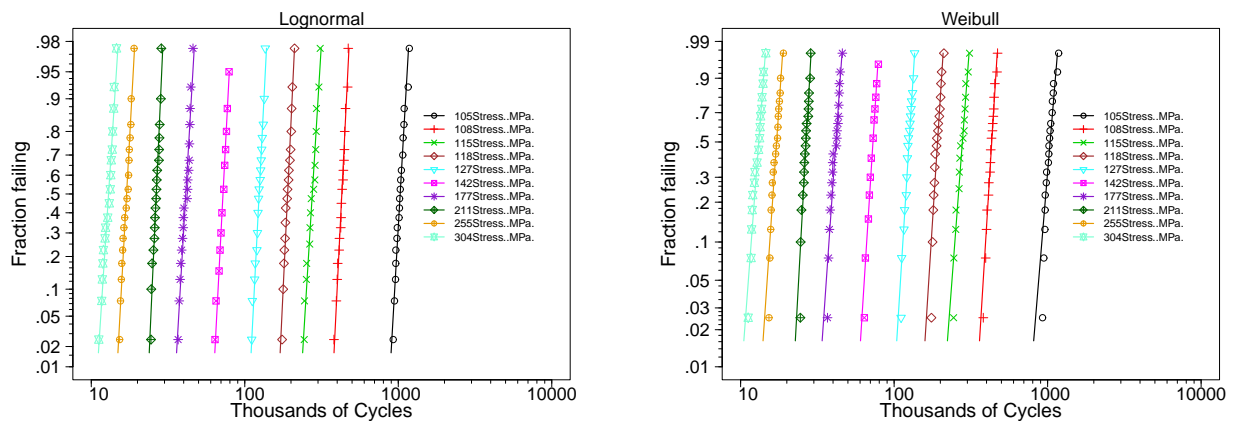
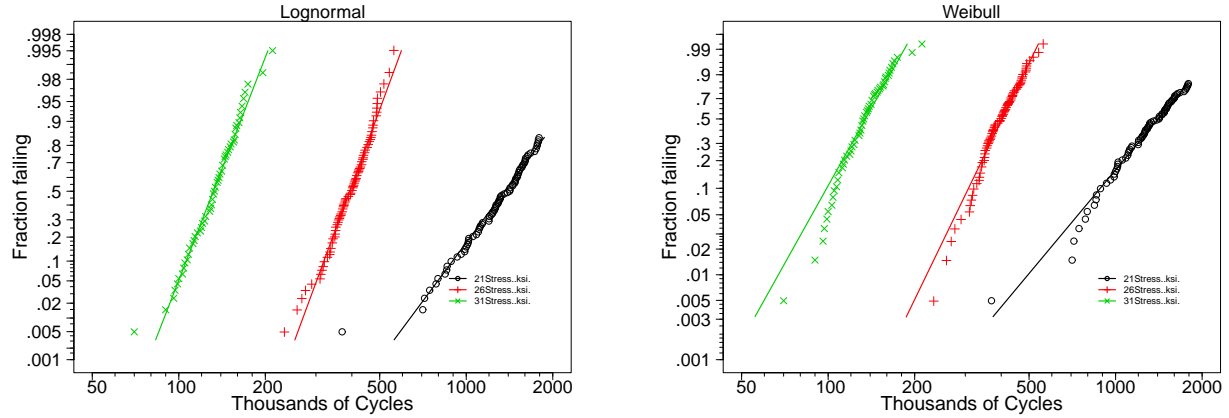
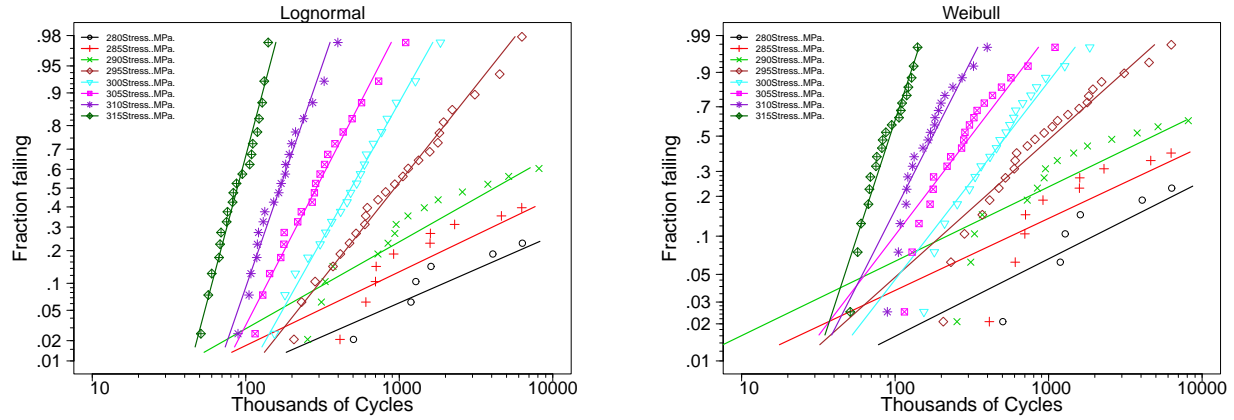


Figure 16: Comparison of lognormal (left) and Weibull (right) distribution probability plots for the annealed aluminum wire, annealed electrolytic copper wire, and annealed ARMCO iron wire *S-N* data.

### Aluminum 6061-T6 Coupons *S-N* Data



### C35 Steel Slightly Notched Specimens *S-N* Data (systematic subset of stress levels)



### Holman Concrete *S-N* Data

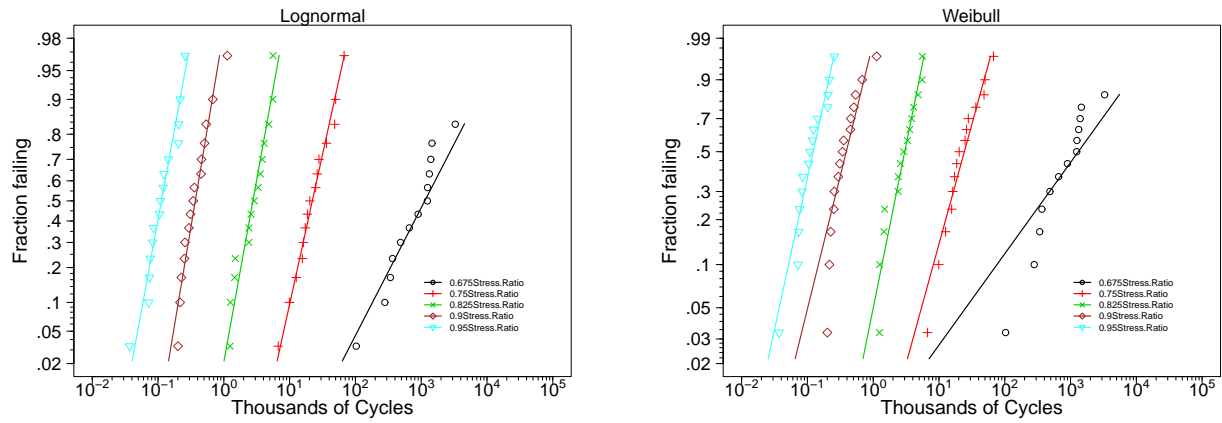
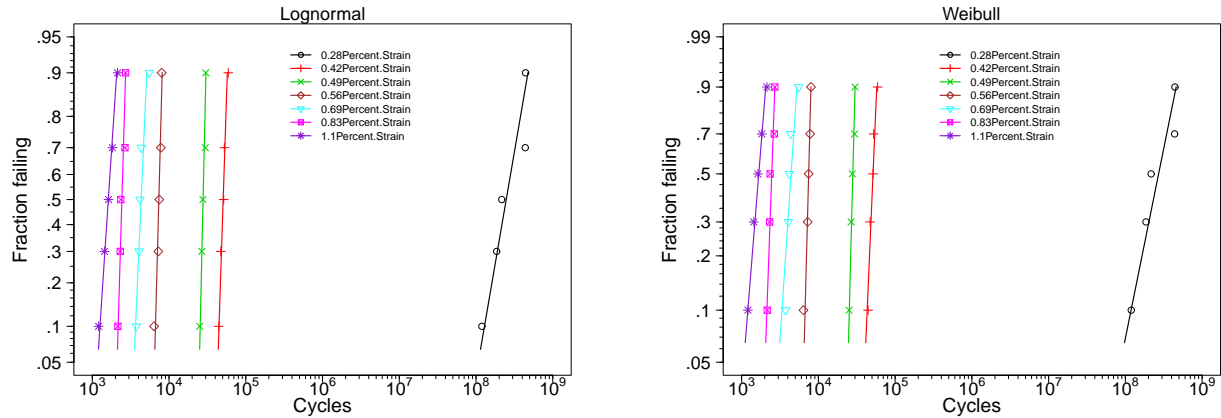
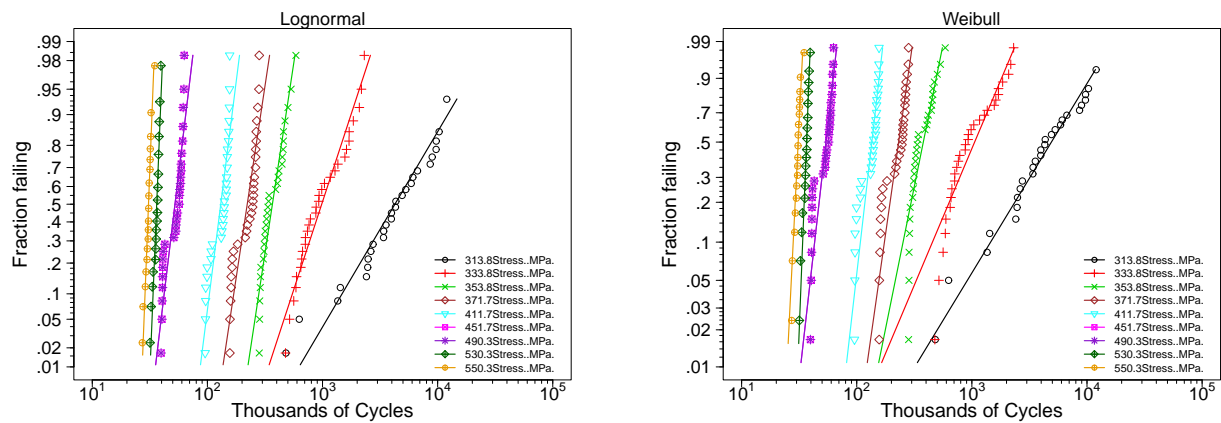


Figure 17: Comparison of lognormal (left) and Weibull (right) distribution probability plots for the aluminum 6061-T6 coupons, slightly notched C35 steel specimens, and the Holman concrete *S-N* data.

Nitinol Wire Rotating Bend *S-N* Data with 0.56 Strain Omitted



Sharply Notched Specimens of Aluminum 2024-T4 *S-N* Data



Ti64 350F  $R = -1$  *S-N* Data

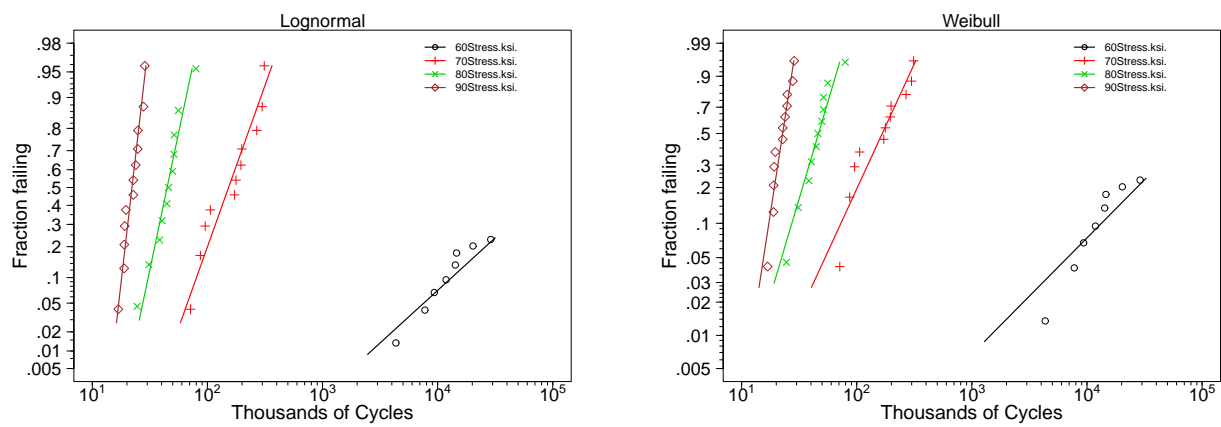


Figure 18: Comparison of lognormal (left) and Weibull (right) distribution probability plots for the nitinol wire rotating bend, sharply notched aluminum 2024-T4 Specimens, and the Ti64 350F  $R = -1$  *S-N* data.

### F.1.1 Proof of the equivalence of fatigue-life and fatigue-strength quantile curves when there is neither a horizontal nor a vertical asymptote

Consider the quantile function for the specified fatigue-strength distribution in (14). Changing variable names  $x_p(N_e)$  to  $S_e$  and  $N_e$  to  $t_p(S_e)$  gives

$$S_e = \exp(\log[h(t_p(S_e); \beta)] + \Phi^{-1}(p)\sigma_X). \quad (45)$$

Solving (45) for  $t_p(S_e)$  gives

$$t_p(S_e) = h^{-1}(\exp[\log(S_e) - \Phi^{-1}(p)\sigma_X]; \beta),$$

which agrees with the quantile function for the induced fatigue-life model in (17), giving the needed result. There is a similar and parallel result showing the equivalence of the quantiles curves for a specified fatigue-life model and an induced fatigue-strength model.

### F.1.2 The effect of coordinate asymptotes on the equivalence of fatigue-life and fatigue-strength quantile curves

This section describes the effect that coordinate asymptotes, when they exist, have on the behavior of quantile curves and the equivalence of fatigue-life and fatigue-strength quantile curves. For the *specified* fatigue-life and fatigue-strength distributions, the quantiles functions are defined for all values of  $0 < p < 1$ . This can be seen for a *specified* fatigue-life distribution by comparing (2) and (4) in Section 2.4 and for a *specified* fatigue-strength distribution by comparing (13) and (14) in Section 3.2.2 and noting that there are no restrictions on the error  $\epsilon$ .

If the  $S$ - $N$  relationship has a coordinate asymptote (horizontal or vertical or both), the behavior of the *induced* fatigue-strength and fatigue-life distributions have special properties for some extreme values of  $p$ . Table 2 summarizes detailed information given in Sections 2.4.2, 2.4.3, 3.2.4, and 3.2.5 about the effect that coordinate asymptotes have on the *induced* fatigue-strength quantiles functions  $x_p(N_e)$  and the *induced* fatigue-life quantile functions  $t_p(S_e)$  for some extreme values of  $p$ . The table illustrates an interesting duality. The following describes each of the four special cases outlined in Table 2.

- Following the development in Section 2.4.3 for an induced fatigue-strength model, because of the discrete atom of probability at infinity, for a given  $p$ , the quantile will be at infinity until cycles level  $N_e = \exp[B + \Phi^{-1}(p)\sigma_N]$  after which it will follow (11) and the fatigue-life and fatigue-strength quantile curves will agree.
- Following the development in Section 3.2.4, for an induced fatigue-life model, because of the discrete atom of probability at infinity, for a given  $p$ , the quantile will be at infinity until stress level  $S_e = \exp[E + \Phi^{-1}(p)\sigma_X]$  after which it will follow (4) and the fatigue-life and fatigue-strength quantile curves will agree.

Table 2: Description of Quantile Function Behavior for Extreme Values of  $p$  for the Induced Fatigue Distributions When There is One or Two Coordinate Asymptotes

Induced Distribution	Horizontal Asymptote $E$	Vertical Asymptote $B$
Fatigue Strength $X$ cdf $F_X(x; N_e)$ Quantile Function $x_p(N_e)$	Section 2.4.2  The fatigue-strength cdf $F_X(x; N_e)$ has a discrete atom of probability of size $1 - \Phi\left(\frac{\log(N_e) - E}{\sigma_N}\right)$ at $\infty$ corresponding to the limiting probability that fatigue life $N$ is greater than $N_e$ when $x$ is large. Finite fatigue-strength quantiles exist only for $0 < p < \Phi\left(\frac{\log(N_e) - E}{\sigma_N}\right)$ .	Section 2.4.3  The fatigue-strength cdf $F_X(x; N_e)$ has a discrete atom of probability of size $1 - \Phi\left(\frac{\log(N_e) - B}{\sigma_N}\right)$ at $\infty$ corresponding to the limiting probability that fatigue life $N$ is greater than $N_e$ when $x$ is large. Finite fatigue-strength quantiles exist only for $0 < p < \Phi\left(\frac{\log(N_e) - B}{\sigma_N}\right)$ .
Fatigue Life $N$ cdf $F_N(t; S_e)$ Quantile Function $t_p(S_e)$	Section 3.2.4  The fatigue-life cdf $F_N(t; S_e)$ has a discrete atom of probability of size $1 - \Phi\left(\frac{\log(S_e) - E}{\sigma_X}\right)$ at $\infty$ corresponding to the limiting probability that fatigue strength $X$ is greater than applied stress $S_e$ when $t$ is large. Finite fatigue-life quantiles exist only for $0 < p < \Phi\left(\frac{\log(S_e) - E}{\sigma_X}\right)$ .	Section 3.2.5  The fatigue-life cdf $F_N(t; S_e)$ has a discrete atom of probability of size $1 - \Phi\left(\frac{\log(S_e) - B}{\sigma_X}\right)$ at $\infty$ corresponding to the limiting probability that fatigue strength $X$ is greater than applied stress $S_e$ when $t$ is large. Finite fatigue-life quantiles exist only for $0 < p < \Phi\left(\frac{\log(S_e) - B}{\sigma_X}\right)$ .

- Following the development in Sections 2.4.2 and 3.2.5 the induced cdfs have a threshold parameter. In either case, however, the quantile functions  $t_p(S_e)$  and  $x_p(N_e)$  map out the same curve (because one is the inverse function of the other, as shown by the proof in Section F.1.1) even though one of the quantile functions approaches the threshold parameter as  $p \rightarrow 0$ .

## F.2 Poof that Concave-up Curvature in the *S-N* Relationship Induces Fatigue-Life Distributions with Increasing Spread at Lower Stress Levels

Suppose that a fatigue-stress model with constant  $\sigma_X$  is specified and the induced fatigue-life model is as given in Section 3.2.3 of the main paper, resulting in a quantile function

$$\begin{aligned} t_p(S_e) &= h^{-1}(\exp[\log(S_e) - \sigma_X \Phi^{-1}(p)]) \\ &= g(\exp[\log(S_e) - \sigma_X \Phi^{-1}(p)]), \end{aligned} \quad (46)$$

which is the same as (17) in the main paper except here we suppress the dependency on the parameter vector  $\beta$  and introduce  $g(x)$  to simplify notation. Suppose  $t_p(S_e)$  is differentiable, decreasing, and strictly concave-up in  $\log(S_e)$ , the latter implying

$$\frac{\partial^2 \log[t_p(S_e)]}{\partial[\log(S_e)]^2} > 0. \quad (47)$$

Consider  $t_p(S_e) = g(w_p)$  where  $w_p = \exp[\log(S_e) - \sigma_X \Phi^{-1}(p)]$  can be interpreted as the *pseudo reverse* fatigue-strength  $p$  quantile (pseudo reverse because of the minus sign and that the center of the fatigue-strength distribution is taken to be  $S_e$ ), which then, according to (46), gets mapped, through the *S-N* relationship  $g(x)$ , to the fatigue-life quantile  $t_p(S_e)$  at stress  $S_e$ .

First note that  $\partial w_p / \partial \log(S_e) = w_p$ . Using the chain rule, the first partial derivative with respect to  $\log(S_e)$ , is

$$\frac{\partial \log[t_p(S_e)]}{\partial \log(S_e)} = \frac{\partial \log[g(w_p)]}{\partial \log(S_e)} = \frac{\partial \log[g(w_p)]}{\partial w_p} \frac{\partial w_p}{\partial \log(S_e)} = \frac{g'(w_p) w_p}{g(w_p)}, \quad (48)$$

where  $g'(w_p) = dg(w_p)/dw_p$ . Using the result in (48) and the chain rule again, the second partial derivative with respect to  $\log(S_e)$  is

$$\begin{aligned} \frac{\partial^2 \log[t_p(S_e)]}{\partial[\log(S_e)]^2} &= \frac{\partial}{\partial \log(S_e)} \left[ \frac{g'(w_p) w_p}{g(w_p)} \right] = \frac{\partial}{\partial w_p} \left[ \frac{g'(w_p) w_p}{g(w_p)} \right] \frac{\partial w_p}{\partial \log(S_e)} \\ &= \frac{\partial}{\partial w_p} \left[ \frac{g'(w_p) w_p}{g(w_p)} \right] w_p = w_p \frac{\partial}{\partial w_p} \left[ \frac{g'(w_p) w_p}{g(w_p)} \right] \end{aligned} \quad (49)$$

which, from the concave-up property in (47), is positive. Then, because  $w_p$  is positive

$$\frac{\partial}{\partial w_p} \left[ \frac{g'(w_p) w_p}{g(w_p)} \right] > 0. \quad (50)$$

Using the result in (48) and the chain rule again, the second mixed partial derivative with respect to  $p$  is

$$\begin{aligned}\frac{\partial^2 \log[t_p(S_e)]}{\partial p \partial \log(S_e)} &= \frac{\partial}{\partial p} \left[ \frac{g'(w_p) w_p}{g(w_p)} \right] = \frac{\partial}{\partial w_p} \left[ \frac{g'(w_p) w_p}{g(w_p)} \right] \frac{\partial w_p}{\partial p} \\ &= \frac{\partial}{\partial w_p} \left[ \frac{g'(w_p) w_p}{g(w_p)} \right] \left[ -\frac{\sigma_X}{\phi[\Phi^{-1}(p)]} \right] w_p,\end{aligned}\quad (51)$$

where

$$\frac{\partial w_p}{\partial p} = \left[ -\frac{\sigma_X}{\phi[\Phi^{-1}(p)]} \right] w_p$$

and  $\phi(z) = d\Phi(z)/dz$ . Then, because  $\partial w_p/\partial p$  is negative and (50),

$$\frac{\partial^2 \log[t_p(S_e)]}{\partial p \partial \log(S_e)} < 0. \quad (52)$$

Now we show that the difference between two fatigue-life quantiles decreases when  $\log(S_e)$  increases. Consider  $0 < p_L < p_U < 1$ . The sign of the derivative in (52) implies that

$$\frac{\partial \log[t_{p_U}(S_e)]}{\partial \log(S_e)} < \frac{\partial \log[t_{p_L}(S_e)]}{\partial \log(S_e)}.$$

Equivalently,

$$\frac{\partial \log[t_{p_U}(S_e)]}{\partial \log(S_e)} - \frac{\partial \log[t_{p_L}(S_e)]}{\partial \log(S_e)} < 0. \quad (53)$$

Let  $\Delta[\log(t_p)] = \log[t_{p_U}(S_e)] - \log[t_{p_L}(S_e)]$  be the difference between the two fatigue-life quantiles on the log scale. Using (53), the derivative of the difference of the log-quantiles is

$$\begin{aligned}\frac{\partial \Delta[\log(t_p)]}{\partial \log(S_e)} &= \frac{\partial}{\partial \log(S_e)} (\log[t_{p_U}(S_e)] - \log[t_{p_L}(S_e)]) \\ &= \frac{\partial \log[t_{p_U}(S_e)]}{\partial \log(S_e)} - \frac{\partial \log[t_{p_L}(S_e)]}{\partial \log(S_e)} < 0.\end{aligned}$$

Consequently, the difference between the fatigue-life quantiles decreases when the stress increases which implies that the spread in the fatigue-life distribution increases when the stress decreases.

### F.3 Proof of the Equivalence of Likelihood-Based Confidence Intervals for Fatigue Life and Fatigue Strength

Hong et al. (2008) showed that pointwise confidence interval bands for a cdf are exactly the same as pointwise confidence interval bands for quantiles if the confidence intervals are computed using the likelihood ratio method. Section 4.1 stated the result that likelihood-based bands of confidence

intervals for fatigue life and fatigue strength are equivalent and describes how confidence intervals for fatigue life cdf values and quantiles (available in much existing software) can be used to obtain confidence intervals for fatigue-strength cdf values and quantiles.

In this section we provide results for the case when the fatigue-life model is specified and the fatigue-strength model is induced. When the fatigue-strength model is specified and the fatigue-life model is induced, there are similar results but we do not provide the details here.

The rest of section is organized as follows:

- Section F.3.1 introduces needed notation.
- Section F.3.2 shows how to obtain likelihood-based confidence intervals for the *specified* fatigue-life model.
- Section F.3.3 shows how to obtain likelihood-based confidence intervals for *induced* fatigue-strength model.
- Section F.3.4 shows that the fatigue-life cdf and fatigue-life distribution quantile confidence bands are equivalent.
- Section F.3.5 shows that the fatigue-strength cdf and fatigue-strength distribution quantile confidence bands are equivalent.
- Section F.3.6 shows that the fatigue-strength distribution quantile confidence bands and fatigue-life distribution quantile bands are equivalent.
- Section F.3.7 shows how the above results can be extended to a model with nonconstant  $\sigma_N$  using a loglinear model component like that described at the end of Section 2.3 of the main paper.

### F.3.1 Notation

Let  $N$  be the number of cycles to failure, and  $S_e$  be the applied stress. The  $S$ - $N$  model can be written as

$$\log(N) = \log[g(S_e; \boldsymbol{\beta})] + \sigma_N \epsilon, \quad (54)$$

where  $g(S_e; \boldsymbol{\beta})$  is a positive nonlinear monotonically decreasing function of the specified stress level  $S_e$  with regression parameter vector  $\boldsymbol{\beta}$ . The error term  $\epsilon$  has a location-scale distribution with  $\mu = 0$  and  $\sigma = 1$  and  $\sigma_N$  is a shape parameter for the log-location distribution of  $N$ . Then  $\boldsymbol{\theta} = (\boldsymbol{\beta}', \sigma_N)'$  is a vector containing the unknown parameters in the regression model.

To simplify the presentation in this section we will also assume that  $\log[g(S_e; \boldsymbol{\beta})]$  has neither a vertical nor a horizontal asymptote. When such asymptotes exist, the results are similar but require some minor adjustments, as indicated in Section B and C.

As in Section 1.2 of the main paper, the  $S$ - $N$  data, possibly with right censoring, are denoted by  $(N_i, S_i, \delta_i)$ ,  $i = 1, \dots, n$ . Here  $N_i$  is the observed cycles to failures or running time for a runout,  $S_i$  is the constant applied stress, and  $\delta_i$  is the failure indicator. Let  $\mathcal{L}(\boldsymbol{\theta}) = \mathcal{L}(\boldsymbol{\beta}, \sigma_N)$  denote the log-likelihood function given in (21). The ML estimator is denoted by  $\hat{\boldsymbol{\theta}}$ .

### F.3.2 Confidence bands for the specified fatigue-life distribution

The model in (54) implies that  $N$  has a log-location-scale distribution with log-location parameter

$$\mu(S_e) = \log[g(S_e; \boldsymbol{\beta})],$$

and shape parameter  $\sigma_N$  for a specified stress level  $S_e$ . Let

$$p = F_N(t; S_e) = \Pr(N \leq t) = \Phi\left[\frac{\log(t) - \mu(S_e)}{\sigma_N}\right].$$

The logarithm of the  $p$  quantile of  $N$  is  $\log[t_p(S_e)] = \mu(S_e) + \sigma_N \Phi^{-1}(p)$ . We can reparameterize using

$$\sigma_N = \frac{\log[t_p(S_e)] - \mu(S_e)}{\Phi^{-1}(p)} > 0.$$

Then

$$2\left\{\mathcal{L}(\hat{\boldsymbol{\beta}}, \hat{\sigma}_N) - \max_{\boldsymbol{\beta}} \mathcal{L}\left[\boldsymbol{\beta}, \frac{\log[t_p(S_e)] - \mu(S_e)}{\Phi^{-1}(p)}\right]\right\} \underset{(55)}{\sim} \chi_1^2,$$

for fixed  $0 < p < 1$ . Likelihood-based confidence intervals for  $t_p(S_e)$  can be obtained by inverting likelihood ratio tests. In particular, a  $100(1 - \alpha)\%$  likelihood-based confidence interval for the  $t_p(S_e)$  using (55) is

$$[t_p(S_e), \tilde{t}_p(S_e)] \quad (56)$$

where

$$\begin{aligned} t_p(S_e) &= \min\left\{t_p(S_e) : t_p(S_e) \text{ satisfying } \max_{\boldsymbol{\beta}} \mathcal{L}\left[\boldsymbol{\beta}, \frac{\log[t_p(S_e)] - \mu(S_e)}{\Phi^{-1}(p)}\right] \geq \mathcal{L}(\hat{\boldsymbol{\beta}}, \hat{\sigma}_N) - \frac{1}{2}\chi_{(1-\alpha;1)}^2\right\} \\ \tilde{t}_p(S_e) &= \max\left\{t_p(S_e) : t_p(S_e) \text{ satisfying } \max_{\boldsymbol{\beta}} \mathcal{L}\left[\boldsymbol{\beta}, \frac{\log[t_p(S_e)] - \mu(S_e)}{\Phi^{-1}(p)}\right] \geq \mathcal{L}(\hat{\boldsymbol{\beta}}, \hat{\sigma}_N) - \frac{1}{2}\chi_{(1-\alpha;1)}^2\right\}, \end{aligned}$$

and  $\chi_{(p;1)}^2$  is the  $p$  quantile of a chi-square distribution with 1 degree of freedom.

Similarly, a likelihood-based confidence interval for the fatigue-life cdf  $F_N(t; S_e)$  at stress level  $S_e$  and specified time  $t$  is

$$[ \tilde{F}_N(t; S_e), \tilde{\tilde{F}}_N(t; S_e) ], \quad (57)$$

where

$$\begin{aligned}\underline{F}_N(t; S_e) &= \min \left\{ p : p \text{ satisfying } \max_{\beta} \mathcal{L} \left[ \beta, \frac{\log(t) - \mu(S_e)}{\Phi^{-1}(p)} \right] \geq \mathcal{L}(\hat{\beta}, \hat{\sigma}_N) - \frac{1}{2} \chi^2_{(1-\alpha;1)} \right\} \\ \widetilde{F}_N(t; S_e) &= \max \left\{ p : p \text{ satisfying } \max_{\beta} \mathcal{L} \left[ \beta, \frac{\log(t) - \mu(S_e)}{\Phi^{-1}(p)} \right] \geq \mathcal{L}(\hat{\beta}, \hat{\sigma}_N) - \frac{1}{2} \chi^2_{(1-\alpha;1)} \right\}.\end{aligned}$$

Note that (56) also provides pointwise confidence bands for the fatigue-life distribution quantile function  $t_p(S_e)$  for a given range of values of  $p$ . Similarly, (57) provides pointwise confidence bands for  $F_N(t; S_e)$ , the fatigue-life distribution cdf at stress level  $S_e$  for a given range of values of  $t$ .

### F.3.3 Confidence bands for the induced fatigue-strength model

To obtain the fatigue-strength distribution at a specified number of cycles  $N_e$ , start with (54) but replace  $N$  by  $N_e$  and  $S_e$  by  $X$  giving

$$\log(N_e) = \log[g(X; \beta)] + \sigma_N \epsilon,$$

switching the random variable driven by  $\sigma_N \epsilon$  from  $N$  at specified  $S_e$  to  $X$  at specified  $N_e$ . Then we can solve for the fatigue-strength random variable  $X$  giving

$$X = g^{-1}[\exp(\log(N_e) - \sigma_N \epsilon); \beta].$$

The cdf of  $X$  is

$$\begin{aligned}F_X(x; N_e) &= \Pr(X \leq x) = \Pr(\log[g(X; \beta)] \leq \log[g(x; \beta)]) \\ &= \Pr(\log(N_e) - \sigma_N \epsilon \geq \log[g(x; \beta)]) \\ &= \Pr\left[\epsilon \leq \frac{\log(N_e) - \log[g(x; \beta)]}{\sigma_N}\right] \\ &= \Phi\left[\frac{\log(N_e) - \log[g(x; \beta)]}{\sigma_N}\right].\end{aligned}$$

The quantile function of  $X$  is  $x_p(N_e) = g^{-1}[\exp[\log(N_e) - \sigma_N \Phi^{-1}(p)]; \beta]$ . We can reparameterize using

$$\sigma_N = \frac{\log(N_e) - \log[g(x_p(N_e); \beta)]}{\Phi^{-1}(p)}.$$

Using the reparameterization, the log-likelihood can be written as

$$\mathcal{L} \left[ \beta; \frac{\log(N_e) - \log[g(x_p(N_e); \beta)]}{\Phi^{-1}(p)} \right].$$

Thus, likelihood-based confidence bands for the fatigue-strength distribution quantiles and fatigue-strength distribution cdf can be obtained in a manner similar to that used for the fatigue-life distribution. We

have

$$2 \left\{ \mathcal{L}(\hat{\beta}, \hat{\sigma}_N) - \max_{\beta} \mathcal{L} \left[ \beta; \frac{\log(N_e) - \log[g(x_p(N_e); \beta)]}{\Phi^{-1}(p)} \right] \right\} \sim \chi^2_1, \quad (58)$$

for fixed  $0 < p < 1$ . Likelihood-based confidence intervals for  $x_p(N_e)$  can be obtained by inverting likelihood ratio tests. In particular, a  $100(1 - \alpha)\%$  likelihood-based confidence interval for the  $x_p(N_e)$  using (58) is

$$[\underline{x}_p(N_e), \quad \tilde{x}_p(N_e)] \quad (59)$$

where

$$\begin{aligned} \underline{x}_p(N_e) &= \min \left\{ x_p(N_e) : x_p(N_e) \text{ satisfying } \max_{\beta} \mathcal{L} \left[ \beta; \frac{\log(N_e) - \log[g(x_p(N_e); \beta)]}{\Phi^{-1}(p)} \right] \geq \mathcal{L}(\hat{\beta}, \hat{\sigma}_N) - \frac{1}{2} \chi^2_{(1-\alpha;1)} \right\} \\ \tilde{x}_p(N_e) &= \max \left\{ x_p(N_e) : x_p(N_e) \text{ satisfying } \max_{\beta} \mathcal{L} \left[ \beta; \frac{\log(N_e) - \log[g(x_p(N_e); \beta)]}{\Phi^{-1}(p)} \right] \geq \mathcal{L}(\hat{\beta}, \hat{\sigma}_N) - \frac{1}{2} \chi^2_{(1-\alpha;1)} \right\}. \end{aligned}$$

Similarly, the likelihood-based confidence interval for  $F_X(x; N_e)$ , the fatigue-strength cdf for a specified value  $N_e$  cycles at a given  $x$  is

$$[\underline{F}_X(x; N_e), \quad \tilde{F}_X(x; N_e)] \quad (60)$$

where

$$\begin{aligned} \underline{F}_X(x; N_e) &= \min \left\{ p : p \text{ satisfying } \max_{\beta} \mathcal{L} \left[ \beta; \frac{\log(N_e) - \log[g(x; \beta)]}{\Phi^{-1}(p)} \right] \geq \mathcal{L}(\hat{\beta}, \hat{\sigma}_N) - \frac{1}{2} \chi^2_{(1-\alpha;1)} \right\} \\ \tilde{F}_X(x; N_e) &= \max \left\{ p : p \text{ satisfying } \max_{\beta} \mathcal{L} \left[ \beta; \frac{\log(N_e) - \log[g(x; \beta)]}{\Phi^{-1}(p)} \right] \geq \mathcal{L}(\hat{\beta}, \hat{\sigma}_N) - \frac{1}{2} \chi^2_{(1-\alpha;1)} \right\}. \end{aligned}$$

Note that (59) also provides pointwise confidence bands for  $x_p(N_e)$ , the fatigue-strength distribution quantile function at  $N_e$  cycles for a given range of values of  $p$ . Similarly, (60) provides pointwise confidence bands for  $F_X(x; N_e)$ , the fatigue-strength distribution cdf for a given range of values of  $x$ .

#### F.3.4 Equivalence of the fatigue-life distribution cdf and quantile confidence bands

This section shows that the confidence bands for the fatigue-life distribution quantile function in (56) are equivalent to the confidence bands for the fatigue-life cdf in (57) if the bands are based on likelihood methods. To show the relationship between the likelihood-based confidence bands obtained from (56) and (57), we define a likelihood-based procedure confidence interval for  $F_N(t; S_e)$  by inverting the

confidence band for  $t_p(S_e)$ , which is

$$[\underline{p}, \bar{p}] \quad (61)$$

where  $\underline{p}$  and  $\bar{p}$  are obtained by solving from equations  $t = \tilde{t}_{\underline{p}}(S_e)$  and  $t = \tilde{t}_{\bar{p}}(S_e)$ . That is,  $\underline{p}$  is chosen such that the upper endpoint of the confidence interval for the  $\underline{p}$  quantile is  $t$ . Similarly,  $\bar{p}$  is chosen such that the lower endpoint of the confidence interval for the  $\bar{p}$  quantile is  $t$ .

**Result 0.1.** The likelihood-based confidence interval procedures (57) and (61) for  $F_N(t; S_e)$  are equivalent.

This result shows that if one uses the likelihood-based procedures, it makes no difference whether one computes pointwise confidence bands for  $F_N(t; S_e)$  or  $t_p(S_e)$ ; the bands will be the same. The proof is similar to the one in Hong et al. (2008). In particular, we show  $\underline{p}$  in (61) is the same as  $\underline{F}_N(t; S_e)$  in (57) here, to illustrate the main idea in the proof. The proof for the equivalence of  $\bar{p}$  and  $\tilde{F}_N(t; S_e)$  is similar.

Let  $(t_0, p_L)$  and  $(t_0, p_U)$  (with  $p_L < p_U$ ) be the points at which the vertical line through any given  $t_0$  intersects the confidence bands for the quantile function  $t_p(S_e)$ . First note that  $t_0$  is the upper end point of the confidence interval for  $t_{p_L}(S_e)$ . That is,

$$t_0 = \max \left\{ t_{p_L}(S_e) : t_{p_L}(S_e) \text{ satisfying } \max_{\beta} \mathcal{L} \left[ \beta, \frac{\log[t_{p_L}(S_e)] - \mu(S_e)}{\Phi^{-1}(p_L)} \right] \geq k \right\},$$

where  $k = \mathcal{L}(\hat{\beta}, \hat{\sigma}_N) - \frac{1}{2}\chi^2_{(1-\alpha;1)}$ . Thus,

$$\max_{\beta} \mathcal{L} \left[ \beta, \frac{\log(t_0) - \mu(S_e)}{\Phi^{-1}(p_L)} \right] \geq k \quad (62)$$

$$\max_{\beta} \mathcal{L} \left[ \beta, \frac{\log(t_0 + \delta) - \mu(S_e)}{\Phi^{-1}(p_L)} \right] < k \text{ for all } \delta > 0. \quad (63)$$

Consider  $p < p_L$  and suppose that  $\tilde{\beta}$  maximizes  $\mathcal{L} \left[ \beta, \frac{\log(t_0) - \mu(S_e)}{\Phi^{-1}(p)} \right]$ . It follows that

$$\begin{aligned} \max_{\beta} \mathcal{L} \left[ \beta, \frac{\log(t_0) - \mu(S_e)}{\Phi^{-1}(p)} \right] &= \mathcal{L} \left[ \tilde{\beta}, \frac{\log(t_0) - \mu(S_e)}{\Phi^{-1}(p)} \right] \\ &= \mathcal{L} \left[ \tilde{\beta}, \frac{\log(t_0 + \delta) - \mu(S_e)}{\Phi^{-1}(p_L)} \right] < k, \end{aligned} \quad (64)$$

for some  $\delta > 0$  and the inequality in (64) follows from (63). Then from (62) and (64), it follows that

$$p_L = \min \left\{ p : p \text{ satisfying } \max_{\beta} \mathcal{L} \left[ \beta, \frac{\log(t_0) - \mu(S_e)}{\Phi^{-1}(p)} \right] \geq k \right\},$$

which means  $p_L$  is the lower end point of confidence interval for  $F_N(t; S_e)$  from (57). That is,  $\underline{p}$  in (61) is the same as  $\underline{F}_N(t; S_e)$  in (57).

### F.3.5 Equivalence of the fatigue-strength cdf and fatigue-strength distribution quantile confidence bands

This section shows that the likelihood-based confidence bands for the fatigue-strength distribution quantile function in (59) are equivalent to the confidence bands for the fatigue-strength cdf in (60) if the bands are based on likelihood methods. To show the relationship between the likelihood-based confidence bands obtained from (59) and (60), we define a likelihood-based procedure confidence interval for  $F_X(x; N_e)$  by inverting the confidence band for  $x_p(N_e)$ , which is

$$[\underline{p}, \bar{p}] \quad (65)$$

where  $\underline{p}$  and  $\bar{p}$  are obtained by solving from equations  $x = \tilde{x}_{\underline{p}}(N_e)$  and  $x = \tilde{x}_{\bar{p}}(N_e)$ . That is,  $\underline{p}$  is chosen such that the upper endpoint of the confidence interval for the  $\underline{p}$  quantile is  $x$ . Similarly,  $\bar{p}$  is chosen such that the lower endpoint of the confidence interval for the  $\bar{p}$  quantile is  $x$ .

**Result 0.2.** The likelihood-based confidence interval procedures (60) and (65) for  $F_X(x; N_e)$  are equivalent.

This result shows that if one uses the likelihood-based procedures, it makes no difference whether one computes pointwise confidence bands for  $F_X(x; N_e)$  or  $x_p(N_e)$ ; the bands will be the same. The proof is similar to the one in [Hong et al. \(2008\)](#) and thus is omitted.

### F.3.6 Equivalence of fatigue-strength distribution quantile confidence bands and fatigue-life distribution quantile bands

Consider the need to find a safe level of stress  $S_e$  such that  $\underline{t}_p(S_e) = N_e$ . If computed using the likelihood-based method, this  $S_e$  value is equivalent to the lower confidence bound  $\underline{x}_p(N_e)$  of the fatigue strength distribution. More generally, if likelihood-based pointwise confidence intervals for  $\underline{t}_p(S_e) = N_e$  are used to obtain bands of such  $S_e$  values for a range of  $N_e$  values, they will be equivalent to the confidence bands for  $x_p(N_e)$  in (59) over the same range of  $N_e$ . We have the following result.

**Result 0.3.** The fatigue-strength distribution quantile confidence bands in (59) and the fatigue-life distribution quantile bands in (56) are equivalent.

Here we give a brief proof. For a fixed  $p$  and  $S_e$ , a point on the quantile line for the cycles to failure distribution is  $(S_e, \exp(\mu_{\beta} + \sigma_N z_p))$ , where  $\mu_{\beta} = \log[g(S_e; \beta)]$  and  $z_p = \Phi^{-1}(p)$ . We can see that this point is also on the  $p$  quantile line for the strength distribution for a fixed  $N_e = \exp(\mu_{\beta} + \sigma_N z_p)$ . The quantile function of  $X$  is

$$\begin{aligned} x_p(N_e) &= g^{-1}[\exp(\log(N_e) - \sigma_N z_p); \beta] \\ &= g^{-1}[\exp(\log[\exp(\mu_{\beta} + \sigma_N z_p)] - \sigma_N z_p); \beta] \\ &= g^{-1}[\exp(\mu_{\beta}); \beta] = S_e, \end{aligned}$$

which is the same point as  $(S_e, \exp(\mu_{\beta} + \sigma_N z_p))$ . Thus the two likelihood-based confidence bands are equivalent.

### F.3.7 Extension for nonconstant $\sigma_N$ model

Sections F.3.2–F.3.6 showed how to compute likelihood intervals for the  $S$ - $N$  model cdfs and quantile functions for  $S$ - $N$  models with constant  $\sigma_N$ . This section indicates how those results can be extended to models with nonconstant  $\sigma_N$ . As described in Section 2.3, to allow for nonconstant  $\sigma_N$ , the  $S$ - $N$  model can be written as

$$\log(N) = \log[g(S_e; \beta)] + \sigma_N(S_e; \beta^{[\sigma]})\epsilon, \quad (66)$$

where

$$\sigma_N(S_e; \beta^{[\sigma]}) = \exp[\beta_0^{[\sigma]} + \beta_1^{[\sigma]} \log(S_e)],$$

$$\text{and } \beta^{[\sigma]} = (\beta_0^{[\sigma]}, \beta_1^{[\sigma]})'.$$

Under this model, the fatigue-life cdf is

$$p = F_N(t) = \Phi\left[\frac{\log(t) - \mu(S_e)}{\sigma_N(S_e; \beta^{[\sigma]})}\right],$$

and the quantile function is  $\log(t_p(N_e)) = \mu(S_e) + \sigma_N(S_e; \beta^{[\sigma]})\Phi^{-1}(p)$ .

Note that

$$\Phi^{-1}(p) = \frac{\log(t) - \mu(S_e)}{\sigma_N(S_e; \beta^{[\sigma]})}.$$

Thus,

$$\sigma_N(S_e; \beta^{[\sigma]}) = \exp[\beta_0^{[\sigma]} + \beta_1^{[\sigma]} \log(S_e)] = \frac{\log(t) - \mu(S_e)}{\Phi^{-1}(p)}.$$

That is

$$\beta_0^{[\sigma]} + \beta_1^{[\sigma]} \log(S_e) = \log\left[\frac{\log(t) - \mu(S_e)}{\Phi^{-1}(p)}\right],$$

leading to a reparameterization where

$$\beta_0^{[\sigma]} = \log\left[\frac{\log(t) - \mu(S_e)}{\Phi^{-1}(p)}\right] - \beta_1^{[\sigma]} \log(S_e).$$

Using this reparameterization, the log-likelihood  $\mathcal{L}(\boldsymbol{\beta}, \beta_0^{[\sigma]}, \beta_1^{[\sigma]})$  can be written as

$$\mathcal{L}\left\{\boldsymbol{\beta}, \log\left[\frac{\log(t) - \mu(S_e)}{\Phi^{-1}(p)}\right] - \beta_1^{[\sigma]} \log(S_e), \beta_1^{[\sigma]}\right\}.$$

Thus, likelihood-based confidence bands for the fatigue-life cdf and distribution quantiles for the nonconstant- $\sigma_N$  model can be obtained in a manner similar to that used for the constant- $\sigma_N$  model. For example, the CI for  $t_p(N_e)$  can be obtained using the result,

$$2\left\{\mathcal{L}(\hat{\boldsymbol{\theta}}) - \max_{\boldsymbol{\beta}, \beta_1^{[\sigma]}} \mathcal{L}\left\{\boldsymbol{\beta}, \log\left[\frac{\log[t_p(N_e)] - \mu(S_e)}{\Phi^{-1}(p)}\right] - \beta_1^{[\sigma]} \log(S_e), \beta_1^{[\sigma]}\right\}\right\} \stackrel{\sim}{\sim} \chi_1^2. \quad (67)$$

## G An Algorithm to Compute the Distribution of Fatigue Strength From the Distribution of Fatigue Life When There is No Closed-Form Expression

For some models where the fatigue-life model is specified, there is not a closed-form expression for the fatigue-strength distribution. In such cases, however, we can numerically compute the fatigue-strength cdf, quantiles, and pdf. Suppose it is possible to compute the fatigue-life distribution  $\Pr(N \leq t) = F_N(t, S_e)$  and corresponding quantiles  $t_p(S_e)$  directly. Then the fatigue-strength distribution can be computed in the following way:

1. Use the quantile-line equivalence property (and interpolation) to compute the fatigue-strength quantiles  $x_{0.001}$  and  $x_{0.999}$  for each  $N_e$  point where the fatigue-strength distribution is needed.
2. Compute the fatigue-strength cdf using  $F_X(x; N_e) = \Pr(X \leq x; N_e) = F_N(N_e; x)$  for say 200 values of  $x$  between  $x_{0.001}$  and  $x_{0.999}$ .
3. Interpolate in the  $F_X(x; N_e)$  values to get any needed quantiles.
4. Use finite differences of the  $F_X(x; N_e)$  values to get the density values.

Note that, unlike fatigue-life quantiles, finite fatigue-strength quantiles always exist and are well behaved except when the cdfs cross (as they will in the lower tail of the fatigue-life distribution when there is loglinear component for  $\sigma_N$ ).

## H Further Explanation of the Castillo et al. S-N Model

This section provides additional technical details for the Castillo et al. model given in (27) and described in Section 5.7 of the main paper. In particular, we provide explicit expressions for the Weibull parameters and quantile functions for the fatigue life  $N$  and fatigue strength  $X$  random variables.

## H.1 The Distribution of Fatigue Life

Starting with (27) in the main paper, it was shown that by replacing  $x$  with  $S_e$  the result can be interpreted as the cdf for fatigue life  $N$  at a specified level of stress  $S_e$ :

$$\begin{aligned}\Pr(N \leq t; S_e) &= F_N(t; S_e) = F(t, S_e) \\ &= 1 - \exp\left\{-\left[\frac{\log(t) - \gamma_N}{\eta_N}\right]^\beta\right\}, \quad t > \exp(\gamma_N), S_e > \exp(E)\end{aligned}\quad (68)$$

where  $\gamma_N = B + \gamma/[\log(S_e) - E]$  and  $\eta_N = \eta/[\log(S_e) - E]$ . Also, it can be shown that  $Y_N = \log(N)$  given  $S_e$  has a three-parameter Weibull distribution with scale parameter  $\eta_N$ , threshold parameter  $\gamma_N$ , and shape parameter  $\beta$ . Also,

$$W = \left(\frac{Y_N - \gamma_N}{\eta_N}\right)^\beta = \left(\frac{\log(N) - \gamma_N}{\eta_N}\right)^\beta$$

at a given  $S_e$  has an exponential distribution with scale parameter 1 or, equivalently, a two-parameter Weibull distribution with scale and shape parameters both equal to 1. Then

$$\epsilon = \log(W) = \log\left[\left(\frac{Y_N - \gamma_N}{\eta_N}\right)^\beta\right] = \log\left[\left(\frac{\log(N) - \gamma_N}{\eta_N}\right)^\beta\right] \quad (69)$$

has a smallest extreme value (Gumbel) distribution with location parameter  $\mu = 0$  and scale parameter  $\sigma = 1$ . Solving for  $N$  in (69) gives

$$N = \exp\left[\gamma_N + \eta_N[\exp(\epsilon)]^{1/\beta}\right] = \exp\left[\left(B + \frac{\gamma}{\log(S_e) - E}\right) + \left(\frac{\eta}{\log(S_e) - E}\right)[\exp(\epsilon)]^{1/\beta}\right]. \quad (70)$$

## H.2 Distribution of Fatigue Strength

Starting with (27) in the main paper, it was shown that by replacing  $t$  with  $N_e$  the result can be interpreted as the cdf for fatigue strength  $X$  at a specified number of cycles  $N_e$ :

$$\begin{aligned}\Pr(X \leq x; N_e) &= F_X(x; N_e) = F(N_e, x) \\ &= 1 - \exp\left\{-\left[\frac{\log(x) - \gamma_X}{\eta_X}\right]^\beta\right\}, \quad x > \exp(\gamma_X), N_e > \exp(B)\end{aligned}\quad (71)$$

where  $\gamma_X = E + \gamma/[\log(N_e) - B]$  and  $\eta_X = \eta/[\log(N_e) - B]$ . Also, it can be shown that  $Y_X = \log(X)$  given  $N_e$  has a three-parameter Weibull distribution with scale parameter  $\eta_X$ , threshold parameter  $\gamma_X$ , and shape parameter  $\beta$ . Then, parallel to (69),

$$\epsilon = \log\left[\left(\frac{Y_X - \gamma_X}{\eta_X}\right)^\beta\right] = \log\left[\left(\frac{\log(X) - \gamma_X}{\eta_X}\right)^\beta\right] \quad (72)$$

has a standard smallest extreme value (Gumbel) distribution. Solving for  $X$  in (72) gives

$$X = \exp\left[\gamma_X + \eta_X[\exp(\epsilon)]^{1/\beta}\right] = \exp\left[\left(E + \frac{\gamma}{\log(N_e) - B}\right) + \left(\frac{\eta}{\log(N_e) - B}\right)[\exp(\epsilon)]^{1/\beta}\right]. \quad (73)$$

### H.3 Quantiles of the Fatigue-life and the Fatigue-Strength Distributions

The fatigue-life  $p$  quantile curve is obtained by setting  $p = F_N[t_p(S_e); S_e]$  in (68). Solving for  $t_p(S_e)$  gives

$$\begin{aligned} t_p(S_e) &= \exp\left[\gamma_N + \eta_N[-\log(1-p)]^{1/\beta}\right] \\ &= \exp\left[\left(B + \frac{\gamma}{\log(S_e) - E}\right) + \left(\frac{\eta}{\log(S_e) - E}\right)[- \log(1-p)]^{1/\beta}\right], \quad 0 < p < 1, S_e > \exp(E). \end{aligned}$$

Similarly, the fatigue-strength  $p$  quantile is obtained by setting  $p = F_X[x_p(N_e); N_e]$  in (71), from which  $x_p(N_e)$  is derived as

$$\begin{aligned} x_p(N_e) &= \exp\left[\gamma_X + \eta_X[-\log(1-p)]^{1/\beta}\right] \\ &= \exp\left[\left(E + \frac{\gamma}{\log(N_e) - B}\right) + \left(\frac{\eta}{\log(N_e) - B}\right)[- \log(1-p)]^{1/\beta}\right], \quad 0 < p < 1, N_e > \exp(B). \end{aligned}$$

### H.4 Comments

Observe that

- The error terms  $\epsilon$  for the random variables  $N$  in (70) and  $X$  in (73) have the same distribution and that either of these equations leads back to the cdfs derived from (27) in the main paper.
- Setting  $p = F[t_p(S_e), S_e]$  in (27) in the main paper leads to

$$[\log(t_p(S_e)) - B][\log(S_e) - E] = \gamma + \eta[-\log(1-p)]^{1/\beta}. \quad (74)$$

Analogously, setting  $p = F[N_e, x_p(N_e)]$  in (27) in the main paper leads to

$$[\log(N_e) - B][\log(x_p(N_e)) - E] = \gamma + \eta[-\log(1-p)]^{1/\beta}. \quad (75)$$

Equations (74) and (75) correspond to Equation (18) of Castillo et al. (1985) and the Castillo et al. (1985) model in Table A.21 on page 195 and Equation (A.26) on page 204 of Castillo and Fernández-Canteli (2009).

- The respective  $p$  quantiles of  $N$  and  $S$  coincide as illustrated in Figure 19. The right-hand side of (74) and (75) decreases as  $\gamma \rightarrow 0$  which implies that the  $p$  quantile curve moves closer to the vertical asymptote  $\exp(B)$  and horizontal asymptote  $\exp(E)$ .

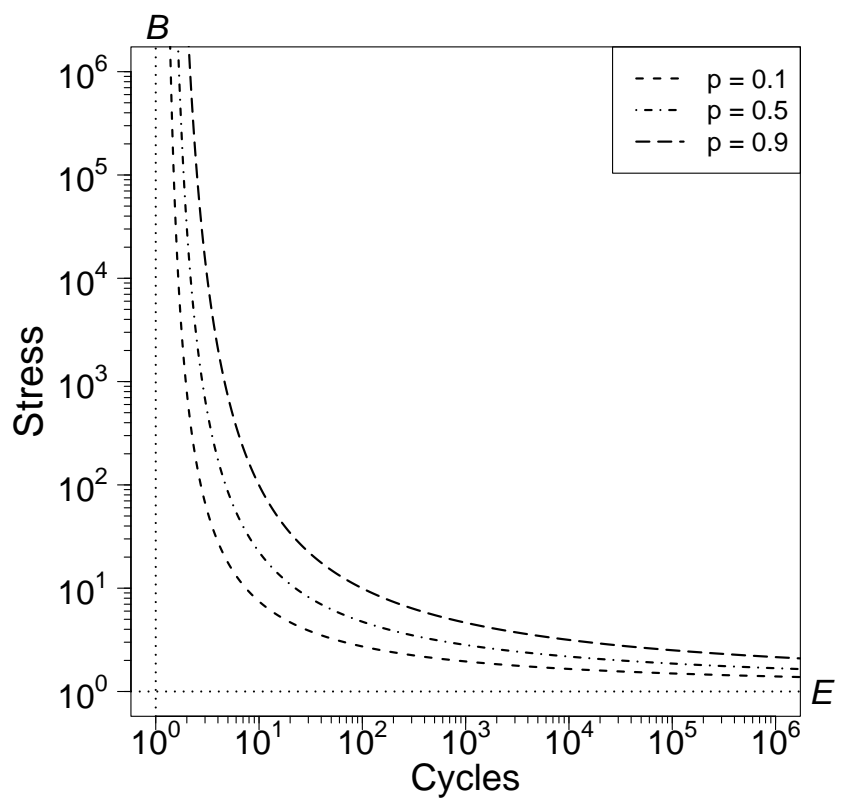


Figure 19: The 0.10, 0.50, and 0.90 quantile curves for the Castillo et al. rectangular-hyperbola Weibull  $S$ - $N$  model with  $E = B = \log(1)$ ,  $\gamma = 3$ ,  $\beta = 2$ , and  $\eta = 5$ .

# I Numerical Methods for Nonlinear Regression Models Used in Fatigue $S$ - $N$ Modeling

As mentioned briefly in Section 4.2.4 of the main paper, robust algorithms for estimating the parameters of nonlinear regression models (using either maximum likelihood (ML) or Bayesian estimation) require

- Careful attention to parameterization,
- Methods for finding “initial values” for the parameters to start the ML optimization, and
- When doing Bayesian estimation, default noninformative priors.

Section I.1 outlines the general strategy in more detail while Sections I.2–I.5 provide implementation details for the four main models described and used in the main paper.

## I.1 The General Strategy

In our general strategy for having robust numerical methods for fitting nonlinear regression models, we do the following, separately, for each model.

### I.1.1 Steps for ML estimation

Even when the final goal is a Bayesian analysis, we find it useful (for reasons described in Section I.1.4) to start with ML estimation. Thus, whether doing ML or Bayesian estimation, we start with the following procedures for ML estimation.

1. Scale both the stress/strain variable  $S$  and the response variable  $N$ . Dividing all values of  $S$  and  $N$  by the maximum value of these variables (denoted by  $S_{\max}$  and  $N_{\max}$ ) works well. This will assure that the performance of the estimation algorithms will not depend on the units of the variables.
2. If needed, replace model parameters that have no practical meaning with alternative interpretable parameters. This step is especially important when Bayesian estimation will be used and prior distributions have to be specified. For example, the intercept  $\beta_0$  in the Box–Cox model (Section 2.3.4) has no practical meaning and should be replaced by a quantile (e.g., the median) at some level of stress in the usual range of experimentation. We call these the “traditional parameters.”
3. Find simple “ball park” preliminary estimates for the traditional parameters. Often these can be obtained by using simple moment estimates (e.g., sample means, variances, and ordinary least squares). In some cases (e.g., with a nonlinear regression relationship having three or four parameters), it is necessary to do the preliminary estimation stage-wise. For example, one might get initial estimates for two of the parameters, hold these fixed, and then compute preliminary

estimates for the other parameters. When finding these preliminary estimates, one can ignore censoring by treating censored observations as failures.

4. Define “stable parameters” (as defined by [Ross, 1970, 1990](#)) that will not be highly correlated, that do not have limits depending on other parameters, and that can be identified from available data (e.g., parameters that can be identified as a feature of a plot of the data). Also, see [Seber and Wild](#) (Chapters 3 and 4 in [2003](#)). It is appealing if the stable parameters are interpretable (and usually they are, almost by definition). Because appropriate stable parameters are not unique and can be usefully defined in different ways, finding such stable parameters is as much art as science and often requires some trial-and-error experimentation for a particular model by using a collection of typical data sets. The goal is to have parameter estimates that are not highly correlated, improving the performance of estimation algorithms. Also, when Bayesian methods are to be used, stable parameters will generally simplify prior specification because such parameters typically have an easy-to-understand interpretation.

For some nonlinear regression models, it might be better to skip Step 3 and compute preliminary estimates directly for the stable parameters (because they are usually interpretable).

5. If needed, further transform the stable parameters so that they are unrestricted (e.g., take logs of positive parameters). Most estimation algorithms (ML or Bayesian MCMC) perform better when parameters are unrestricted. For clarity and consistency, we call this parameterization the “unrestricted stable parameterization” although it could also be called the “estimation parameterization.” Then one maps the preliminary estimates from Step 3 or 4 into estimates of the unrestricted stable parameters and use these as initial values to start the ML optimization.
6. Do the ML estimation. Check the results by computing the gradient vector (the elements should be close to zero) and the Hessian matrix (the eigenvalues should all be negative) of the log-likelihood evaluated at the maximum.
7. To check for estimability and as a diagnostic, especially in situations with a new model and kind of data, it is important to examine profile likelihood plots for individual parameters and parameter pairs, as described and illustrated in [Pascual and Meeker \(1999\)](#).
8. Translate ML parameter estimates back to ML estimates of the traditional parameterization that users would expect to see if unscaled data had been used. Also obtain the variance-covariance matrix for the traditional parameters using the vector version of the delta method (e.g., Section C.2 of [Meeker et al., 2022](#)).

### I.1.2 Summary of terminology

The steps for ML estimation outlined in Section I.1.1, as the first part of our “stable estimation” strategy, introduced several different layers of parameterization that have different purposes in the

model-building/inference process. Correspondingly, the section also described different levels of preliminary estimates leading to initial values to start the ML optimization. This section reviews the terminology relating to those definitions and the related rationale.

There is a hierarchy of parameterizations. To make the explanations concrete, we use Basquin model (Section 2.3.2 in the main paper) as a simple example. Thus the model is

$$\log(N) = \beta_0 + \beta_1 \log(S) + \sigma_N \epsilon.$$

- The *traditional parameters* for the original unscaled data are  $(\beta_0, \beta_1, \sigma_N)$ .
- After scaling data by dividing values of  $S$  by  $S_{\max}$  and values of  $N$  by  $N_{\max}$  the model form is the same but some of the parameters are scaled in a simple way. To simplify discussion and notation we will continue to use  $(\beta_0, \beta_1, \sigma_N)$  to denote these traditional parameterization after data scaling. For each of the particular models in the following sections, we will give explicit mappings between the estimates for the unscaled and the scaled data.
- For some models, there will be a modification to the traditional parameterization so that all parameters are interpretable. This step is especially important when prior distributions need to be specified by the analyst. For example an intercept (which may not have a practical interpretations) might be replaced by a quantile at a level of the explanatory variable(s) within the range of experience (e.g., where past data are available). This parameterization, in an application where a quantile replaces the intercept could be denoted by  $(t_p(S_0), \beta_1, \sigma_N)$  for some particular values of  $p$  and  $S_0$  will be called the “interpretable traditional parameters.”
- For some models, the interpretable traditional parameterization may have strong correlations between certain pairs of parameters. In that case, it is useful to find a stable parameterization. For example, with some of the  $S$ - $N$  models considered here, using fatigue life quantiles at extreme stress levels where failures were observed work well. We call these the “stable parameters.” Note that for some models, the interpretable traditional parameters will be stable so the additional changes described here will not be needed. For the Basquin model, the traditional parameters  $(t_p(S_0), \beta_1, \sigma_N)$  are also stable parameters.
- In some cases, the stable parameters will have restrictions (e.g., to be positive). Such parameters will be transformed to be unrestricted (e.g., by taking logarithms of any positive parameters) and the resulting parameters will be called “unrestricted stable parameters.” These are the parameters that are used in the optimization algorithms (both ML and Bayesian MCMC). For the Basquin model, the unrestricted stable parameters are  $(\log[t_p(S_0)], \beta_1, \log(\sigma_N))$ .

Initial values of the unrestricted stable parameters are needed to start the ML optimization algorithm. These are generally found by following steps.

- As described in Step 3 in Section I.1.1, one generally starts with simple preliminary estimates of the traditional parameters.

- The preliminary estimates are then used in a model-dependent manner (described for each of our models in Sections I.2–I.5) to make refinements to the preliminary estimates to assure that the resulting refined preliminary estimates will be in a part of the parameter space where the likelihood is nonnegligible and thus will provide safe “initial values” to start the ML optimization.
- Assuming that there are no serious estimability problems (see Section I.1.3), the optimization algorithm should produce valid ML estimates.

### I.1.3 Potential estimability problems

Sections I.1.1 and I.1.2 mentioned the important concept of stable parameters defined by Ross (1970, 1990). Sections I.2–I.5 provide the details of algorithms that we have tailored for the four five-parameter models that we have used for fatigue  $S$ - $N$  data that tend to exhibit convex-up curvature and increased spread at lower levels of stress. In situations where there is little or no concave-up curvature in the data plotted on log-log scales (e.g., low-cycle fatigue where all units are exposed to high levels of stress), the three-parameter Basquin model (Section 2.3.2 in the main paper) would likely be appropriate. In such situations, attempting to estimate all five unrestricted parameters could lead to situations where the maximum of the likelihood is in a region of the parameter space where one or more parameters is approaching minus infinity and/or the maximum may not be unique (due to flatness in the likelihood surface). We have designed our algorithms to detect such situations and provide suitable warnings. In such situations, one should attempt to fit the simpler Basquin model and carefully check model-fitting diagnostics (Section 4.3 of the main paper) to assure that the model is adequate.

### I.1.4 Steps for Bayesian prior specification and estimation

If continuing on to Bayesian estimation (where for now we use the same unrestricted stable parameters as estimation parameters and suppose that there is a desire or need to use noninformative or weakly informative prior distributions), we use the following steps to obtain default prior distributions, MCMC initial values and posterior draws via MCMC. In all cases, it is important to carefully examine MCMC diagnostics (especially trace plots for three or four independently drawn chains) and check the adequacy of the fit to the data.

1. Combining flat (i.e., uniform over the entire real line) marginal priors provide a natural default joint prior distribution for the stable, not highly correlated, unrestricted estimation parameters described in Steps 4 and 5 in Section I.1.1. In many cases, the flat prior for the estimation parameters will provide a good approximation to a reference prior (which would be difficult to establish exactly because of the right censoring typically seen at low levels of stress).
2. While the flat prior suggested in the previous step might work well for some model/data combinations, often it will lead to difficulties for the MCMC sampler attempting to obtain draws from the joint posterior (e.g., because the prior puts non-zero probability in nonsensical parts of the

parameter space where the log-likelihood evaluations are in the noise of the numerical computations). In extreme cases, the posterior may be improper (e.g., when there is little information in the data about one or more parameters). In such cases, one can replace the flat prior with an approximately flat normal (Gaussian) distribution with an extremely large standard deviation. Such an approximately noninformative (or weakly informative) prior will assure that the posterior is proper but will not assure that the MCMC sampler will accurately sample from the correct joint posterior distribution. We have encountered situations where the MCMC sampler finishes, the MCMC diagnostics look good, but the fitted model does not agree with the data (because “posterior draws” were being taken from one part of the approximately flat prior, far away from the likelihood).

3. When specifying a non-flat prior distribution (whether informative or weakly informative) we recommend using the “parameter-range” method of specifying a prior distribution, as used, for example, in [Meeker et al.](#) (Chapter 10 of [2022](#)). Instead of specifying a prior distribution and its parameters, specify instead the distribution and the 0.005 and 0.995 quantiles of the distribution. Such ranges are generally easier to elicit from subject-matter experts.
4. When the extremely wide normal distributions do not provide a satisfactory noninformative prior, it is necessary to use a weakly informative prior, usually represented by normal distributions with standard deviations that are not too large. To choose the center and standard deviation of those normal distribution one can use information such as the scale of ones data, previous experience and other engineering knowledge.
5. From our experience, having to specify weakly informative prior distributions in the manner described in Step 4 can take much time and may require some trial-and-error. Thus there is often a need to automate the process of finding *numerically-stable* default noninformative or minimally informative priors. Technically, one should not use information from the data to help set the prior distribution (doing so violates the likelihood principle). For example, it would be a serious mistake to use 95% or even 99% confidence intervals from the data to choose a prior distribution parameter range (doing so is like using the available data twice!). Nevertheless, from a practical point of view one can use the results of an ML estimation in a manner that can be shown to provide a prior distribution that is effectively noninformative and that avoids reuse of one’s data. For example, if Wald-like confidence intervals were computed using a factor of 50 standard errors instead of 1.96, the prior would be approximately flat over the part of the parameter space and somewhat beyond where the likelihood is nonnegligible. Weakly informative priors chosen in this way should be insensitive to the exact values of the mean and standard deviations of the specified normal distributions and this can be checked by doing sensitivity analysis (e.g., by generating a few hundred joint posterior draws and comparing for different settings of the prior-specification algorithm).
6. Following common practice, we run four independent chains so that we can use standard MCMC

diagnostics to check for convergence. MCMC initial values are obtained by sampling randomly, without replacement, from the vertices of a hyper-rectangle defined by the endpoints of 95% confidence intervals for the parameters. Doing this improves the chances that MCMC sampling will be from the joint posterior instead of some alternative low-level island of probability elsewhere in the parameter space.

7. After draws from the estimation-parameterization posterior have been computed and checked, compute and save posterior draws for the marginal distributions of the traditional parameters so that these can be used for post processing of the results to compute estimates and credible intervals for quantities of interest and make corresponding plots.

Exactly how these ideas are implemented depends on the particular model. Sections [I.2–I.5](#) provide details for the four models used, primarily, in our paper.

## I.2 Parameterization and Initial Values for the Box–Cox/Loglinear- $\sigma_N$ Model

The following is the  $S$ - $N$  curve defined under the traditional Box–Cox/Loglinear- $\sigma_N$  parameterization:

$$\log(N) = \beta_0 + \beta_1 \nu(S; \lambda) + \exp\left[\beta_0^{[\sigma]} + \beta_1^{[\sigma]} \log(S)\right] \Phi^{-1}(0.50),$$

where

$$\nu(S; \lambda) = \begin{cases} \frac{S^\lambda - 1}{\lambda} & \text{if } \lambda \neq 0 \\ \log(S) & \text{if } \lambda = 0, \end{cases}$$

is the Box–Cox power transformation, and  $\Phi^{-1}(0.50)$  is the median of the corresponding standard distribution.

We use the following steps to find the ML estimates:

1. Scale stress and lifetime by dividing by the largest values of each variable.
2. Find preliminary estimates for  $\beta_0$ ,  $\beta_1$ , and  $\lambda$ .
3. Find estimates for the shape parameter of the distribution of  $N$  at a high and a low stress level.
4. Map the preliminary estimates for the traditional parameters into preliminary estimates for the unrestricted stable parameters and use these as initial values to start the ML optimization.
5. Find the ML estimates by optimizing all parameters simultaneously, using the unrestricted stable parameterization (i.e., a parameterization for which parameters have no constraints).
6. Translate the ML estimates and estimated covariance matrix back to the traditional parameterization with unscaled data.

### I.2.1 Stable and unrestricted stable parameterizations

We suggest a parameterization consisting of four stable parameters  $\sigma_{\text{Low}}$ ,  $\sigma_{\text{High}}$ ,  $t_{\text{Low}}$ , and  $t_{\text{High}}$  that are one-to-one functions of the traditional parameterization regression coefficients  $(\beta_0, \beta_1, \beta_0^{[\sigma]}, \beta_1^{[\sigma]})$ . First,

$$\begin{aligned}\sigma_{\text{Low}} &= \exp[\beta_0^{[\sigma]} + \beta_1^{[\sigma]} \log(S_{\text{High}})] \\ \sigma_{\text{High}} &= \exp[\beta_0^{[\sigma]} + \beta_1^{[\sigma]} \log(S_{\text{Low}})]\end{aligned}\tag{76}$$

are the shape parameters of the distribution of  $N$  at stress levels  $S_{\text{High}}$  and  $S_{\text{Low}}$ , respectively. Then

$$\begin{aligned}t_{\text{Low}} &= \exp[\beta_0 + \beta_1 \nu(S_{\text{High}}; \lambda) + \sigma_{\text{Low}} \Phi^{-1}(0.50)] \\ t_{\text{High}} &= \exp[\beta_0 + \beta_1 \nu(S_{\text{Low}}; \lambda) + \sigma_{\text{High}} \Phi^{-1}(0.50)].\end{aligned}\tag{77}$$

are the medians of the distribution of  $N$  at stress levels  $S_{\text{High}}$  and  $S_{\text{Low}}$ , respectively. This stable parameterization avoids the high correlations between  $\lambda$  and regression coefficients in the traditional parameterization. Together with the power parameter  $\lambda$ ,  $\log(\sigma_{\text{Low}})$ ,  $\log(\sigma_{\text{High}})$ ,  $\log(t_{\text{Low}})$ , and  $\log(t_{\text{High}})$  provide an unrestricted stable parameterization.

### I.2.2 Initial values for $\beta_0$ , $\beta_1$ , and $\lambda$

First, fit a simple regression  $\log(N) \sim \log(S)$ , using all of the data. Use the estimates of  $\beta_0$ ,  $\beta_1$  and  $\lambda = 0$  for a nonlinear least squares fitting of the model  $\log(N) \sim \nu(S; \lambda)$ , providing initial values for  $\beta_0$ ,  $\beta_1$ , and  $\lambda$ . To keep this preliminary estimation simple, it is sufficient to ignore censoring (e.g., by taking the censored observations to be failures at the censoring times).

### I.2.3 Initial values for the unrestricted stable estimation parameters

Especially when using a stable parameterization, the initial values to start ML estimation do not have to be accurate. In most cases, they only need to be in the region where the likelihood is nonnegligible. The initial values for  $\log(\sigma_{\text{Low}})$  and  $\log(\sigma_{\text{High}})$  are obtained as follows. Recall that  $\log(\sigma)$  tends to be smaller at larger levels of stress. To find the initial value for  $\log(\sigma_{\text{Low}})$  use the data at the highest levels of stress (e.g., divide the data into two parts), fit the single distribution and take the log of the resulting ML estimate for  $\sigma$ . Do the same using the lowest levels of stress to find the initial value for  $\log(\sigma_{\text{High}})$ . Then calculate the initial values for  $t_{\text{Low}}$  and  $t_{\text{High}}$  by substituting the initial values for  $\beta_0$ ,  $\beta_1$ , and  $\lambda$  from Section I.2.2, into (77) and taking logs.

### I.2.4 ML estimates for the stable parameters

When there is sufficient data for parameters to be estimable, ML iterations using the unrestricted stable estimation parameters and initial values suggested above should be successful. To recover the ML estimates of the traditional parameters from this reparameterization, solve (76) for  $\beta_1^{[\sigma]}$  and  $\beta_0^{[\sigma]}$

giving:

$$\begin{aligned}\beta_1^{[\sigma]} &= \frac{\log(\sigma_{\text{High}}) - \log(\sigma_{\text{Low}})}{\log(S_{\text{Low}}) - \log(S_{\text{High}})} \\ \beta_0^{[\sigma]} &= \log(\sigma_{\text{Low}}) - \beta_1^{[\sigma]} \log(S_{\text{High}}).\end{aligned}$$

Then solve (77) for  $\beta_1$  and  $\beta_0$  giving:

$$\begin{aligned}\beta_1 &= \frac{[\log(t_{\text{High}}) - \log(t_{\text{Low}})] - (\sigma_{\text{High}} - \sigma_{\text{Low}})\Phi^{-1}(0.50)}{\nu(S_{\text{Low}}; \lambda) - \nu(S_{\text{High}}; \lambda)} \\ \beta_0 &= \log(t_{\text{Low}}) - \beta_1 \nu(S_{\text{High}}; \lambda) - \sigma_{\text{Low}}\Phi^{-1}(0.50).\end{aligned}$$

where the evaluations are done at the ML estimates.

### I.2.5 ML estimates for the traditional parameters based on the original unscaled data

In the previous steps, ML estimates were obtained using scaled data, as described in Step 1 of Section I.1.1. We denote the estimates from the scaled data by  $\tilde{\beta}_0$ ,  $\tilde{\beta}_1$ ,  $\tilde{\lambda}$ ,  $\tilde{\beta}_0^{[\sigma]}$ , and  $\tilde{\beta}_1^{[\sigma]}$ , where the scaling values are  $S_{\text{max}}$  and  $N_{\text{max}}$  for stress and number of cycles, respectively. Then the Box–Cox/Loglinear- $\sigma_N$   $S$ - $N$  model under scaled data is:

$$\log(\tilde{N}) = \tilde{\beta}_0 + \tilde{\beta}_1 \nu(\tilde{S}; \tilde{\lambda}) + \exp\left[\tilde{\beta}_0^{[\sigma]} + \tilde{\beta}_1^{[\sigma]} \log(\tilde{S})\right] \Phi^{-1}(0.50),$$

where  $\tilde{S}$  and  $\tilde{N}$  are the scaled stress and number of cycles, respectively. In terms of the original unscaled data, the model is:

$$\begin{aligned}\log(N) &= \log(N_{\text{max}}) + \tilde{\beta}_0 + \tilde{\beta}_1 \nu(\tilde{S}; \tilde{\lambda}) + \exp\left[\tilde{\beta}_0^{[\sigma]} - \tilde{\beta}_1^{[\sigma]} \log(S_{\text{max}}) + \tilde{\beta}_1^{[\sigma]} \log(S)\right] \Phi^{-1}(0.50) \\ &= \log(N_{\text{max}}) + \tilde{\beta}_0 - \frac{\tilde{\beta}_1}{S_{\text{max}}^{\tilde{\lambda}}} \nu(S_{\text{max}}; \tilde{\lambda}) + \frac{\tilde{\beta}_1}{S_{\text{max}}^{\tilde{\lambda}}} \nu(S; \tilde{\lambda}) + \exp\left[\tilde{\beta}_0^{[\sigma]} - \tilde{\beta}_1^{[\sigma]} \log(S_{\text{max}}) + \tilde{\beta}_1^{[\sigma]} \log(S)\right] \Phi^{-1}(0.50),\end{aligned}$$

which follows from the result:

$$\nu(\tilde{S}; \tilde{\lambda}) = \frac{1}{S_{\text{max}}^{\tilde{\lambda}}} \left[ \nu(S; \tilde{\lambda}) - \nu(S_{\text{max}}; \tilde{\lambda}) \right].$$

Therefore, the ML estimates for the traditional parameters based on the original unscaled data are:

$$\begin{aligned}\widehat{\beta}_0 &= \log(N_{\max}) + \widetilde{\beta}_0 - \frac{\widetilde{\beta}_1}{S_{\max}^{\widetilde{\lambda}}} \nu(S_{\max}; \widetilde{\lambda}) \\ \widehat{\beta}_1 &= \frac{\widetilde{\beta}_1}{S_{\max}^{\widetilde{\lambda}}} \\ \widehat{\lambda} &= \widetilde{\lambda} \\ \widehat{\beta}_0^{[\sigma]} &= \widetilde{\beta}_0^{[\sigma]} - \widetilde{\beta}_1^{[\sigma]} \log(S_{\max}) \\ \widehat{\beta}_1^{[\sigma]} &= \widetilde{\beta}_1^{[\sigma]}.\end{aligned}$$

### I.3 Parameterization and Initial Values for the Coffin–Manson Model

The Coffin–Manson model is described in Section 5.5 of the main paper. The following is the Coffin–Manson relationship using the traditional model parameterization:

$$S = A_{el}(2N)^b + A_{pl}(2N)^c,$$

where the parameters are  $A_{el} > 0$ ,  $A_{pl} > 0$ ,  $b < 0$ ,  $c < 0$ , and  $|c| > |b|$ . The last inequality makes the model identifiable.

We use the following steps to find the ML estimates:

1. Scale stress and lifetime by dividing by the largest values of each variable.
2. Find preliminary estimates for the traditional parameters.
3. Find a preliminary estimate for  $\log(\sigma_X)$  using conditional ML, conditioning on the preliminary estimates from Step 2.
4. Map the preliminary estimates for the traditional parameters into preliminary estimates for the unrestricted stable parameters and use these as initial values to start the ML optimization.
5. Find the ML estimates by optimizing all parameters simultaneously, using unrestricted stable parameterization.
6. Translate the ML estimates and estimated covariance matrix back to the traditional parameterization based on the original unscaled data.

#### I.3.1 Stable and unrestricted stable parameterizations

We suggest a parameterization consisting of five positive stable parameters  $x_{\text{Low}}$ ,  $x_{\text{High}}$ ,  $\beta$ , and  $\delta$ , and  $\sigma_X$  that are one-to-one functions of the traditional parameterization regression coefficients ( $A_{el}$ ,  $A_{pl}$ ,

$b$ ,  $c$ , and  $\sigma_X$ ). First,

$$\begin{aligned} x_{\text{Low}} &= A_{el}(2N_{\text{High}})^b + A_{pl}(2N_{\text{High}})^c \\ x_{\text{High}} &= A_{el}(2N_{\text{Low}})^b + A_{pl}(2N_{\text{Low}})^c \end{aligned} \quad (78)$$

are the Coffin–Manson equation values at a large  $N_{\text{High}}$  value and a small  $N_{\text{Low}}$  value, respectively. We use the maximum and minimum uncensored  $N$  values in the data. Then

$$\begin{aligned} \beta &= |b| > 0 \\ \delta &= b - c > 0. \end{aligned} \quad (79)$$

are, respectively, the absolute value of the elastic regime slope and the positive difference between the elastic and plastic regime slopes. This stable parameterization reduces the correlations between pairs of parameters estimates. The quantities  $x_{\text{Low}}$  and  $x_{\text{High}}$  are the Coffin–Manson equation evaluated at a large  $N_{\text{High}}$  value and a small  $N_{\text{Low}}$  value, respectively. Then  $\log(x_{\text{Low}})$ ,  $\log(x_{\text{High}})$ ,  $\log(\beta)$ ,  $\log(\delta)$ , and  $\log(\sigma_X)$  are unrestricted stable parameters used in ML estimation.

### I.3.2 Initial values for the traditional parameters

As described in Section 5.5, the Coffin–Manson  $S$ - $N$  relationship can be interpreted as the sum of two Basquin relationships. These two Basquin relationships are asymptotes for the  $S$ - $N$  relationship. As such, the model is quite flexible. Section 5.8 of the main paper describes the effect that coordinate asymptotes (either horizontal or horizontal) have on modeling  $S$ - $N$  data. In our extensive numerical experiments (using 18 different data sets) we discovered that more than one method was needed to find initial values for the traditional parameters, depending on whether the data suggested that one of the Basquin lines approaches either a horizontal (not uncommon and occurs when there is evidence in the data that a fatigue limit exists) or a vertical (uncommon, but such data sets do exist) asymptote or not. The three different methods are described in the rest of this section. We suggest trying all three methods, evaluating the likelihood as the resulting estimates (if there are no NaNs returned) and then choosing as initial values for starting the ML iterations the estimates from the method that has the highest likelihood.

**Method 1** This method generally works well unless one of the Basquin lines approaches a coordinate asymptote.

1. Fit a simple regression:  $\log(S) \sim \log(2N)$ , using all data (treating runouts as failures). The estimates of intercept and slope are  $\hat{b}_0$  and  $\hat{b}_1$ .
2. Set initial values of four parameters using the estimates from the previous step:  $A_{el} = A_{pl} = \hat{b}_0/2$ , and  $b = c = \hat{b}_1$ .

3. Fit a nonlinear least squares:  $S \sim A_{el}(2N)^b + A_{pl}(2N)^c$  (again treating runouts as failures) to get better starting values of the four parameters.
4. Reorder the parameters to obey the inequality constraints.

**Method 2** This method works well when one of the Basquin lines approaches a horizontal asymptote.

1. Do the same as the Step 1 in Method 1.
2. Set initial values of the plastic Basquin-line parameters using the estimates from the previous step:  $A_{pl} = \hat{b}_0$ , and  $c = \hat{b}_1$ . And set  $A_{el}$  to some value a little bit lower than the lowest level of stress (e.g. 0.9 times the lowest level of stress). Set  $b$  to a number close to zero, e.g.  $b = c \times 10^{-5}$ .
3. Fit a nonlinear least squares (again, treating runouts as failures):  $S \sim A_{el}(2N)^b + A_{pl}(2N)^c$  to get a better value for  $A_{pl}$ , while fixing all other three parameters.

**Method 3** This method works well when one of the Basquin lines approaches a vertical asymptote.

1. Do the same as the Step 1 in Method 1.
2. Slightly different from Step 2 in Method 2, set initial values of the elastic Basquin-line parameters by using the estimates from previous step:  $A_{el} = \hat{b}_0$ , and  $b = \hat{b}_1$ . Then In the log-log plot of the  $S$ - $N$  curve, find a straight line with a steep slope (e.g.  $c = b \times 100$ ) and also through a point which is to the left of the top-left observation in the plot. We choose a line which is not very distant from the observations, but also far enough so that the line does not pass through observations in the plot.
3. Similar to the Step 3 in Method 2, we find a better value for  $A_{el}$  by fixing the other three parameters and use nonlinear least squares to fit:  $S \sim A_{el}(2N)^b + A_{pl}(2N)^c$ .

### I.3.3 Initial value for $\log(\sigma_X)$

Using the preliminary estimates for the four traditional parameters, we can obtain a preliminary estimate of  $\log(\sigma_X)$  by maximizing the conditional log-likelihood, conditioning on the preliminary estimates for the four traditional parameters.

### I.3.4 Initial values for the unrestricted stable estimation parameters

Especially when using a stable parameterization, the initial values to start ML estimation do not have to be accurate. In most cases, they only need to be in the region where the likelihood is nonnegligible. The initial values for  $\log(x_{\text{Low}})$ ,  $\log(x_{\text{High}})$ ,  $\log(\beta)$ ,  $\log(\delta)$ , and  $\log(\sigma_X)$  are obtained by evaluating the equations in Section I.3.1 at the initial values for traditional parameters found in Section I.3.2.

### I.3.5 ML estimates for the stable parameters

When there is sufficient data for parameters to be estimable, ML iterations using the unrestricted stable estimation parameters and initial values suggested above should be successful. To recover the traditional parameters from the unrestricted ones, first one needs to recover  $b$  and  $c$  from  $\beta$  and  $\delta$  by:

$$\begin{aligned} b &= -\beta \\ c &= -\beta - \delta. \end{aligned}$$

Then solve (78) for  $A_{el}$  and  $A_{pl}$ , giving

$$\begin{aligned} A_{pl} &= \frac{x_{\text{Low}}/(2N_{\text{High}})^b - x_{\text{High}}/(2N_{\text{Low}})^b}{(2N_{\text{High}})^c/(2N_{\text{High}})^b - (2N_{\text{Low}})^c/(2N_{\text{Low}})^b} \\ A_{el} &= \frac{x_{\text{High}}}{(2N_{\text{Low}})^b} - \frac{(2N_{\text{Low}})^c}{(2N_{\text{Low}})^b} A_{pl}, \end{aligned}$$

where the evaluations are done at the ML estimates.

### I.3.6 ML estimates for the traditional parameters based on the original, unscaled data

In the previous steps, ML estimates were obtained using scaled data, as described in Step 1 of Section I.1.1. We denote the estimates from the scaled data by  $\tilde{A}_{pl}$ ,  $\tilde{b}$ ,  $\tilde{A}_{el}$ , and  $\tilde{c}$ , where the scaling values are  $S_{\text{max}}$  and  $N_{\text{max}}$  respectively for stress and number of cycles. Then the Coffin–Manson equation under scaled data is:

$$\tilde{S} = \tilde{A}_{el}(2\tilde{N})^{\tilde{b}} + \tilde{A}_{pl}(2\tilde{N})^{\tilde{c}},$$

where  $\tilde{S}$  and  $\tilde{N}$  are scaled stress and lifetime. In terms of the original data and scaling factor, the relationship is:

$$S = S_{\text{max}}\tilde{A}_{el}N_{\text{max}}^{-\tilde{b}}(2N)^{\tilde{b}} + S_{\text{max}}\tilde{A}_{pl}N_{\text{max}}^{-\tilde{c}}(2N)^{\tilde{c}}.$$

Therefore, the ML estimates for the traditional parameters based on the original unscaled data are:

$$\begin{aligned} \hat{A}_{el} &= S_{\text{max}}\tilde{A}_{el}N_{\text{max}}^{-\tilde{b}} \\ \hat{A}_{pl} &= S_{\text{max}}\tilde{A}_{pl}N_{\text{max}}^{-\tilde{c}} \\ \hat{b} &= \tilde{b} \\ \hat{c} &= \tilde{c}. \end{aligned}$$

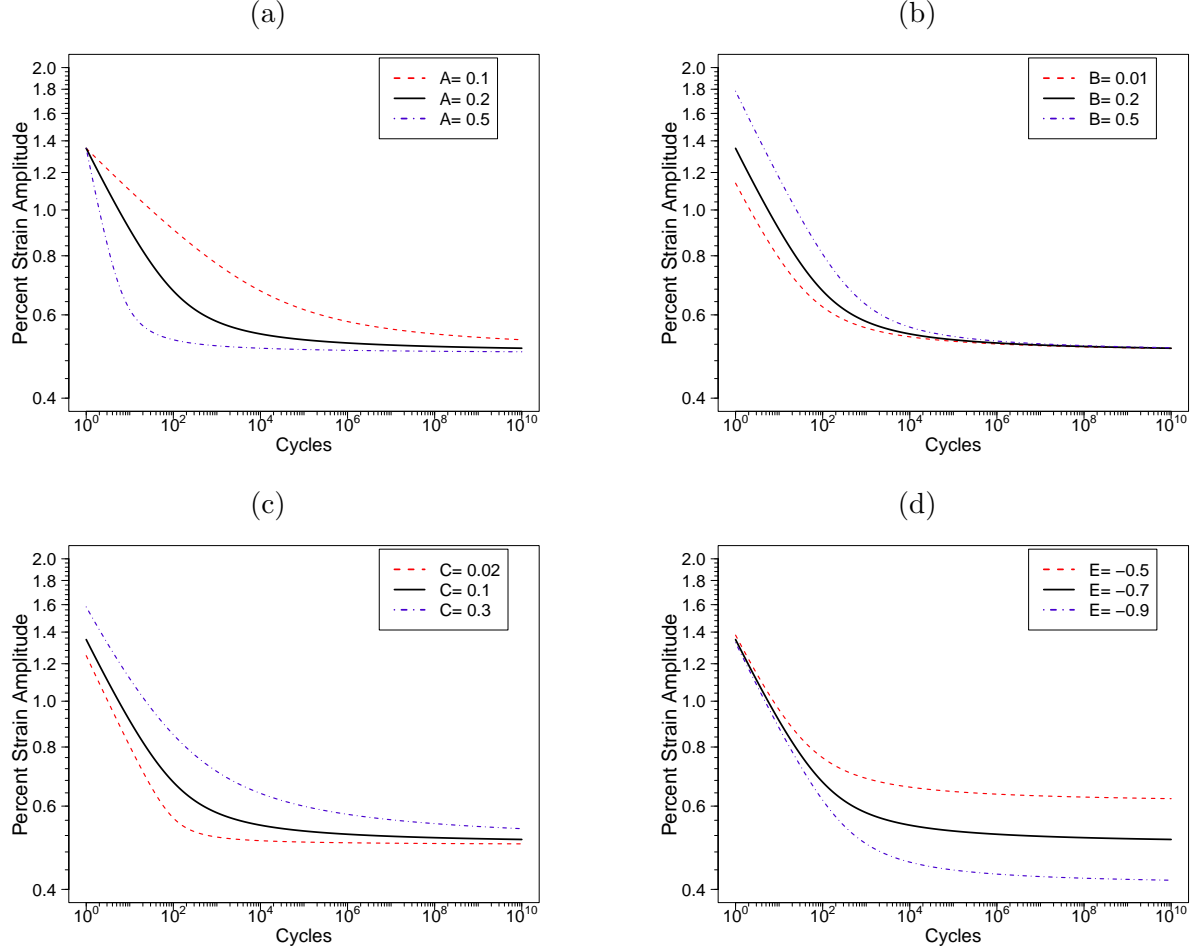


Figure 20: The [Nishijima \(1980, 1985\)](#) hyperbolic  $S$ - $N$  model varying  $A$ , the negative of the slope of the large- $S$  asymptote (a);  $B$ , the intercept of the large- $S$  asymptote (b);  $C$ , the square of the vertical distance between the  $S$ - $N$  curve and the asymptote-intersection point (c); and  $E$ , the horizontal asymptote (log fatigue-limit) (d) parameters.

#### I.4 Parameterization and Initial Values for the Nishijima Hyperbolic Model

The Nishijima hyperbolic model is described in Section 5.4 of the main paper. Figure 5(c) displays the Nishijima  $S$ - $N$  relationship in a way that illustrates the meaning of the relationship parameters. Figure 20 shows the effect of changing one parameter at a time.

The Nishijima relationship, using the traditional model parameterization is

$$S = h(N; \beta) = \exp \left( \frac{-A \log(N) + B + E + \sqrt{[A \log(N) - (B - E)]^2 + 4C}}{2} \right) \quad (80)$$

where  $A$ ,  $B$ ,  $C$ , and  $E$  are the regression model parameters constrained by following inequalities:

$$\begin{aligned} A &> 0, \\ C &> 0. \end{aligned}$$

We use this five-step strategy to find the ML estimates:

1. Scale stress and lifetime by dividing by the largest values of each variable.
2. Find preliminary estimates for the traditional parameters.
3. Find a preliminary estimate for  $\log(\sigma_X)$  using conditional ML, conditioning on the preliminary estimates from the previous step.
4. Find the ML estimates by optimizing all parameters simultaneously, using an unrestricted parameterization.
5. Translate the ML estimates and estimated covariance matrix back to the traditional parameterization.

#### I.4.1 Preliminary estimates for $A$ , $B$ , $C$ , and $E$

The parameter  $A$  is the negative of the slope of the small- $N$  asymptote seen in Figure 5(c). The parameter  $B$  is the  $\log(N) = 0$  intercept of the small- $N$  asymptote. It usually suffices to use a simple linear regression  $\log(N) \sim b_0 + b_1 \log(S)$  on the upper left portion of the data (larger levels of stress) as a first step and denote these estimates of the intercept and slope by  $\hat{b}_0$  and  $\hat{b}_1$ . Here we fit a regression along the vertical axis of the log-log scaled  $S$ - $N$  plot, not the conventional horizontal axis. Then the initial value of  $A$  is  $-1/\hat{b}_1$ .

When experimental data are collected at a few stress levels, using a couple of the highest stress levels works well. When data are scattered at various levels, and there are just a few observations at individual levels, using a proportion (say 30%) of the data points with the highest stress values should suffice. Then we shift the fitted line to the left to depict the initial guess of the asymptote line associated with the upper left  $S$ - $N$  hyperbola. We found the algorithm behaves well by shifting by the size of a prediction interval  $\Delta$  of the regression within the data range. The initial asymptote line is  $\log(N) = \hat{b}_0 - \Delta + \hat{b}_1 \log(S)$ .

To find the initial value for  $E$ , use the logarithm of a value that is slightly smaller than the smallest stress level where there were failures. Find the horizontal coordinate of the intersection between the horizontal asymptote  $E$  and the previously obtained hyperbola asymptote line. The x-coordinate of the intersection is  $x = \hat{b}_0 - \Delta + \hat{b}_1 E$ . Solve  $x = (B - E)/A$  to get  $B$ . That is  $B = xA + E$ .

Then use a simple optimization to get the initial value for  $C$  while fixing other parameters to their initial values. This can be treated as a root finding problem for  $C$ , by solving  $\sqrt{C} = h(N; \beta) - E$ , where  $h$  function is defined in (80). Or it can also be treated as a nonlinear least

squares curve fitting problem, by fitting the  $S$ - $N$  curve using  $h(N; \beta)$ . To start, use the relationship  $[\log(S) - E][\log(S) + A \log(N) - B] = C$ , with any pair of stress-life values in the data and initial values for  $A$ ,  $B$ , and  $E$  to get an initial value for  $C$  using this optimization.

#### I.4.2 Initial value for $\log(\sigma_X)$

Using the preliminary estimates for the four parameters, we can obtain a preliminary estimate of  $\log(\sigma_X)$  by maximizing the conditional log-likelihood, conditioning on the four traditional parameters. The initial value for  $\log(\sigma_X)$  is obtained by fitting stress observations to the specified strength distribution type.

#### I.4.3 Unrestricted likelihood reparameterization

After finding the preliminary estimates for all parameters, the next step is to use them to define an unrestricted parameterization. We found a stable unrestricted parameterization that uses five parameters  $\log(x_{\text{Low}})$ ,  $\log(x_{\text{High}})$ ,  $\log(C)$ ,  $E$ , and  $\log(\sigma_X)$ , where

$$\begin{aligned}\log(x_{\text{Low}}) &= \log[h(N_{\text{High}}; \beta)] \\ \log(x_{\text{High}}) &= \log[h(N_{\text{Low}}; \beta)]\end{aligned}$$

and the  $h$  function is defined in (80). This parameterization results in relatively low correlations among the parameters. The quantities  $x_{\text{Low}}$  and  $x_{\text{High}}$  correspond to  $h(N; \beta)$  evaluated at  $N_{\text{High}}$  and  $N_{\text{Low}}$  the maximum and minimum values of  $N$  in the data, respectively. Correspondingly, in that case,  $x_{\text{Low}}$  and  $x_{\text{High}}$  are close to the lowest and highest stress levels in the data.

To recover  $A$  and  $B$  from the above parameterization, solve the following small system of linear equations to recover  $A$  and  $B$ :

$$\begin{aligned}A \log(N_{\text{High}}) - B &= C/(\log(x_{\text{Low}}) - E) - \log(x_{\text{Low}}) \\ A \log(N_{\text{Low}}) - B &= C/(\log(x_{\text{High}}) - E) - \log(x_{\text{High}})\end{aligned}$$

in which  $A$  and  $B$  are the only unknown quantities.

#### I.4.4 ML estimates for the traditional parameters based on the original unscaled data

In the previous steps, ML estimates were obtained using scaled data, as described in Step 1 of Section I.1.1. We denote the estimates from the scaled data by  $\tilde{A}$ ,  $\tilde{B}$ ,  $\tilde{C}$ , and  $\tilde{E}$ , where the scaling values are  $S_{\text{max}}$  and  $N_{\text{max}}$  respectively for stress and number of cycles. The ML parameter estimates for the

traditional parameter based on the original unscaled data are:

$$\begin{aligned}
\hat{A} &= \tilde{A} \\
\hat{C} &= \tilde{C} \\
\hat{E} &= \tilde{E} + \log(S_{\max}) \\
\hat{B} &= \tilde{B} + \log(S_{\max}) + \tilde{A} \log(N_{\max}).
\end{aligned} \tag{81}$$

To see why, we express  $[\log(S) - \hat{E}] [\log(S) + \hat{A} \log(N) - \hat{B}] = \hat{C}$  in terms of scaling values and parameters for scaled data as follows:

$$\left[ \log\left(\frac{S}{S_{\max}}\right) - \tilde{E} \right] \left[ \log\left(\frac{S}{S_{\max}}\right) + \tilde{A} \log\left(\frac{N}{N_{\max}}\right) - \tilde{B} \right] = \tilde{C}.$$

After rearrangement, the above expression is equivalent to the following expression:

$$\left[ \log(S) - (\tilde{E} + \log(S_{\max})) \right] \left[ \log(S) + \tilde{A} \log(N) - (\tilde{B} + \log(S_{\max}) + \tilde{A} \log(N_{\max})) \right] = \tilde{C},$$

which implies the parameter mapping in (81).

## I.5 Parameterization and Initial Values for the Random Fatigue Limit Model

The following is the  $S$ - $N$  curve defined by the traditional Random Fatigue Limit (RFL) model parameterization from Section 5.6 of the main paper. In particular, the logarithm of the fatigue-life random variable median is

$$\log(N) = \beta_0 + \beta_1 \log(S - \gamma) + \sigma_\epsilon \Phi^{-1}(0.50), \tag{82}$$

where  $\gamma$  is a random parameter having a log-location-scale distribution and  $\Phi^{-1}(0.50)$  is the median of the corresponding standard distribution for  $N$ . The cdf of the logarithm of  $\gamma$  is

$$\Pr[\log(\gamma) < \log(c)] = \Phi_\gamma\left(\frac{\log(c) - \mu_\gamma}{\sigma_\gamma}\right).$$

If  $\gamma$  is a fixed parameter, (82) is the median of the Stromeier model.

We suggest the following five-step strategy to find the ML estimates for the RFL model:

1. Scale stress and lifetime by dividing by the largest values of each variable.
2. Fit the data to the Stromeier model and get ML estimates for  $\beta_0$ ,  $\beta_1$ ,  $\gamma$ , and  $\sigma_\epsilon$ .
3. Find a preliminary estimate for  $\sigma_\gamma$ .
4. Using the results from Steps 2 and 3, find the ML estimates for the RFL model by optimizing all parameters simultaneously, using an unrestricted parameterization.

5. Translate the ML estimates and estimated covariance matrix back to the traditional parameters based on the original unscaled data.

### I.5.1 ML estimates for the Stromeier model

First, fit a simple regression  $\log(N) \sim \log(S)$ , using all of the data. The estimates of the intercept and slope are  $\hat{b}_0$  and  $\hat{b}_1$ , respectively. Fit the nonlinear least squares model  $\log(N) \sim \log(S - \gamma)$ , using  $\hat{b}_0$  and  $\hat{b}_1$  as starting values for two corresponding coefficients and 0 as the starting value for  $\gamma$  in the nonlinear model. The results provide initial values for  $\beta_0$ ,  $\beta_1$ , and  $\gamma$ . If the preliminary estimate of  $\gamma$  in the previous step is not positive, fix its value to be half of the smallest stress level where there was at least one failure. Then fit the nonlinear least squares model again to get the estimates for  $\beta_0$  and  $\beta_1$ .

Then use all data to obtain a preliminary estimate for  $\sigma_\epsilon$ . After finding the preliminary estimates for the Stromeier model parameters, we use them to find ML estimates of the Stromeier model parameters. Notice,  $\gamma$  must be between zero and the smallest stress level where there was at least one failure. We use an unrestricted reparameterization to estimate the parameters. Then we use the logarithm of the estimate of  $\gamma$  as the preliminary estimate for  $\mu_\gamma$  in the RFL model.

### I.5.2 Initial value for $\sigma_\gamma$

To get an initial value for  $\sigma_\gamma$ , we maximize the conditional log-likelihood of the RFL model, conditioning on the preliminary estimates of other parameters.

### I.5.3 Stable unrestricted likelihood parameterization

We found stable unrestricted parameters that are one-to-one functions of the traditional parameters:

$$\begin{aligned}\log(t_{\text{Low}}) &= \beta_0 + \beta_1 \log(S_{\text{High}} - \gamma_0) + \sigma_\epsilon \Phi^{-1}(0.50) \\ \log(t_{\text{High}}) &= \beta_0 + \beta_1 \log(S_{\text{Low}} - \gamma_0) + \sigma_\epsilon \Phi^{-1}(0.50) \\ \log(c_\gamma) &= \mu_\gamma + \sigma_\gamma \Phi_\gamma^{-1}(0.50)\end{aligned}$$

as well as  $\log(\sigma_\gamma)$  and  $\log(\sigma_\epsilon)$  where  $\gamma_0$  is a value between zero and the smallest stress level where there was at least one failure,  $\Phi^{-1}(0.50)$  is the median of the standard location-scale distribution for  $N$ , and  $\Phi_\gamma^{-1}(0.50)$  is the median of the standard location-scale distribution for  $\gamma$ . In our experiments, we use the ML estimate of  $\gamma$  from the Stromeier model for  $\gamma_0$ . In this parameterization,  $\log(t_{\text{Low}})$  is the median of  $\log(N)$  at a high stress level  $S_{\text{High}}$ , conditional on  $\gamma = \gamma_0$ . Similarly,  $\log(t_{\text{High}})$  is the median of  $\log(N)$  at a low stress level  $S_{\text{Low}}$ . We used the largest stress level for  $S_{\text{High}}$  and the smallest stress level with at least one failure for  $S_{\text{Low}}$ . The parameter  $\log(c_\gamma)$  is the logarithm of the median of  $\gamma$ . The initial values for the new parameters are calculated using initial values for  $\beta_0$ ,  $\beta_1$ ,  $\mu_\gamma$ ,  $\sigma_\gamma$ , and  $\sigma_\epsilon$  from the previous steps.

To recover the traditional parameters from this reparameterization, one first recovers three parameters:

$$\begin{aligned}\sigma_\gamma &= \exp[\log(\sigma_\gamma)] \\ \mu_\gamma &= \log(c_\gamma) - \sigma_\gamma \Phi_\gamma^{-1}(0.50) \\ \sigma_\epsilon &= \exp[\log(\sigma_\epsilon)].\end{aligned}$$

Then to recover  $\beta_0$  and  $\beta_1$ , solve the simple system of linear equations:

$$\begin{aligned}\log(t_{\text{Low}}) &= \beta_0 + \beta_1 \log(S_{\text{High}} - \gamma_0) + \sigma_\epsilon \Phi^{-1}(0.50) \\ \log(t_{\text{High}}) &= \beta_0 + \beta_1 \log(S_{\text{Low}} - \gamma_0) + \sigma_\epsilon \Phi^{-1}(0.50).\end{aligned}$$

#### I.5.4 ML estimates for the traditional parameters based on the original unscaled data

From previous steps, the ML estimates using scaled data are denoted by  $\tilde{\beta}_0$ ,  $\tilde{\beta}_1$ ,  $\tilde{\mu}_\gamma$ ,  $\tilde{\sigma}_\gamma$ , and  $\tilde{\sigma}_\epsilon$ . The scaling values were  $S_{\text{max}}$  and  $N_{\text{max}}$  for stress and lifetime, respectively. The RFL model  $S$ - $N$  equation using scaled data is

$$\log(\tilde{N}) = \tilde{\beta}_0 + \tilde{\beta}_1 \log(\tilde{S} - \tilde{\gamma}) + \tilde{\sigma}_\epsilon \Phi^{-1}(0.50),$$

where  $\tilde{S}$  and  $\tilde{N}$  are scaled stress and lifetime and the cdf of the logarithm of the random fatigue limit in the scaled model is

$$\Pr[\log(\tilde{\gamma}) < \log(c)] = \Phi_\gamma\left(\frac{\log(c) - \mu_\gamma}{\sigma_\gamma}\right).$$

In terms of the original data and scaling values, the relationship is:

$$\log(N) = \log(N_{\text{max}}) + \tilde{\beta}_0 - \tilde{\beta}_1 \log(S_{\text{max}}) + \tilde{\beta}_1 \log(S - S_{\text{max}} \tilde{\gamma}) + \tilde{\sigma}_\epsilon \Phi^{-1}(0.50).$$

Therefore, the ML parameter estimates for the traditional parameters based on the original unscaled data are:

$$\begin{aligned}\hat{\beta}_0 &= \log(N_{\text{max}}) + \tilde{\beta}_0 - \tilde{\beta}_1 \log(S_{\text{max}}) \\ \hat{\beta}_1 &= \tilde{\beta}_1 \\ \hat{\mu}_\gamma &= \log(S_{\text{max}}) + \tilde{\mu}_\gamma \\ \hat{\sigma}_\gamma &= \tilde{\sigma}_\gamma \\ \hat{\sigma}_\epsilon &= \tilde{\sigma}_\epsilon.\end{aligned}$$

## J More Details from the Data Analysis/Modeling Examples

The data analysis/modeling examples in the main paper focus on the main features of the fitted models. To save space, less interesting, but potentially useful details are presented in this section.

### J.1 More Details for the Box–Cox/Loglinear- $\sigma_N$ $S$ - $N$ Model Fit to the Laminate Panel Data

Example 2.2 in the main paper gives a summary of the results of fitting the Box–Cox/loglinear- $\sigma_N$   $S$ - $N$  model to the laminate panel data.

#### J.1.1 Model and prior distributions

The lognormal distribution regression model fit to the laminate panel data was

$$\begin{aligned}\log(N) &= \mu(S) + \sigma(S)\epsilon. \\ \mu(S) &= \beta_0 + \beta_1[\nu(S/S_{\max}; \lambda) - \nu(S_{\mu 0}; \lambda)] \\ &= \beta_0^* + \beta_1\nu(S/S_{\max}; \lambda). \\ \sigma(S) &= \beta_0^{[\sigma]} + \beta_1^{[\sigma]}[\log(S/S_{\max}) - \log(S_{\sigma 0})] \\ &= \beta_0^{*[\sigma]} + \beta_1^{[\sigma]}\log(S/S_{\max}),\end{aligned}\tag{83}$$

where stress  $S$  was scaled for numerical reasons,  $S_{\mu 0}$  and  $S_{\sigma 0}$  are centering values that can be used to reduce the correlation between the model's intercept and slope, and

$$\nu(S; \lambda) = \begin{cases} \frac{S^\lambda - 1}{\lambda} & \text{if } \lambda \neq 0 \\ \log(S) & \text{if } \lambda = 0, \end{cases}$$

is the Box–Cox power transformation, and  $\epsilon \sim \text{NORM}(0, 1)$ .

The prior distribution for  $\beta_0^*$ ,  $\beta_1$ ,  $\beta_0^{*[\sigma]}$ , and  $\beta_1^{[\sigma]}$  were flat and the prior distribution for  $\lambda$  was  $\text{NORM}(-8, 2)$  (a normal distribution with its 0.005 quantile equal to  $-8$  and its 0.995 quantile equal to  $2$ ).

#### J.1.2 Posterior draws and parameter estimates

The following table is a summary of the posterior draws.

```
Inference for Stan model: BoxCoxLogLinSigma. 4 chains, each with
iter=30000; warmup=5000; thin=5; post-warmup draws per chain=5000,
total post-warmup draws=20000.
```

mean	se_mean	sd	2.5%	25%	50%	75%	97.5%	n_eff	Rhat
------	---------	----	------	-----	-----	-----	-------	-------	------

intercept	4.22	0.001	0.070	4.08	4.17	4.22	4.265	4.357	19563	1
slope	-11.01	0.007	0.987	-13.02	-11.65	-10.99	-10.346	-9.155	19536	1
intercept_log_sigma	-1.02	0.001	0.121	-1.25	-1.11	-1.03	-0.944	-0.776	19427	1
slope_log_sigma	-1.60	0.004	0.542	-2.65	-1.97	-1.60	-1.232	-0.531	18892	1
lambda	-2.13	0.003	0.487	-3.09	-2.45	-2.13	-1.804	-1.173	19560	1

Figure 21(a) shows trace plots for the parameters (indicating good mixing) and Figure 21(b) the corresponding pairs plot.

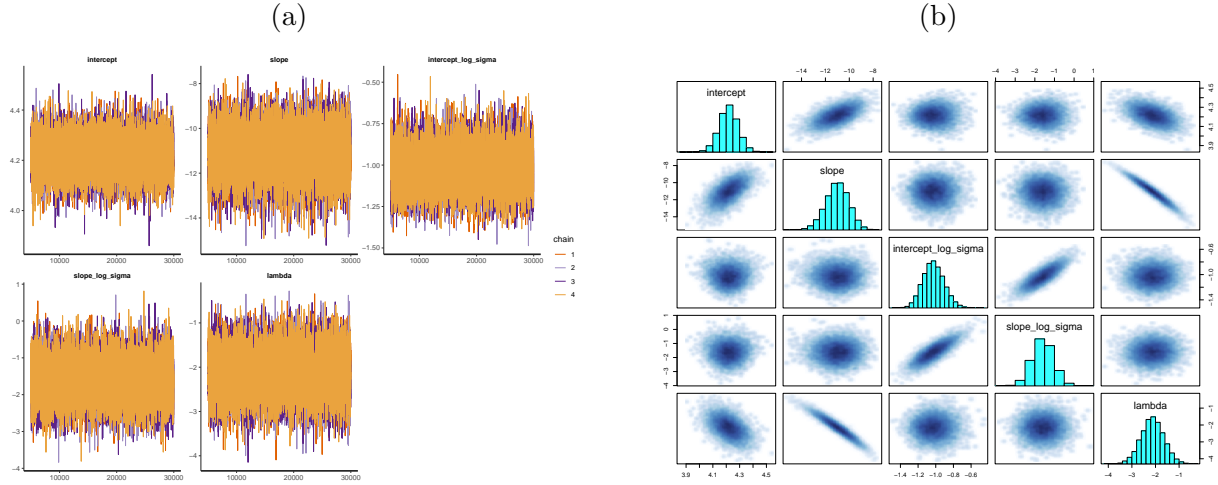


Figure 21: Trace plots (a) and a pairs plot (b) of the posterior draws for the Box–Cox/loglinear- $\sigma_N$  model fit to the laminate panel data.

## J.2 More Details for the Nishijima Hyperbolic *S-N* Model Fit to the Ti64 Data

### J.2.1 Comparison of lognormal and Weibull distributions

Figure 22 uses lognormal and Weibull probability plots to compare the two distributions fit to the Ti64 data. The lognormal distribution fits better.

### J.2.2 Prior distributions

Example 5.1 in the main paper gives a summary of the results of fitting the Nishijima hyperbolic *S-N* model to the Ti64 data. The weakly informative prior distributions used for this example were  $A \sim \text{LNORM}(0.1, 3.0)$ ,  $B \sim \text{NORM}(3.0, 9.0)$ ,  $C \sim \text{LNORM}(0.01, 5.0)$ ,  $E \sim \text{NORM}(2.0, 10.0)$ , and  $\sigma_\epsilon \sim \text{LNORM}(0.01, 1.0)$ .

### J.2.3 Posterior draws and parameter estimates

The following table is a summary of the posterior draws.

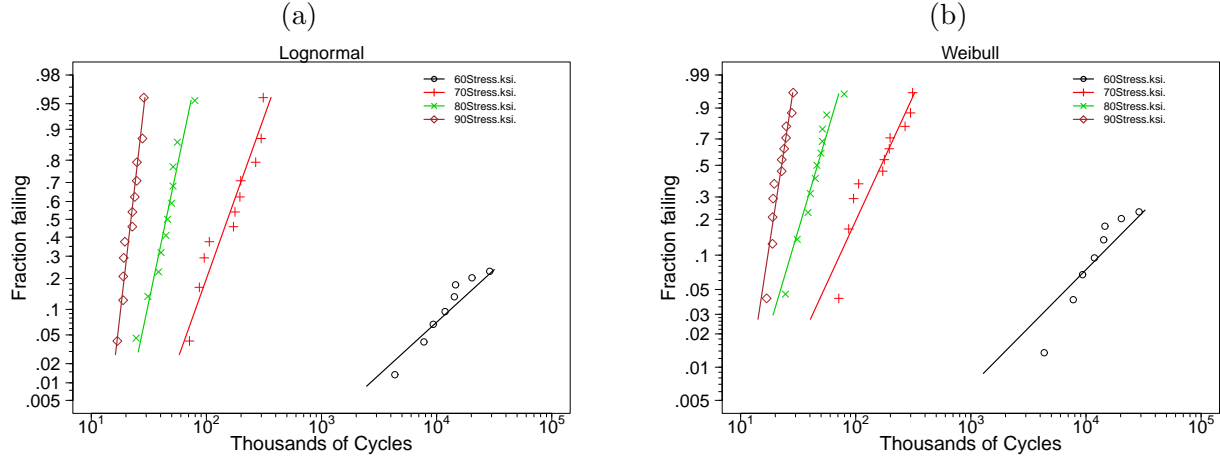


Figure 22: A comparison of lognormal (a) and Weibull (b) probability plots for the Ti64 data.

```
Inference for Stan model: HyperbolicFatigue. 4 chains, each with
iter=30000; warmup=5000; thin=5; post-warmup draws per chain=5000,
total post-warmup draws=20000.
```

	mean	se_mean	sd	2.5%	25%	50%	75%	97.5%	n_eff	Rhat
Ahyp	0.793	0.003	0.374	0.322	0.525	0.709	0.966	1.734	14716	1
Chyp	0.567	0.003	0.384	0.126	0.302	0.469	0.727	1.568	15276	1
Bhyp	5.724	0.004	0.441	5.137	5.407	5.631	5.944	6.821	15378	1
Ehyp	4.039	0.000	0.020	3.998	4.026	4.039	4.053	4.078	17712	1
sigma_error	0.037	0.000	0.004	0.030	0.034	0.036	0.039	0.046	19532	1

Figure 23(a) shows trace plots for the parameters (indicating good mixing) and Figure 23(b) the corresponding pairs plot.

#### J.2.4 Additional residual analyses

Figure 24 shows plots of the standardized strength residuals based on the fit of the Nishijima model fit to the Ti64 data versus lifetime (a) and strength (b) fitted values. In the residuals versus lifetime fitted values plot, each column of residuals corresponds to one of the four stress levels that were used in the experiment. Taking into account the 28 out of 37 runouts at 60 ksi, there is no evidence of any departure from the assumed model.

In the residuals versus strength fitted values plot, again, each group corresponds to a level of stress used in the experiment. The plot of residuals versus strength fitted values is, however, harder to interpret because the fitted values also depend on the number of cycles for each data point.

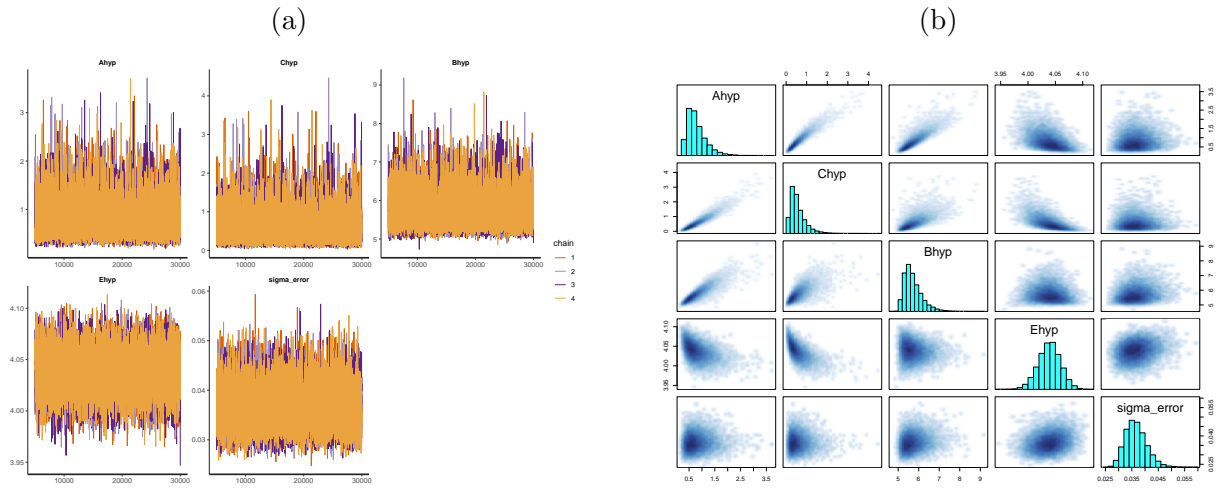


Figure 23: Trace plots (a) and a pairs plot (b) of the posterior draws for the Nishijima Hyperbolic model fit to the Ti64 data.

### J.3 More Details for the Coffin–Manson *S-N* Model Fit to the Superelastic Nitinol Data

#### J.3.1 Comparison of lognormal and Weibull distributions

Figure 25 uses lognormal and Weibull probability plots to compare the two distributions fit to the nitinol data. Both distributions fit well.

#### J.3.2 Prior distributions

Example 5.2 in the main paper gives a summary of the results of fitting the superelastic nitinol *S-N* data to the Coffin–Manson model. The weakly informative prior distributions used for this example were  $A_{el} \sim \text{LNORM}(0.60, 1.5)$ ,  $b \sim \text{NORM}(-0.05, -0.02)$ ,  $A_{pl} \sim \text{LNORM}(1500, 3000)$ ,  $c \sim \text{NORM}(-0.99, -0.70)$ , and  $\sigma_\epsilon \sim \text{LNORM}(0.08, 1.0)$ .

#### J.3.3 Posterior draws and parameter estimates

The following table is a summary of the posterior draws.

```
Inference for Stan model: CoffinManson. 4 chains, each with
iter=30000; warmup=5000; thin=5; post-warmup draws per chain=5000,
total post-warmup draws=20000.
```

	mean	se_mean	sd	2.5%	25%	50%	75%	97.5%	n_eff	Rhat
Ael	0.857	0.00	0.052	0.762	0.821	0.855	0.891	0.964	18963	1
Apl	2207.211	1.99	275.319	1716.451	2013.713	2190.657	2381.767	2790.224	19195	1
bel	-0.028	0.00	0.003	-0.034	-0.030	-0.028	-0.025	-0.021	18960	1

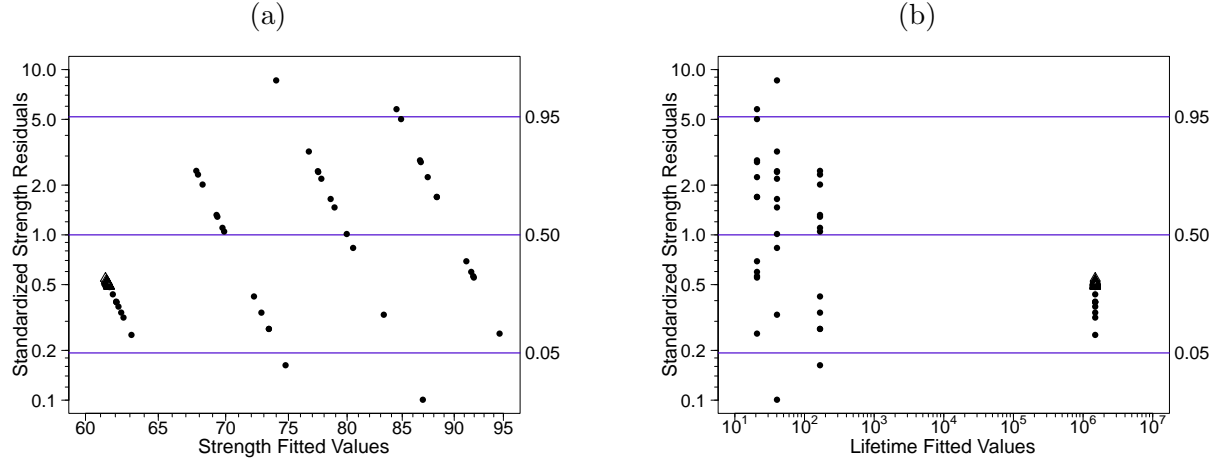


Figure 24: Residuals from the Nishijima model fit to the Ti64 data versus lifetime fitted values (a) and strength fitted values (b).

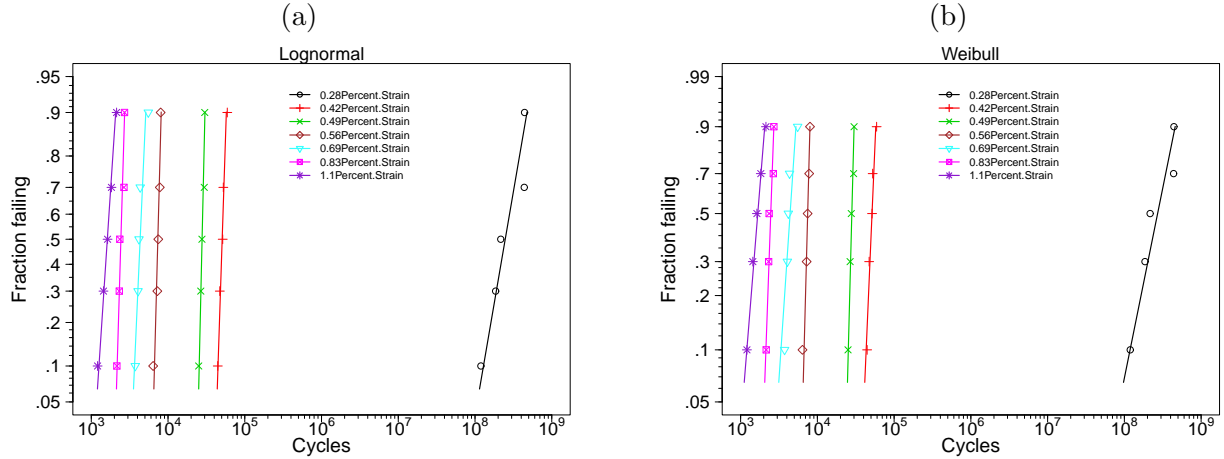


Figure 25: A comparison of lognormal (a) and Weibull (b) probability plots for the nitinol data with the bimodal data at 0.56% strain removed.

cpl	-0.878	0.00	0.015	-0.908	-0.888	-0.877	-0.867	-0.848	19025	1
sigma_error	0.096	0.00	0.011	0.078	0.089	0.095	0.103	0.121	19774	1

Figure 26(a) shows trace plots for the parameters (indicating good mixing) and Figure 26(b) the corresponding pairs plot.

### J.3.4 Additional residual analyses

Figure 27 shows plots of the standardized strength residuals based on the fit of the Coffin Manson model to the nitinol data versus lifetime (a) and strength (b) fitted values.

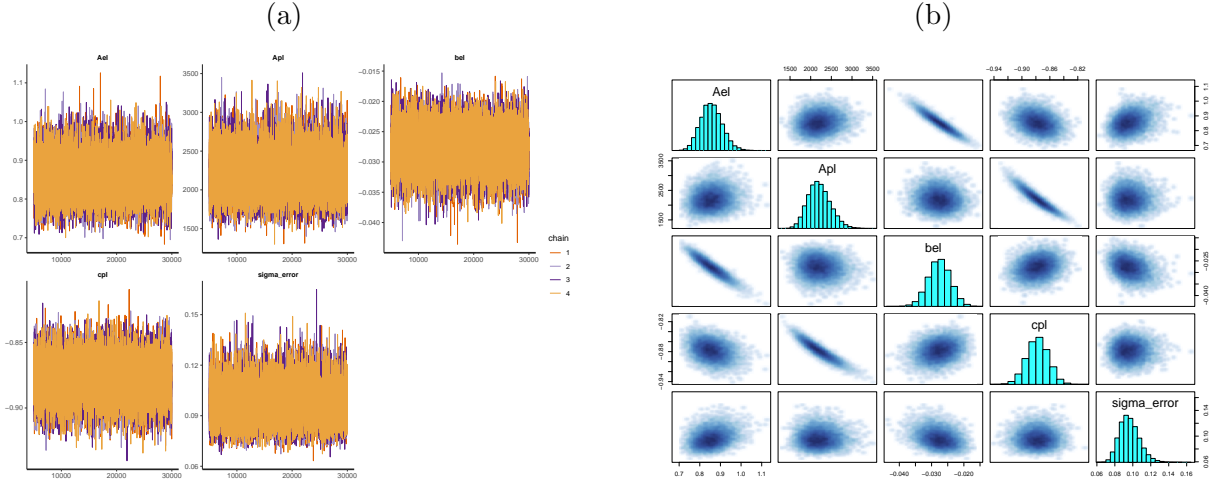


Figure 26: Trace plots (a) and a pairs plot (b) of the posterior draws for the Coffin–Manson model fit to the nitinol data.

## References

ASTM (2015). *Standard Practice for Statistical Analysis of Linear or Linearized Stress-Life (S-N) and Strain-Life ( $\epsilon$ -N) Fatigue Data*. ASTM International. [\[2\]](#)

Awad, M., M. DeJack, and V. Krivtsov (2004). Evaluation of fatigue life regression models. Technical report, SAE Technical Paper 2004-01-0625. [\[18\]](#)

Babuška, I., Z. Sawlan, M. Scavino, B. Szabó, and R. Tempone (2016). Bayesian inference and model comparison for metallic fatigue data. *Computer Methods in Applied Mechanics and Engineering* 304, 171–196. [\[6\]](#)

Basquin, O. H. (1910). The exponential law of endurance tests. In *Proceedings of the American Society for Testing and Materials*, Volume 10, pp. 625–630. [\[9\]](#)

Bastenaire, F. A. (1972). New method for the statistical evaluation of constant stress amplitude fatigue-test results. In *Probabilistic Aspects of Fatigue*. American Society for Testing and Materials International. [\[17, 27\]](#)

Bathias, C. (1999). There is no infinite fatigue life in metallic materials. *Fatigue & Fracture of Engineering Materials & Structures* 22, 559–565. [\[10\]](#)

Birnbaum, Z. W. and S. C. Saunders (1969). Estimation for a family of life distributions with applications to fatigue. *Journal of Applied Probability* 6, 328–347. [\[49\]](#)

Castillo, E. and A. Fernández-Canteli (2009). *A Unified Statistical Methodology for Modeling Fatigue Damage*. Springer. [\[6, 15, 17, 32, 66\]](#)

Castillo, E., A. Fernández-Canteli, V. Esslinger, and B. Thürlimann (1985). Statistical model for fatigue analysis of wires, strands and cables. In *IABSE Proceedings*, pp. 1–40. [\[32, 66\]](#)

Castillo, E., A. Fernández-Canteli, A. Hadi, and M. López-Aenlle (2007). A fatigue model with local sensitivity analysis. *Fatigue & Fracture of Engineering Materials & Structures* 30, 149–168. [\[49\]](#)

Castillo, E., A. Fernández-Canteli, H. Pinto, and M. López-Aenlle (2008). A general regression model for statistical analysis of strain–life fatigue data. *Materials Letters* 62, 3639–3642. [\[32\]](#)

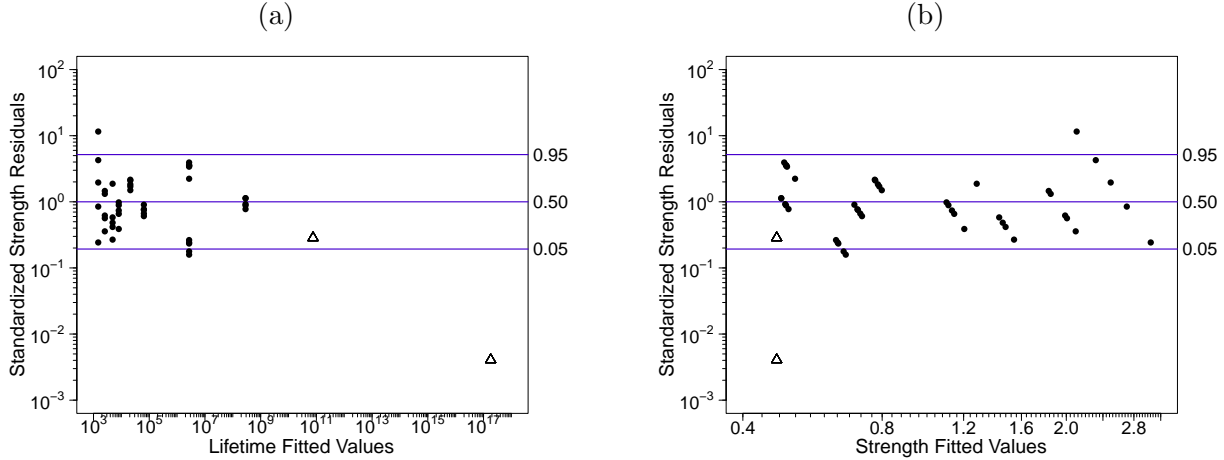


Figure 27: Residuals from the Coffin–Manson model fit to the nitinol data versus lifetime fitted values (a) and strength fitted values (b).

Castillo, E. and J. Galambos (1987). Lifetime regression models based on a functional equation of physical nature. *Journal of Applied Probability* 24, 160–169. [32, 49]

Castillo, E. and A. S. Hadi (1995). Modeling lifetime data with application to fatigue models. *Journal of the American Statistical Association* 90, 1041–1054. [49]

Castillo, E., M. Muniz-Calvente, A. Fernández-Canteli, and S. Blasón (2019). Fatigue assessment strategy using Bayesian techniques. *Materials* 12, 3239. [6, 32, 49]

Crowder, M. J., A. C. Kimber, R. L. Smith, and T. J. Sweeting (1994). *Statistical Analysis of Reliability Data* (Paperback ed.). Chapman & Hall. [15]

Dowling, N. (2013). *Mechanical Behavior of Materials: Engineering Methods for Deformation, Fracture, and Fatigue* (Fourth ed.). Pearson. [30, 37]

Efron, B. and R. J. Tibshirani (1993). *An Introduction to the Bootstrap*. Chapman & Hall. [22]

Falk, W. (2019). A statistically rigorous fatigue strength analysis approach applied to medical devices. In *Fourth Symposium on Fatigue and Fracture of Metallic Medical Materials and Devices*. ASTM International. [7, 18, 35]

Freudenthal, A. (1952). Planning and interpretation of fatigue tests. In *Symposium on Statistical Aspects of Fatigue*. ASTM International. [49]

Freudenthal, A. M. and E. J. Gumbel (1953). On the statistical interpretation of fatigue tests. *Proceedings of the Royal Society of London. Series A. Mathematical and Physical Sciences* 216, 309–332. [6]

Freudenthal, A. M. and E. J. Gumbel (1954). Minimum life in fatigue. *Journal of the American Statistical Association* 49, 575–597. [6]

Freudenthal, A. M. and E. J. Gumbel (1956). Physical and statistical aspects of fatigue. *Advances in Applied Mechanics* 4, 117–158. [6, 7]

Gelman, A., D. Simpson, and M. Betancourt (2017). The prior can often only be understood in the context of the likelihood. *Entropy* 19, 555. [23]

Gnedenko, B. V., Y. K. Belyayev, and A. D. Solovyev (1969). *Mathematical Methods of Reliability Theory*. Academic Press. [15]

Grove, D. and F. Campean (2008). A comparison of two methods of analysing staircase fatigue test data. *Quality and Reliability Engineering International* 24, 485–497. [18]

Hanaki, S., Y. Iwao, M. Yamashita, H. Uchida, M. Zako, and T. Kurashiki (2003). On a decision method of the S-N curve based on fatigue strength distribution (in Japanese). *Journal-Society of Materials Science Japan* 52, 23–27. [18]

Hanaki, S., M. Yamashita, H. Uchida, and M. Zako (2010). On stochastic evaluation of S-N data based on fatigue strength distribution. *International Journal of Fatigue* 32, 605–609. [18]

Hauteville, R., X. Hermite, and F. Lefebvre (2022). A new generic method to analyse fatigue results. *Procedia Structural Integrity* 38, 507–518. [27]

Holmen, J. O. (1979). *Fatigue of concrete by constant and variable amplitude loading*. Ph. D. thesis, Norwegian Institute of Technology, University of Trondheim. [49]

Holmen, J. O. (1982). Fatigue of concrete by constant and variable amplitude loading. In S. P. Shah (Ed.), *Fatigue of Concrete Structures*, Volume 75, pp. 71–110. American Concrete Institute. [49]

Hong, Y., W. Q. Meeker, and L. A. Escobar (2008). The relationship between confidence intervals for failure probabilities and life time quantiles. *IEEE Transactions on Reliability* 57, 260–266. [22, 56, 61, 62]

ISO (2012). *ISO 12107: Metallic Materials-Fatigue Testing-Statistical Planning and Analysis of Data* (Second ed.). ISO. [2, 27]

Johnson, V. E., M. Fitzgerald, and H. F. Martz (1999). Estimating fatigue curves with the random fatigue-limit model: Discussion. *Technometrics* 41, 294–296. [23]

King, C. B., Y. Hong, S. P. Dehart, P. A. Defeo, and R. Pan (2016). Planning fatigue tests for polymer composites. *Journal of Quality Technology* 48, 227–245. [36]

Little, R. E. and E. H. Jebe (1975). *Statistical Design of Fatigue Experiments*. Halsted Press. [18]

Maennig, W. W. (1968). Calculation of the fatigue strength values of steel using an arctan transformation according to R. Müller. *Materials Testing* 10, 191–199. [49]

Mann, N. R., R. E. Schafer, and N. D. Singpurwalla (1974). *Methods for Statistical Analysis of Reliability and Life Data*. Wiley. [15]

Meeker, W. Q. and L. A. Escobar (1995). Teaching about approximate confidence regions based on maximum likelihood estimation. *The American Statistician* 49, 48–53. [22]

Meeker, W. Q., L. A. Escobar, and F. G. Pascual (2022). *Statistical Methods for Reliability Data* (Second ed.). Wiley. [3, 8, 9, 10, 15, 34, 36, 69, 72]

Meeker, W. Q., L. A. Escobar, and S. Zayac (2003). Use of sensitivity analysis to assess the effect of model uncertainty in analyzing accelerated life test data. In W. R. Blischke and D. N. P. Murthy (Eds.), *Case Studies in Reliability and Maintenance*, Chapter 12, pp. 269–292. Wiley. [10]

Meeker, W. Q., G. J. Hahn, and L. A. Escobar (2017). *Statistical Intervals: A Guide for Practitioners and Researchers*. Wiley. [22, 26]

MMPDS (2021). *Metallic Materials Properties Development and Standardization (MMPDS-16): Chapters 1-9*, Volume 2. Battelle Memorial Institute. [2, 37]

Müller, C., M. Wächter, R. Masendorf, and A. Esderts (2017). Accuracy of fatigue limits estimated by the staircase method using different evaluation techniques. *International Journal of Fatigue* 100, 296–307. [18]

Nelson, W. B. (1973). Analysis of residuals from censored data. *Technometrics* 15, 697–715. [24]

Nelson, W. B. (1984). Fitting of fatigue curves with nonconstant standard deviation to data with runouts. *Journal of Testing and Evaluation* 12, 69–77. [6, 11, 17, 36]

Nelson, W. B. (2004). *Accelerated Testing: Statistical Models, Test Plans, and Data Analyses* (Paperback ed.). Wiley. [6, 10, 18, 36]

Nishijima, S. (1980). Statistical analysis of small sample fatigue data (in Japanese). *Transactions of Japanese Society Mechanical Engineering Series A* 46, 1303–1313. [28, 80]

Nishijima, S. (1985). Statistical analysis of small sample fatigue data. *Transactions of National Research Institute for Metals* 27, 234–245. [28, 80]

Pascual, F. (2003). The random fatigue-limit model in multi-factor experiments. *Journal of Statistical Computation and Simulation* 73, 733–752. [36]

Pascual, F. G. and W. Q. Meeker (1997). Regression analysis of fatigue data with runouts based on a model with nonconstant standard deviation and a fatigue limit parameter. *Journal of Testing and Evaluation* 25, 292–301. [11]

Pascual, F. G. and W. Q. Meeker (1999). Estimating fatigue curves with the random fatigue-limit model (with discussion). *Technometrics* 41, 277–302. [3, 22, 32, 49, 69]

Pawitan, Y. (2013). *In All Likelihood: Statistical Modelling and Inference Using Likelihood* (Paperback ed.). Oxford University Press. [21]

Pollak, R., A. Palazotto, and T. Nicholas (2006). A simulation-based investigation of the staircase method for fatigue strength testing. *Mechanics of Materials* 38, 1170–1181. [18]

R Core Team (2022). *R: A Language and Environment for Statistical Computing*. R Foundation for Statistical Computing. [23]

Ross, G. J. S. (1970). The efficient use of function minimization in non-linear maximum-likelihood estimation. *Journal of the Royal Statistical Society: Series C (Applied Statistics)* 19, 205–221. [69, 71]

Ross, G. J. S. (1990). *Nonlinear Estimation*. Springer-Verlag. [69, 71]

Seber, G. A. F. and C. J. Wild (2003). *Nonlinear Regression*. Wiley. [69]

Severini, T. A. (2000). *Likelihood Methods in Statistics*. Oxford University Press. [21]

Shen, C.-L. (1994). *The Statistical Analysis of Fatigue Data*. Ph. D. thesis, The University of Arizona. [49]

Shimokawa, T. and Y. Hamaguchi (1979). Relationship between fatigue life distributions and S-N curve of sharply notched specimens of 2024-T4 aluminum alloy. *Japan Society for Aeronautical and Space Sciences* 21, 225–237. [49]

Shimokawa, T. and Y. Hamaguchi (1987). Statistical evaluation of fatigue life and fatigue strength in circular-hole notched specimens of a carbon eight-harness-satin/epoxy laminate. In T. Tanaka, S. Nishijima, and M. Ichikawa (Eds.), *Statistical Research on Fatigue and Fracture*, pp. 159–176. Elsevier Science. [3]

Smith, R. L. (1985). Maximum likelihood estimation in a class of nonregular cases. *Biometrika* 72, 67–90. [\[14\]](#)

Spindel, J. and E. Haibach (1979). The method of maximum likelihood applied to the statistical analysis of fatigue data. *International Journal of Fatigue* 1, 81–88. [\[6\]](#)

Stan Development Team (2022a). *RStan: The R Interface to Stan*. R Package Version 2.30. [\[23\]](#)

Stan Development Team (2022b). *Stan User's Guide, Version 2.30*. [\[23\]](#)

Stromeyer, C. (1914). The determination of fatigue limits under alternating stress conditions. *Proceedings of the Royal Society of London. Series A, Containing Papers of a Mathematical and Physical Character* 90, 411–425. [\[10\]](#)

Toasa Caiza, P. D. and T. Ummenhofer (2018). A probabilistic Stüssi function for modelling the SN curves and its application on specimens made of steel S355J2+N. *International Journal of Fatigue* 117, 121–134. [\[35\]](#)

Weaver, J., G. Sena, K. Aycock, A. Roiko, W. Falk, S. Sivan, and B. Berg (2022). Rotary bend fatigue of nitinol to one billion cycles. *Submitted xx, xxx–xxx*. [\[5, 31, 37, 47, 49\]](#)

Woo, S. (2020). *Reliability Design of Mechanical Systems* (Second ed.). Springer. [\[6\]](#)

Wu, C. J. and Y. Tian (2014). Three-phase optimal design of sensitivity experiments. *Journal of Statistical Planning and Inference* 149, 1–15. [\[18\]](#)